

ABSTRACT

Anti-Tumor Properties of CD40 Ligand when Delivered as a Transgene by the Conditional Replicative Oncolytic Adenovirus AdEH to Breast Cancer Cells

Erica Manuela Gomes

Mentor: Alex. W. Tong, Ph.D.

Cancer-selective biotherapy and gene therapy have been considered to be the next horizon towards developing a cure for breast cancer. CD40 ligand (CD40L), a member of the tumor necrosis factor superfamily, relays critical growth signals in various hematological malignancies and carcinomas. We previously demonstrated that recombinant CD40L can directly inhibit breast cancer cell growth. However a potential limitation of CD40L therapy is systemic toxicity. To improve efficacy of gene delivery and limit CD40L expression to the tumor micro-environment, we have generated a conditionally replicative virus (AdEHCD40L) that delivers CD40L selectively to breast carcinomas. Tumor/tissue-specific promoters (hypoxic/HIF-1 α response and estrogen response elements) were incorporated to limit CD40L expression to the tumor microenvironment. Viral E1A and CD40L transgene expression was examined in breast cancer lines with low constitutive (T47D) or no (BT-20) HIF-1 α expression. Both cell lines displayed significantly increased CD40L expression under viral- permissive conditions (T47D: $65.5 \pm 3.9\%$ with increased HIF-1 α vs. $38.5 \pm 2.8\%$ under uninduced condition, $p = 0.01$; BT20: $43.2 \pm 14.9\%$ vs. $10.6 \pm 0.2\%$, $p = 0.03$). AdEHCD40L

produced markedly stronger inhibition compared to the parental construct (T47D: $53.7 \pm 15.2\%$ vs. $32.1 \pm 11.7\%$, $p = 0.02$; BT20: $25.8 \pm 10.2\%$ vs. $15.2 \pm 6.8\%$, $p = 0.03$), suggesting that growth inhibition encompassed CD40L-mediated and viral oncolytic events. Replicative activity of AdEHCD40L was comparable to the wild type adenovirus in breast cancer cells and attenuated in normal lung fibroblast cells, with reduced growth inhibitory impact. Preliminary findings on mechanisms of AdEHCD40L cytotoxicity indicated increased apoptotic (Annexin V+) and necrotic (propidium iodide incorporation) activities that were accompanied by reduced I κ B α , phosphorylation, G₂M/S cell cycle arrest, culminating in an increased sub-G₀ fraction, and altered chemokine/cytokine expression. AdEHCD40L biodistribution and its maximum tolerated dose (2×10^8 pfu) evaluated in mice were comparable to that of other conditional-replicative adenoviruses. Anti-tumor efficacy of AdEHCD40L showed a reduction in mean tumor diameter of MDA-MB-231 (44-58%) and T47D (49%) human breast cancer xenografts in SCID mice. These findings illustrate the applicability of CD40L gene transfer approach for experimental treatment of human breast cancer.

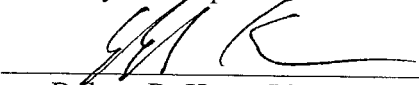
Anti-Tumor Properties of CD40 Ligand when Delivered by the Conditional Replicative
Oncolytic Adenovirus AdEH to Breast Cancer Cells

by

Erica Manuela Gomes, M.S.

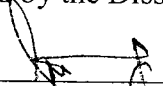
A Dissertation

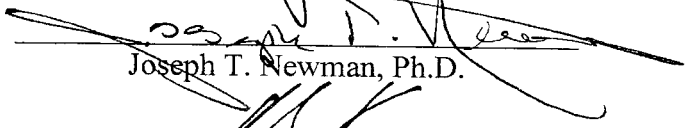
Approved by the Department of Biomedical Studies

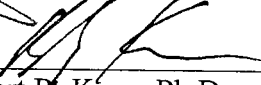

Robert R. Kane, Ph.D., Chairperson

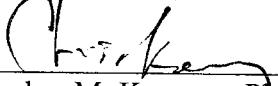
Submitted to the Graduate Faculty of
Baylor University in Partial Fulfillment of the
Requirements for the Degree
of
Doctor of Philosophy

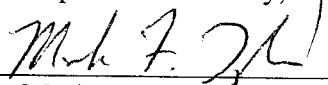
Approved by the Dissertation Committee


Alex W. Tong, Ph.D., Chairperson

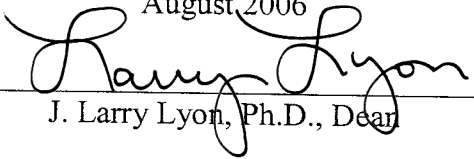

Joseph T. Newman, Ph.D.


Robert R. Kane, Ph.D.


Christopher M. Kearney, Ph.D.


Mark F. Taylor, Ph.D.

Accepted by the Graduate School
August 2006


J. Larry Lyon, Ph.D., Dean

Copyright 2006 by Erica Manuela Gomes

All rights reserved

TABLE OF CONTENTS

	Page
List of figures	vi
List of tables	viii
Abbreviations	ix
Acknowledgments	xiii
Dedication	
Chapter	
1. Introduction	
Breast cancer	1
CD40 and CD40L	2
CD40-CD40L for cancer therapy	5
CD40-CD40L signaling pathway	6
Adenovirus for cancer gene therapy	7
Conditional replicative oncolytic adenovirus for cancer therapy	11
Adenovirus and CD40L delivery	13
Adenoviral gene therapy for breast cancer	14
Rationale for Study	16
Aim of Study	17

	Page
2. Characterization of the Adenovirus vectors	
Material and Methods	19
Results	25
Discussion	36
3. Growth regulatory activities of AdEHCD40L	
Material and Methods	39
Results	42
Discussion	52
4. In vivo growth regulatory activities of AdEHCD40L	
Material and Methods	56
Results	60
Discussion	69
5. Tumor growth inhibitory mechanisms of AdEHCD40L	
Material and Methods	75
Results	79
Discussion	90
6. Conclusion and Future Studies	96
Appendices	
A Cloning of the AdEH recombinant adenoviral constructs	101
B Purification, titration and genomic validation of AdEHCD40L	
Material and Methods	105
Results	110

	Discussion	112
C	CD40L sequence	115
	References	116

LIST OF FIGURES

Figure	Page
1.1 Adenovirus structural components	10
1.2 Adenoviral early and late genes	12
2.1 Schematic representation of genetic modifications in AdEHCD40L	22
2.2 Viral E1A expression in cancer cells	30
2.3 Flow cytometric analysis of CD40L protein following AdEHCD40L infection	31
2.4 CD40L transgene expression in ZR-75-1 breast cancer cells	32
2.5 CD40L transgene expression in cancer cells on CoCl ₂ induction	33
2.6 Effect of cobalt chloride on cell viability	34
2.7 RT-PCR for viral E1A and CD40L	35
3.1 Time dependent growth regulatory outcome of AdEHCD40L	43
3.2 Relative anti-tumor efficacy of AdEHCD40L and AdEHNull	44
3.3 Viral replication of AdEHCD40L is comparable to the control construct	46
3.4 AdEHCD40L is more potent than the recombinant CD40L	47
3.5 Crystal violet staining for cytopathic effect in non malignant and malignant cell lines	48
3.6 AdEHCD40L attenuated in non permissive BT20 cancer cells	49
3.7 Viral replication in non malignant and malignant cell lines	50
4.1 Schematic representation of biodistribution and maximum tolerated experimental design	57

Figure	Page
4.2	Biodistribution of AdEHCD40L in organs of female Balb/c mice 62
4.3	Biodistribution of AdEHCD40L in serum of female Balb/c mice 63
4.4	H&E and HIF-1 α staining of T47D xenografts 64
4.5	AdEHCD40L evaluation in T47D xenografts SCID xenografts 66
4.6	Anti-tumor responses of AdEHCD40L in MDA-MB-231 68
5.1	Schematic of CD40-CD40L signaling pathways 73
5.2	Annexin V/ PI staining of T47D infected cultures 80
5.3	Cell cycle analysis 82
5.4	Western blot analysis for p38 and p42/p44 84
5.5	Western blot analysis for AKT and I κ B α 85
5.6	Western blot analysis for cell cycle regulator p21 ^{waf1/cip-1} 87
5.7	Effect of blocking I κ B α phosphorylation on growth regulation 88
5.8	Luminex analysis of chemokines and cytokines 91
5.9	Putative mechanism of AdEHCD40L perturbation of NF κ B pathway 93
5.10	Schematic of pathways affected by AdEHCD40L 95
6.1	Hypothetical anti-tumor activity of AdEHCD40L 98
B.1	Schematic for viral purification, quantification and validation of genomic integrity 106
B.2	Primer sequences and schematic of primer position used for PCR amplification of E1, E3 and E4 modified sequences 107
B.3	Sequence specific amplification of the viral construct 111
B.4	Bidirectional DNA sequencing data of the CD40L transgene by the dye terminator labeling 112

LIST OF TABLES

Table	Page
1.1 Biological therapies for breast cancer	3
1.2 Growth regulation of CD40-CD40L in hematopoietic cells	8
1.3 Growth regulation of CD40-CD40L in non hematopoietic cells	9
2.1 Immunophenotype analysis of cancer and normal cell lines	26
2.2 Immunophenotype of cancer and normal cell lines for viral permissive conditions	28
3.1 Quantification of soluble CD40L by ELISA	52
4.1 Determination of maximum tolerated dose (MTD) of AdEHCD40L in vivo	61
5.1 Western blot analysis of transcription mediators	89
B.1 Quantification of viral yield by spectrophotometry and plaque forming assay	113

LIST OF ABBREVIATIONS

AdEH	Adenovirus with HRE/ERE and E2F-1 promoters
AdEHCD40L	AdEH carrying the CD40L transgene
AdEHNull	AdEH lacking the CD40L transgene.
Adv-WT	Adenovirus wild type
AP-1	Activation protein-1
APC	Antigen presenting cell
ATCC	American Type Culture Collection
AU	Absorbance units
bp	Base pair
BSA	Bovine serum albumin
CAR	Coxsackie adenovirus receptor
CD	Cluster of differentiation
Cdk	Cyclin dependent kinase
cDNA	Complementary deoxyribonucleic acid
CLL	Chronic lymphocytic leukemia
CoCl ₂	Cobalt chloride
CsCl	Cesium chloride
CTL	Cytotoxic T lymphocyte
D	Mean tumor diameter
DCs	Dendritic cells

DMEM	Dulbecco's Modified Eagles Media
DNA	Deoxyribonucleic acid
ECL	Enhanced chemiluminescence
ED ₅₀	Effective dose 50
ERE	Estrogen response element
Erk	Extracellular regulated kinase
FAM	6-carboxytetramethylrhodamine
FBS	Fetal bovine serum
FITC	Fluorescein isothiocyanate
GM-CSF	Granulocyte Macrophage colony stimulating factor
gp	Glycoprotein
Her-2/ neu	Human epidermal growth factor
HIF	Hypoxia inducible factor
HIGM	X linked hyper IgM syndrome
HMEC	Human mammary epithelial cells
HRE	Hypoxic response element
ICAM	Intracellular adhesion molecules
IFN γ	Interferon gamma
IKK	I κ B α kinase
IL	Interleukin
I κ B α	Inhibitor of NF-kappaB α
JNK	c-jun-N-terminal kinase
LFA	Lymphocyte function associated

MAPK	Mitogen activated protein kinase
MIP-1 α	Macrophage inflammatory protein-1 alpha
MOI	Multiplicity of infection
MTT	3-[4,5-dimethylthiazol-2-yl]-2,5-diphenyltetrazolium bromide
ND	Not determined
NF κ B	Nuclear factor-kappa B
ng	Nanogram
NGFR	Nerve growth factor receptor
nM	Nanomolar
PBS	Phosphate buffer saline
PCR	Polymerase chain reactions
PE	Phycoerythrin
pfu	Plaque forming units
PI	Propidium iodide
PI3Kinase	Phosphatidylinositol-3 kinase
PVDF	PolyVinylidene DiFluoride
qPCR	Quantitative PCR
RANTES	Regulated on activation normal T cell expressed and secreted
rCD40L	Recombinant CD40L
RGD	Arginine-glycine aspartic acid
RT	Room temperature
SAPK	Stress activated protein kinase
sCD40L	Soluble CD40L

SCID	Severe combined immunodeficiency
SDS	Sodium dodecylsulfate
Ser	Serine
STAT	Signal transducer and activator of transcription
TAMRA	6-carboxyfluorescein
TCR	T cell receptor
TGF	Transforming growth factor
Th1	T helper 1
Thr	Threonine
TMB	Tetramethyl-benzidine
TNF	Tumor necrosis factor
TNFRSF	Tumor necrosis receptor factor superfamily
TRAF	Tumor necrosis receptor associated factor
TRAIL	TNF related apoptosis inducing ligand
TSR	Template suppression reagent
Tyr	Tyrosine
UV	Ultra violet
VEGF	Vascular endothelial growth factor
Vp	Viral particles
XIAP	X-linked inhibitor of apoptosis
μg	Microgram
μl	Microliter
μM	Micromolar

ACKNOWLEDGMENTS

It gives me immense pleasure to thank my advisor Dr. Alex W. Tong for providin me an opportunity to work on this exciting project. His priceless help, unfailing support, guidance and financial assistance through the duration of this project is deeply appreciated. I thank the director of the Sammons cancer center, Dr. Marvin J.Stone for encouraging me, reviewing my abstracts/ posters that were sent to various international scientific meets and extending his laboratory facilities during my work period. Thanks also goes to our collaborators, Dr. Ruben Alcocoeba Hernandez and Dr. Michael Clarke for providing the cloned adenovirus. Dr. Joseph T. Newman for his constant encouragement, intellectual input, not to forget his tremendous sense of humor and all the weekends he brought me donuts. His commitment to his job has been inspirational. He is a wonderful professor and made up experience doing research memorable. I also thank Dr. Maria Papayoti, who worked with me during the first six months of this project, got me started on this project. Though I worked with her briefly, I learnt all my technical skills and the ability to think as a scientist through interacting with her. Joe Kansopon, for his contribution on the quantitative PCR work done. Margret Rodrigues, who I worked in close association on this project. She willingly waited late with me, was there for me through every part of this project making sure I never doubted myself, and gave me the reassurance I needed through this process. Her ability to maintain a cheerful environment is deeply appreciated. I thank Dr. Yu- An Zhang, Dr. Padmasini Kumar,

Patrick Chen and Dan Su who helped me, supported me and put up with me even when I was unreasonable. Appreciation go to all the staff at the immunology research laboratory, especially Yolanda, Elga, Laura and Latisha for always accommodating me and allowing me to use their equipment. They were always fun to be around. The employees at the Baylor research institute and the staff at the Sammons Cancer Center for their help. Dr. Jack Chang and Mao from the pathology department, for helping me with the histological aspects of this project. Dr. Ajay Joel and Erin Hotchkiss from the gastroenterology laboratory for their insight on the cell cycle analysis. Chun-i Yu my colleague from the department of biomedical studies. Interacting with her was always a pleasure. She gave me the mental stimulation I needed, thought me my animal skills and was always willing to have a discussion on any scientific topic. Sam Ho, for rendering his expertise with the sequencing done on this project. My initial contact to Baylor University and the institute of Biomedical studies was with Dr. Darden Powers. Had he not given me this opportunity to come to Baylor I would have never had these wonderful experiences and met everyone that I did. I thank Lori Banas and Diana Balderas, secretaries of the institute of biomedical institute for always being there to help me and were fun to interact with. My committee member's Dr. Robert Kane, Dr Christopher Kearney and Dr. Mark Taylor for their invaluable advice and time taken out of their busy schedules to serve on my committee. The graduate school and the international office of Baylor University for all their support and help rendered. My friends and family in the US and scattered world wide need to be acknowledged. Dr. Daniel Menezes for keeping me focused on my goal, advising me and making sure I completed writing my dissertation in a timely manner. Every time I doubted myself or felt like I was not going

to pull through, he always reassured me that I was doing what I loved to do-research. Last but not the least, my mother Maria Ligia D'Abreu and brother Ashley Savio Gomes for, their constant moral support, believing in me and patience. Though they were not physically here with me and worlds apart, they were always a phone call away and reminded me that I was not alone. My mother has been an icon of strength and inspiration to me who sacrificed a lot and sent me to the USA to pursue my dreams. She never complained and believed in me despite of her challenges for which I am deeply indebted. My grandmother and the main reason I pursued a career in cancer was always been proud of me and my accomplishments. Though she is no longer alive, her strength, unfailing love and belief in me live on. I would not be where I am in life today and accomplished my goals had it not been for everyone acknowledged. Thank you.

DEDICATION

To

My mother, Maria Ligia D'Abreu

My brother, Ashley Savio Gomes

and

In loving memory of

My grandparents, Dr. Jose Mariano D'Abreu, Rosalia Pinto D'Abreu

My brother, Anil Carlos Gomes.

May their souls rest in peace.

CHAPTER ONE

Introduction

Breast Cancer

Breast cancer poses a major health problem worldwide with more than 1,000,000 new cases and 370,000 deaths per year ¹. In the United States an estimated 40,410 women are expected to die from breast cancer as anticipated by the American cancer society for the years 2005 - 2006. Though the overall survival rate of breast cancer patients has improved due to improved screening programs, early surgical intervention, and a better understanding of cancer biology, relatively few therapeutics are currently available for treating patients with advanced metastatic diseases ¹. Thus novel treatment strategies are particularly needed for patients with metastatic disease, and cancers unresponsive to standard radiation, hormone and chemotherapy.

Conventional therapy for breast cancer includes surgery (removal of lymph nodes, lumpectomy, mastectomy and ovarian ablation), chemotherapy (cyclophosphamide, methotrexate, anthracyclines, taxanes), radiation therapy and hormonal therapy (tamoxifen, fulvestran). Although these treatment strategies provide acceptable response rates and improve overall survival in patients with breast cancer, they are generally not selective and induce cytotoxicity in normal as well as cancer cells ^{2,3}. Cancer-selective biotherapy or gene therapy approaches have widely been considered to be the next horizon towards developing a cure for breast cancer. An increasing

knowledge on the biological pathways and genes associated with breast carcinogenesis has lead to the development of targeted therapeutics, namely antibodies, small synthetic molecules, cytokines and gene therapy for breast cancer (Table 1.1) ⁴. These targeted approaches aim to specifically block the carcinogenesis and tumor growth, rather than simply interfering with rapidly dividing cells. Success with targeted therapy for the well known antigen human epidermal receptor (HER)-2/ neu (human epidermal growth factor receptor), over-expressed in breast cancers ⁵ suggests it to be a feasible alternative for the treatment of breast cancer.

CD40 and CD40L

Our study focuses on the interaction of CD40, a membrane receptor and member of the tumor necrosis factor receptor superfamily (TNFRSF) and its natural ligand CD40 ligand (CD40L) which is also referred to as CD154, gp39, T-BAM or TRAP ⁶. The TNFRSF are a group of related molecules characterized as type I and II transmembrane glycoproteins that includes the Fas antigen (Fas), CD27 (T cell antigen), 4-1BB, nerve growth factor receptor (NGFR), and CD30 ⁷. Most of them have been assigned functions related to immune effector function and cell growth regulation ⁷⁻⁹.

The CD40 receptor is a 45-50 KDa phosphorylated glycoprotein, and consists of 277 amino acids with a large 193 amino acid extracellular region, 22 amino acid transmembrane domain and a short 62 amino acid cytoplasmic C terminus ¹⁰. It is best known for its role in regulation of cellular and humoral immune responses ¹¹. The CD40 receptor has been found on early CD34+ B cell precursors and shown to be expressed during all stages of B cell development until their terminal differentiation into plasma

Table 1.1: Biological therapies for breast cancer

Therapeutic agent	Examples	Mechanisms
Monoclonal antibodies	Trastumzumab/ Herception	Targeting Her-neu receptor
Antiangiogenic	Bevacizumab	Blocks formation of new blood vessels by targeting vascular endothelial growth factor (VEGF)
Hormone antagonist/ endocrine therapy	Tamoxifen	Estrogen antagonist
	Faslodex, Fulvestran	Down-regulates estrogen receptors
	Aromatase inhibitors (Steroidal: exemestane; Non steroidal: anastrozole, letrozole).	Inhibitors of estrogen synthesis
Cytokines	IL-2	Immunostimulatory and anti-tumor activity
	IFN α	Immunostimulatory
Vaccines	Her-2 neu peptide and granulocyte macrophage colony stimulating factor (GM-CSF)	T cell antigen specific immune response
Gene therapy	Adenoviral E1A	Down-regulation of Her-neu

cells¹². It has also been found to be expressed on monocytes/macrophages, dendritic cells (DCs), eosinophils and CD8+ T cells¹³. By comparison, CD40L is tightly regulated and expressed transiently on T cells¹⁰. The CD40L has also been described on other cell types such as basophils, eosinophils, platelets, activated B cells, monocytes and natural killer cells^{10, 14-16}. It is found to exist both in a soluble form and a 39 KDa type II transmembrane bound form where it appears to form a trimeric protein structure¹⁰.

The cross-linking of CD40 by CD40 ligand (CD154) is a well known requirement for initiating the regulation of cellular and humoral immune responses ¹¹. CD40 activation has been shown to be important in B cell activation, proliferation, isotype switching and induction of apoptosis ¹⁷. The functional outcome is dependent on B cell maturation stage. Germinal center B cells cultured with IL-2, IL-10 and CD40L differentiate into memory B cells ¹⁸ while resting B cells treated with CD40L undergo Fas mediated apoptosis ¹⁹.

CD40L also stimulates B cells and dendritic cells to express a number of co-stimulatory molecules [CD80/B7-1, CD86/B7-2, intracellular adhesion molecules (ICAM)-1/CD54 and lymphocyte function associated (LFA)-3/CD58] which increases the efficiency by which antigen presenting cells (APCs) interact with T cells ¹⁵. The physiological importance of CD40-CD40L interaction was ascertained by the findings that patients suffering from X linked hyper IgM syndrome (HIGM), an X linked immunodeficiency disease, had a genetic alteration in the CD40L gene ^{20, 21}. These patients were characterized by an impairment in T cell mediated antibody response, over-production of IgM, absence of IgG, IgA, IgE, no memory B cells and accompanied by severe recurrent infection ^{22, 23}.

CD40 has also been found on non-hematopoietic cells like fibroblasts, thymic epithelial cells and endothelial cells ¹¹ where it appears to play a role in growth regulation and cytokine/ chemokine secretion ¹¹. In epithelial cells, CD40 expression is restricted to the proliferative basal layer of the nasopharyngeal, tonsillar and ectocervical epithelium ^{11, 24} and presumably plays a role in growth regulation, cytokine and chemokine secretion

CD40-CD40L for Cancer Therapy

Ever since CD40 was first identified on the surface of bladder carcinoma in 1985²⁵, it has subsequently been shown to be expressed on various hematological and epithelial cancers of the lung, ovary, bladder, colon and squamous cell cancer of the head and neck^{11, 26, 27}. Clinical studies evaluating lung and melanoma patients demonstrated that CD40 expression may serve as a prognostic marker which correlates with metastasis and poor prognosis^{28, 29}. Further, we demonstrated that there is > 90% of CD40 expression in breast cancers of various histological types (infiltrating ductal and lobular, carcinoma in situ, mucinous)³⁰.

CD40L can positively and negatively modulate the growth of cancer cells. Totero et al reported that CD40 triggering upregulates IL-21 that mediates pro-apoptotic signals in chronic lymphocytic leukemia (CLL)³¹. For multiple myeloma, a plasma cell neoplasm, reports of growth inhibition and stimulation have been reported depending on the CD40L molecule being used (membrane, soluble, monoclonal antibody)^{32, 33}. The functional role of CD40 and its ability to modulate tumor cell growth has been similarly demonstrated in epithelial cells^{30, 34}. CD40 activation by CD40L recombinant protein or anti-CD40 monoclonal antibodies have shown to induce growth inhibitory and/or apoptosis in mouse renal cancer cells³⁵. We demonstrated that CD40L delivered either as soluble recombinant CD40L, gp39, or a CD40L trimer inhibits CD40+ breast cancer cells³⁰. However, others have shown that the co-expression of CD40 and CD40L on B cell lymphoma's and breast carcinoma's plays an autocrine anti-apoptotic role and that blocking CD40-CD40L interactions sensitizes cells to drug induced apoptosis³⁶.

Altogether, this suggests that CD40 is commonly expressed on cancer cells and can be used to modulate cancer cell growth.

CD40-CD40L Signaling Pathway

The ability of CD40L to induce cell proliferative and growth inhibitory responses in hematological and epithelial malignancies, suggests that a better understanding of the mechanisms underlying anti-tumor responses is required. The various growth regulatory outcomes have been attributed due to differences in concurrent intracellular signaling via the CD40 cytoplasmic domain. Goldstein et al demonstrated that residues at position 227 and 234 in the cytoplasmic domain play an important role in the induction of the costimulatory molecule B7-1 but have a lesser importance in CD40 mediated growth inhibition. This suggests that there are distinct domains in the cytoplasmic region of the CD40 molecule that mediate B7-1 induction or growth inhibition³⁷. Following receptor trimerization, the recruitment of tumor necrosis receptor associated factor (TRAF) by the CD40 cytoplasmic tail is mediated by a membrane proximal region containing amino acids Gln²³⁴Glu²³⁵ responsible for TRAF6 binding, and a membrane distal region Pro²⁵⁰XGln²⁵²XThr²⁵⁴ motif that has been shown to be critical for interactions with TRAF1, TRAF2, TRAF3, and indirectly with TRAF 5³⁸. Localization of these adaptor molecules is cell type dependent and triggers multiple signaling pathways that leads to the activation of c-Jun N terminal kinase (JNK), p38 mitogen activated protein (MAPK), extracellular regulated kinase (Erk), the transcription factor NFkB, signal transducer and activator of transcription (STAT), and the phosphatidylinositol 3-Kinase (PI3Kinase) cascade³⁸⁻⁴⁰. These pathways may act in

concert and trigger a plethora of events and growth regulatory outcomes (Tables 1.2, 1.3). Due to the ability of CD40L to impact the immune system that could lead to non specific systemic activation, an appropriate gene delivery vehicle that can localize its growth regulatory outcome is necessary for its administration.

Adenovirus for Cancer Gene Therapy

Several viral vectors like retrovirus, lentivirus, pox virus, herpes simplex virus-1 and adenovirus have been used for experimental cancer gene therapy ⁴¹, particularly for cancers refractory to conventional therapies (surgery, radiation, and chemotherapy). Adenovirus is one of the most widely accepted viral agents for cancer gene therapy. Its capacity for gene transfer (up to 7-8 Kb), in vivo stability, coupled with other factors like its ability to transduce dividing and non dividing cells, well characterized genome, relative ease of production, purification and manipulation, make it an appropriate agent for viral therapy of cancer. Adenovirus does not integrate into the host genome, a safety feature appropriate as a gene transfer agent for cancer therapy. From a clinical point of view, adenovirus is endemic in the human population and its natural pathogenicity is associated with mild respiratory infections, and therefore, manifests a well defined safety profile.

Adenovirus was first isolated and cultured from human tonsils and adenoid tissues ⁴²⁻⁴⁴. Currently 51 human adenovirus serotypes have been identified and grouped into six subgroups (A-F) of which the most widely studied serotype are group C types 2 and 5. Adenovirus is a non-enveloped icosohedral particle which carries a 36 Kb double stranded DNA genome. The capsid consists of three main components: hexon, penton

Table 1.2: Growth regulation of CD40-CD40L in hematopoietic cells

Cell Type	Mechanism of action ^a	
	Prostimulatory	Anti-Proliferative
B cells	<ol style="list-style-type: none"> 1. TRAF 2, 3 involved in activation of p38, JNK, IκBα phosphorylation and not in Ig production. TRAF 6 regulated affinity maturation. 2. TRAF 2, 5, 6 activate JNK, Erk and NFκB that result in increase IL-6, CD54, cIAP1-2, Bcl-XL. 3. JNK, p38, NFκB important for survival. 4. NFκB is critical for some but not all CD40 effector signals. ↑ CD80-dependent; ↑ CD95- partially dependent; ↑ CD11a- independent. 	<ol style="list-style-type: none"> 1. Increase in Fas. However Fas mediated cell death occurs only when CD40L interactions ceases. It is also associated with increase in cFLIP. 2. TRAF 3 is involved in feed back inhibition of activation
Dendritic cells	<ol style="list-style-type: none"> 1. TRAF 6 required for p38 and JNK activation and IL-12 production. 2. NFκB activations involved in DC maturation (via p50/Rel A and Rel c) and anti-apoptotic responses (p52/ Rel B). 	
Monocytes	<ol style="list-style-type: none"> 1. TRAF1,5 caused rapid and transient expression of Erk 1,2 	
T cells	<ol style="list-style-type: none"> 2. TRAF-1 caused ↑ c-Jun mRNA, ↑ SAPK activation, but did not affect Erk 1,2 	
B cell malignancies	<ol style="list-style-type: none"> 1. NFκB, A20, Bcl 2, Bcl XL, FLICE regulate survival. 2. PI3K/TOR and Erk counteract apoptotic signals independent of p38 and NFκB. 3. Blocking NFκB increased apoptosis independent of NFAT and p38 (Ramos B cells) 4. IgG production is mediated by TRAF 3 –p38 activation while apoptosis does not involve TRAF-3 but decreases NFκB (Ramos B cells). 	
Multiple myeloma		<ol style="list-style-type: none"> 1. TRAF 4, 6 involved in apoptosis

^a 17, 45-49

Table 1.3: Growth regulation of CD40-CD40L in non-hematopoietic cells

Cell Type	Mechanism of action ^a	
	Prostimulatory	Anti-Proliferative
Intrahepatic Endothelial cells	1. NFkB activation sustained for 2- 24Hrs and no activation of AP-1 or downstream effectors like Erk-1, 2 and JNK1, 2 was observed.	
Biliary epithelial cells		1. Sustained AP-1 and transient NFkB activation resulted in apoptosis through FasL regulation.
Hepatocytes		1. Sustained AP-1 and transient NFkB activation resulted in apoptosis through FasL regulation and activation of Erk-1, 2 and JNK1, 2.
Carcinomas	1. NFkB and JNK cause increase in ICAM, IL-6, IL-8.	1. Growth Inhibition via modulation of NFkB and JNK.
Rat-1		1. PI3Kinase involved in anti-apoptotic responses.
Ovarian Cancer		1. Growth inhibition observed mediated in presence/ absence of NFkB activation and was cell line dependent. 2. In all lines JNK was activated. 3. Growth inhibition observed in presence/absence of apoptosis.
HeLa	1. Erk activation involved in anti-apoptosis. 2. C40L activates protein synthesis in a PI3Kinase, Erk, mTOR dependent manner. 3. PI3Kinase regulate cFLIPs involved in anti-apoptosis.	1. PI3Kinase involved in anti-apoptotic responses.

^a 17, 45-49

and fiber (Figure 1.1). Hexon is the most abundant structural protein which appears to play a role in coating the virus. The pentameric structure called penton is known to mediate viral internalization. The fiber protrudes from the penton bases and appears to play a role in viral attachment to the cellular receptor namely coxsackie adenovirus receptor (CAR). Attachment via knob-CAR interactions is followed by interactions between cellular integrins and an arginine-glycine aspartic acid motif (RGD-motif) located at the penton base. This binding leads to the formation of endosomes, viral internalization, disassembly and the release of viral nucleic acid. Thereafter viral DNA is transported to the nucleus where the genes are expressed and viral replication occurs.

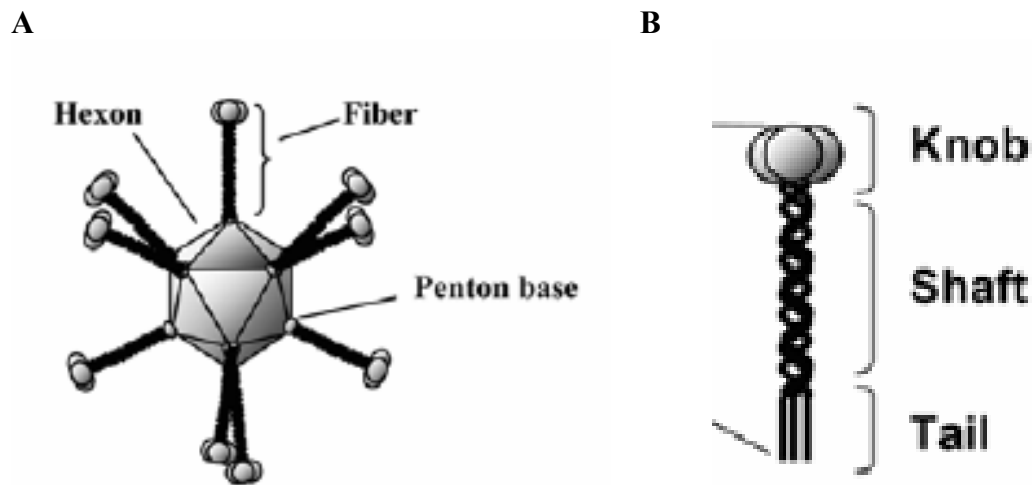


Figure 1.1: Adenovirus structural components. (A) Adenoviral virion showing the main structural components of the virus. (B) Adenoviral fiber consists of the tail, shaft and knob. The knob is involved in CAR mediated high affinity interactions required for cellular attachment. The tail mediates CAR independent low affinity interactions through cellular integrins and is involved mainly in viral penetration and internalization ⁵⁰.

The adenoviral genome can be divided into immediately early (*E1A*), early (*E1B*, *E2*, *E3*, *E4*), intermediate (*IX*, *IVa2*) and late genes (Figure 1.2A). The early genes are expressed prior to viral replication consisting of mainly regulatory proteins that prepare the host cell for virus DNA replication and block antiviral mechanisms. The late viral genes encode for viral structural proteins. Importantly, the E3 region encodes a variety of proteins involved in immune response evasion. A number of these E3 regions have been deleted to provide cloning sites for transgene insertion. This process has found to not compromise adenoviral replicative function (Figure 1.2B) ⁵¹.

Conditional Replicative, Oncolytic Adenovirus for Cancer Therapy

Studies indicate that adenovirus can be safely used for gene delivery. Initially, non replicative adenoviruses were used to cancer therapy. Non replicative adenoviruses have been modified by replacing early genes, E1A and E1B or E3 with the gene of interest. Since the E1 unit is essential for viral replication, the recombinant vector is replicative defective and its replication requires helper functions provided by transacting E1 complementing cells. However, these recombinant constructs have been useful mainly at local/ regional stage. Their therapeutic limitation has been the incomplete infection of tumor cells, transient expression of the transgene, and a lack of systemic efficacy.

Recently, conditional replicative, oncolytic adenoviruses have been shown to replicate and kill tumor cells without harming normal cells, and thus has resulted in them being employed clinically ⁵². The tumor specificity of these viruses has been manifested through the incorporation of tissue or tumor specific promoters that limit viral gene

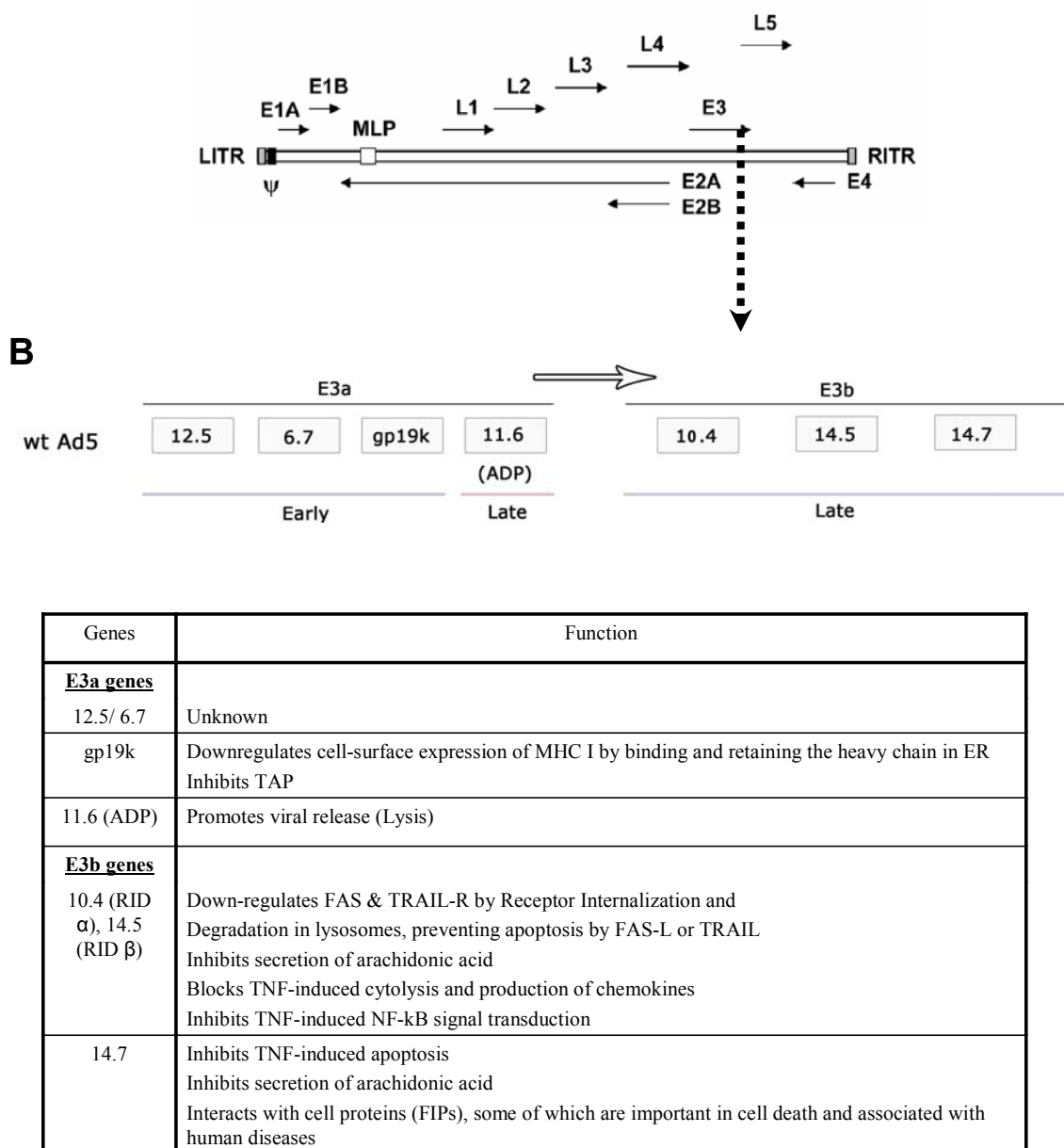


Figure 1.2: Adenoviral early and late genes. A) Schematic representation of the adenoviral genome representing the viral early and late genes⁵⁰. The early genes E1, E2, E3 and E4 encode for regulatory proteins that prepare the host cell for virus DNA replication and block antiviral mechanisms. The late genes encode viral structural proteins. B) The adenoviral E3 genes that have been used for cloning of transgenes along with their cellular functions.

expression to cells that express the requisite transcription factor^{53, 54}. Onyx-015 was the first oncolytic adenovirus that was successfully employed clinically in humans. Deletions in the viral E1A and E1B genes restrict viral replication to cancer cells. Nonetheless, the use of Onyx-015 as a monotherapy, has produced only limited clinical efficacy, although Onyx-015 plus chemotherapy (cisplatin and 5-fluorouracil) has provided effective local tumor control in patients with recurrent squamous cell carcinoma of the head and neck^{55, 56}.

Based on anti-tumor findings of transgenes that are delivered by non-replicative viruses, it appears likely that the incorporation of transgenes with anti-tumor activity into oncolytic adenovirus may enhance cell killing properties of the virus⁵².

Adenovirus and CD40L Delivery

CD40L has been evaluated as an immunotherapeutic agent for cancer therapy. The rationale of this approach is to modify the host tumor interactions by stimulating the host's anti-tumor immune responses. While the capacity of adenoviral delivered CD40L to activate tumor specific immunity is well documented, there are limited studies that examined the direct tumor growth inhibitory impact of this molecule. Dotti et al demonstrated that CD40L, when delivered by a non replicative adenovirus may exert dual effects that favor immune activation against human multiple myeloma⁵⁷. The first is through the induction of apoptosis via the CD40L engagement of CD40 on the tumor cells, in turn leading to the presentation of tumor associated antigens in the form of apoptotic bodies to professional APC. The second mechanism, which was independent of CD40 expression on tumor cells was attained through the activation of CD40L

transgene on tumor cells that stimulates CD40+ DCs to increase their maturation and potential to stimulate cytotoxic T lymphocytes (CTL) ⁵⁷.

Alternatively, adenovirus delivered, CD40L caused a rapid reduction in leukemia cell counts in CLL patients, likely to be attributable to apoptotic induction. CLL cells were resistant to Fas (CD95) mediated apoptosis within the first 3 days of CD40L ligation which was shown to be linked to the expression of X-linked inhibitor of apoptosis protein (XIAP) in CLL cells ⁵⁸.

For solid cancers, the apoptotic impact of adenovirus delivered CD40L was demonstrated in a mouse prostate cancer model ⁵⁹. However, tumor growth inhibitory activity of CD40L to be delivered as a transgene by a replicative oncolytic adenovirus in human epithelial cancers has yet to be defined.

Adenoviral Gene Therapy for Breast Cancer

In view of the limited success of currently available treatment strategies for breast cancer, alternative and complementary strategies need to be developed to improve treatment outcome. Recent successes with adenovirus in treatment of various solid tumors suggest that similar strategies are applicable to breast cancer. A barrier in the use of adenovirus as monotherapy for cancer is the relatively low transduction efficiency in vivo. This has been attributed due to the low and variable levels of the Coxsackie adenovirus receptor (CAR) expression on cancer cells that is required for viral entry into the cell. A recent report suggested that aggressive human breast cancers had a higher expression of the adenoviral CAR receptor ⁶⁰, indicating that breast cancer cells may serve as a favorable target for adenoviral gene delivery ⁶¹.

A number of adenoviral gene therapy agents have been developed for breast cancer treatment. The adenoviral early protein E1A can inhibit breast cancer cells via down regulation of Her-neu a well established breast cancer oncogene and was used subsequently in phase I trials for its anti-Her-neu activity⁶²⁻⁶⁵. Similar, approaches that deliver anti-apoptotic, anti-angiogenic and immunomodulatory genes have resulted in anti-tumor responses in vitro, and in mice models⁶⁶⁻⁶⁸.

The incorporation of tumor specific promoters like hypoxia response element, heparanase promoter have been used to regulate viral gene and transgene expression to the breast tumor micro-environment^{69, 70} while sparing toxicity to normal cells. Hypoxia (low oxygen tension) is a common feature of rapidly growing malignant primary and metastatic tumor cells^{71, 72}. The hypoxic state presents a major barrier for effective treatment, since hypoxic cells are resistant to radiotherapy and often to chemotherapy⁷³. However, severe hypoxia is also a unique physiological condition to tumors and potentially exploitable for targeting cancer cells.

The role of hypoxia in aggressive tumors and unresponsiveness to endocrine therapy have been attributed to its ability to reduce hormone responsiveness and degrade estrogen receptors in human breast cancer cells⁷⁴⁻⁷⁶. Hypoxia inducible factor (HIF)-1 α a protein that is stabilized under hypoxic conditions was expressed in the majority of breast cancer patients and linked to poor prognosis⁷⁷⁻⁷⁹. HIF-1 α may also play a role in modulating cell cycle progression and angiogenesis of breast cancer cells^{80, 81}.

In this study we have utilized a hypoxic response element (HRE) to limit the adenoviral replicative activity and CD40L transgene to breast cancer cells. HRE is regulated by HIF-1 α , a protein that is stable in the hypoxic micro-environment⁷². In

view of the presence of estrogen receptor in > 70% of breast cancers⁸² an estrogen response element (ERE) as an additional component to achieve tumor specific gene expression has been incorporated. This facilitates viral activation by the estrogen/estrogen receptor complex⁸³ in regions of the tumor that are not hypoxic.

Rationale for Study

The ability of CD40L to concomitantly impact cell growth and activate the immune system provides an opportunity to combine two potent anti-cancer activities in a single therapeutic maneuver, offering an attractive option for future clinical trials. Previous findings by us and others demonstrated that CD40 ligation by recombinant CD40L produces a direct growth inhibitory effect in breast cancer cells via cell cycle blockage and/or induction of apoptosis. However, administration of recombinant CD40L may elicit pro-inflammatory and autoimmune responses through non specific immune activation that is detrimental to the host. This study utilizes CD40L as a transgene that is integrated into a selective replicative oncolytic adenovirus that incorporates tumor/tissue-specific promoters (hypoxic/HIF-1 α response and estrogen response elements) into the viral backbone to limit the CD40L expression to the tumor micro-environment. This construct is expected to generate a high transgene expression in response to either estrogen or hypoxia that is common in rapidly dividing cancer cells^{71, 84, 85}. We hypothesize that the use of replicative oncolytic adenoviruses to express CD40L may enhance anti-tumor efficacy and overcome some of the drawbacks of limited gene expression when delivered by a non -replicative adenoviruses. The oncolytic activity of

this virus, coupled with tumor cytotoxic activity of the CD40L transgene, is expected to produce an additive or synergistic CD40L response with minimal toxicity to normal cells.

Aim of Study

1. To characterize the conditional replicative activity of the AdEHCD40L adenovirus and the restricted expression of the CD40L.
2. To validate the selective cytotoxic activity of AdEHCD40L in normal and breast cancer lines.
3. To determine the anti-tumorigenic properties of AdEHCD40L and the growth inhibitory outcome of AdEHCD40L on pre-existing breast cancer heterotransplants in SCID mice models.
4. To determine the cellular and molecular mechanisms of cancer growth inhibition of the AdEH delivered CD40L transgene.

CHAPTER TWO

Characterization of the Adenovirus Vectors

The potential of recombinant CD40L to be exploited for treatment of CD40+ human breast cancer cells was previously demonstrated by us and others^{30, 86, 87}. However, the clinical applicability of CD40L experimental therapy may be limited by the short half life of the recombinant protein, and potential risks of inducing non-specific immune activation, autoimmunity^{13, 88}.

Successes of CD40L gene delivery with non-replicative adenovirus in B cell malignancies, like chronic lymphocytic leukemia (CLL), non Hodgkin's lymphoma, and multiple myeloma, suggest that adenoviral delivery of CD40L is a feasible alternative for the administration of CD40L⁸⁹⁻⁹¹.

Recently, oncolytic adenovirus such as Onyx 015, Onyx 411, and CG7870 have been successfully engineered to selectively replicate and lyse cancer cells, either through modifications of viral early genes and/or integration of early viral gene promoters. Unique or up-regulated transcriptional factors have been used to limit viral gene expression and replication to cancer cells⁹²⁻⁹⁴. While these conditional replicative adenoviruses have been tested in prostate, ovarian, and head and neck carcinomas, there were limited data on its efficacy in breast cancer⁹².

Hernandez-Alcoceba et al demonstrated that restricted replication of an oncolytic adenovirus to breast cancer cells can be achieved by utilizing dual tumor and tissue specific promoters⁷⁰. We in collaboration with Hernandez-Alcoceba, are the first

groups to examine the use of a replication competent oncolytic adenoviral backbone for tumor-restricted delivery of CD40L to human breast cancer cells. To attain selective expression of the CD40L transgene, we have cloned the human CD40L cDNA into the AdEH oncolytic virus ⁷⁰. Prevalence of the estrogen receptors on breast cancers ^{95, 96} and low oxygen tension (hypoxia), that is commonly associated with the malignant state ^{84, 97, 98}, provide the positive selection criteria for AdEH early gene E1A and CD40L expression by incorporating estrogen and hypoxic inducible promoters. In addition, the endogenous viral E4 promoter of AdEH has also been replaced by a human E2F dependent promoter, further limiting viral replication to E2F-1 over-expressing cancer cells (Figure 2.1). This transcriptional-targeting approach is expected to optimize viral replication and transgene expression to target (tumors) cells, and limit its expression in normal cells.

This chapter describes the construction, of the CD40L-carrying adenovector, named AdEHCD40L. The immunophenotype of breast cancer and non-malignant human lines were determined prior to their use for determining AdEHCD40L activity. To validate the parameter of conditional CD40L expression, viral genes (E1A) and the CD40L transgene expression was correlated with that of hypoxia inducing factor and/or estrogen in host cells.

Material and Methods

Cell Lines

The human breast carcinoma (T47D, BT20, MDA-MB-231 and ZR-75-1), lung carcinoma (A549) and normal lung (IMR-90) cell lines were obtained from the American

Type Culture Collection (ATCC, Rockville, MD). Human mammary epithelial cells (HMEC) were obtained from Clonetics (Walkersville, MD). The breast cancer cells were cultured in RPMI 1640 (Invitrogen, Carlsbad, CA) with 10% fetal bovine serum (FBS) (Atlanta Biologicals, Lawrenceville, GA). The medium for T47D and ZR-75-1 was supplemented with 9 µg/ml insulin (Invitrogen); ZR-75-1 was additionally supplemented with 2 mM L-glutamine (Invitrogen) and 1 mM sodium pyruvate (Invitrogen). MDA-MB-231 was supplemented with 2 mM L-glutamine (Invitrogen) and 1 mM sodium pyruvate (Invitrogen). Experiments were performed in phenol red free RPMI 1640 (Invitrogen) and 2% charcoal dextran treated FBS (Hyclone, Logan, UT). For studies involving evaluation of the estrogen response element (ERE) promoter regulation, cells had to be pre-treated for 14 hours with 2 nM estradiol. A549 cells used for viral expansion and titer determination by plaque assay were cultured in 1X Dulbecco's modified Eagles Media (DMEM) (Invitrogen) with 10% FBS. IMR-90 was cultured in minimum essential media with 2 mM L-glutamine, 1 mM sodium pyruvate and 10% FBS while HMEC was cultured in mammary epithelial growth media (Clonetics).

Cloning of Recombinant Adenovirus

The conditional expressing adenovector has been generated in collaboration with Dr. M. Clarke (University of Michigan Medical Center) and explained in detail in appendix A. As starting material, the pSEHE2F plasmid was used (Hernández Alcoceba et al. Human Gene Therapy 2002; 13: 1737-1750). The genome of adenovirus was modified in order to include the following features (Figure 2.1):

1. Deletion of the endogenous E1A promoter and substitution by the 5XEH3 promoter

2. Deletion of the endogenous E4 promoter and substitution by the E2F-1 promoter
3. Introduction of an insulator sequence (bovine growth hormone transcriptional stop signal) between the packaging signal and the E1A promoter.
4. Deletion of the genes encoding the glycoprotein (gp) 19K/6.7K proteins in the E3 region, and substitution with the CD40L complementary deoxyribonucleic acid (cDNA). This location allows the transcriptional control of the transgene by the endogenous adenoviral late promoter, which is active once the viral replication has initiated (Hawkins et al, 2001. Gene Ther. 8: 1123-31).

Purification, titration and validation of the genomic configuration of AdEHCD40L have been described in Appendix B.

CD40L and E1A Expression by Flow Cytometry

To identify C40L and E1A proteins, cells were seeded at 5×10^5 cells/well in RPMI 1640 (without phenol red) + 2% charcoal dextran treated FBS with appropriate supplements, and allowed to adhere overnight. Infection with AdEHCD40L or control virus was done at a multiplicity of infection (MOI) of one in 2 mls of infectious volume, in the presence or absence of 25 μ M CoCl₂. The cultures were incubated for 90 minutes (37°C, 5% CO₂) after which time the volume was brought up to 4 mls to attain a final CoCl₂ concentration of 25 μ M. Cells were maintained at 37°C, 5% CO₂ and harvested at graded time points to determine the expression of E1A or CD40L.

For CD40L staining, single cell suspension obtained after trypsinization was treated with phycoerythrin (PE) conjugated, mouse anti-human CD40L antibody or an isotypic antibody control (IgG1-PE) (both from BD pharmingen, San Jose, CA) and

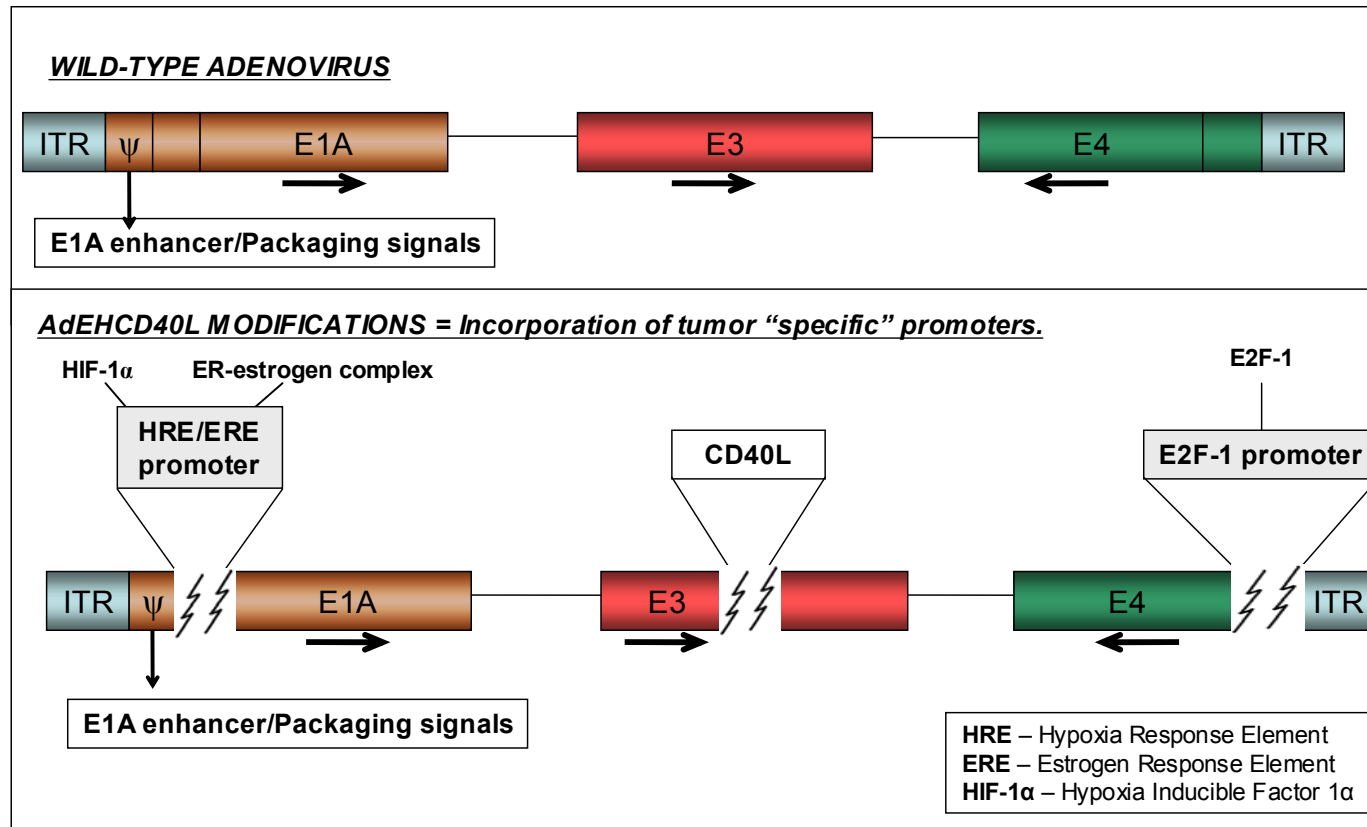


Figure 2.1: Schematic Representation of Genetic Modifications in AdEHCD40L. The 800bp CD40L transgene cassette was inserted in the E3 region of the adenovirus. The E1A promoter was deleted and substituted by an estrogen response element (ERE) and a hypoxia response element (HRE). The wild type E4 promoter region has been substituted by an E2F-1 promoter.

incubated at room temperature for 30 minutes in the dark. The cells were washed twice with 1X PBS containing 0.1% sodium azide and 1% bovine serum albumin (BSA).

For E1A staining, single cell suspension was treated with a permeabilizing reagent (Fix and Perm cell permeabilization kit, Invitrogen Diagnostics, Carlsbad, CA) and PBS (PBS + 1% BSA + 0.1% sodium azide), vortexed and incubated for 15 minutes at room temperature. The permeabilized cells were washed once (300 g, 10 minutes), then resuspended with PBS, reagent B (permeabilization reagent kit, Invitrogen) and stained with either a mouse anti E1A antibody (10 µg/ml) or IgG2a isotypic control antibody (10 µg/ml) (BD pharmingen, San Jose, CA). Washed cells were stained with goat anti-mouse fluorescein isothiocyanate (FITC) conjugated secondary antibody (10 µg/ml) (BD pharmingen) in PBS, incubated for 20 minutes in the dark and then washed twice with PBS containing 0.1% sodium azide and 1 % BSA (300 g, 10 minutes).

Appropriately stained cells were fixed in 500 µl of 1% paraformaldehyde, and analyzed by flow cytometry (Becton Dickinson FACScan, San Jose, CA) with a laser excitation wavelength of 515 nm for fluorescein isothiocyanate (FITC), and 585 nm for phycoerythrin (PE). The frequency of CD40L and E1A positive cells was determined by analysis of 5,000 events using the CELLQuest software (Becton Dickinson).

Immunoblotting Analysis for E2F-1 and HIF-1 α Protein

Immunoblot analysis was carried out to evaluate the expression of E2F-1 and hypoxia inducible factor (HIF)-1 α that can potentially activate the E2F-1 promoter and hypoxia response element (HRE) promoters inserted in AdEH derived viral constructs. Cells (1×10^7) at logarithmic growth phase were incubated with media alone, or CoCl₂

(25 μ M) for 24 hours to achieve a hypoxic state. Total cell protein was extracted and western blot performed as previously described³⁰. Briefly, cells were treated with proteinase inhibitors, protein concentration determined by Coomassie blue (Pierce, Rockford, IL) spectrophotometry (Spectramax 340 System; Molecular Devices, Sunnyvale, CA). Fifty μ g of the protein extract was mixed at 1:2 with electrophoresis sample buffer (Biorad, Hercules, CA), boiled at 95°C for 5 minutes, loaded onto a 7.5% Tris-HCl gel (Biorad) and electrophoresed. The samples were transblotted to a Polyvinylidene difluoride (PVDF) membrane that was briefly soaked in 100% methanol and equilibrated with transfer buffer. Protein transfer was performed at 50 V (120 minutes at 4°C). Membranes were blocked with 5% non-fat milk in 1X PBS. Each sample was treated with a mouse anti-human E2F-1 at a 1:100 dilution (BD pharmingen, Carlsbad, CA) or HIF-1 α (1:250, BD pharmingen, Carlsbad, CA) primary antibody (1 hour), followed by incubation with a goat anti-mouse IgG horseradish peroxidase (HRP) conjugated secondary antibody at a dilution of 1:2000 (Santa Cruz biotechnology, Santa Cruz, CA) for 1 hour, with appropriate washings (1X PBS, 0.1% Tween 20). The reaction was developed by enhanced chemiluminescence (ECL plus detection kit, GE healthcare, Piscataway, NJ) as per manufacturer's specifications, and visualized by autoradiography using Kodak scientific imaging film (Perkin Elmer, Wellesley, MA). For a protein loading reference, membranes were stripped and re-probed with β -actin using mouse anti-human antibody at a dilution of 1:100 (Santa Cruz biotechnology, Santa Cruz, CA) and developed as above. Bands were quantified by densitometric analysis using the Alphamanager 2000D and Scion Image Software.

Viability Mitochondrial Assays

MTT (3-[4, 5 dimethylthiazol-2-yl)-2, 5 diphenyltetrazolium bromide]) assay is based on the quantification of mitochondrial activity as a function of cell viability. The reduction of MTT by metabolically active cells to insoluble purple formazan dye crystals can be solubilized and determined spectrophotometrically. At varying time intervals T47D cells (1×10^5 cells/ml; 100 μ l) cells were treated with MTT (R&D Systems, Minneapolis, MN) for 2 hours (37°C, 5% CO₂). The formazan crystals were solubilized with detergent (overnight, room temperature, dark) and quantified spectrophotometrically at 570 nm with 690 nm as reference wavelength (SpectraMax 340, Molecular Device). Percentage viability was calculated as % of untreated cells based on an average of triplicate absorbance values obtained for each treatment group.

Formulae: % Viability = (Treated/Untreated) x 100

Results

Immunophenotyping of Breast Cancer and Normal Cell Lines

Previous studies showed that > 90% of primary breast cancer tumors expressed CD40^{30, 99}. To develop in vitro breast cancer models appropriate for the characterization of CD40L-based therapy, we examined the surface distribution of CD40 on a panel of breast cancer and normal cell lines (Table 2.1). A high frequency of CD40 expression (> 95%) was observed in the T47D, MDA-MB-231 and BT20 breast cancer lines based on flow cytometric immunofluorescence analysis. In comparison, ZR-75-1 and MCF-7 breast cancer lines lacked CD40 expression (< 1% of CD40 positive cells) when compared to the positive control cell line (Daudi; > 95%). We also evaluated CD40

Table 2.1: Immunophenotype analysis of cancer and normal cell lines.

Cell Lines (Histology)	Expression (% Positive cells)	
	CD40	CD40L
<u>Breast cancer Lines</u>		
T47D (Ductal carcinoma)	++++ (96.6 \pm 2.3 %)	- (< 2 %)
BT-20 (Adenocarcinoma)	++++ (97.9 %)	- (< 1 %)
MDA-MB-231 (Adenocarcinoma)	++++ (93.81%)	- (< 1 %)
ZR-75-1 (Ductal carcinoma)	- (< 1 %)	- (< 1 %)
MCF-7 (Adenocarcinoma)	- (< 1 %)	- (< 1 %)
<u>Normal Lines</u>		
IMR-90 (lung fibroblast)	+ (5.0 \pm 1.1 %)	+ (12.0 \pm 12.8 %)
HMEC (breast epithelium)	- (< 3 %)	- (< 1 %)

The % reactivity cells were determined by direct immunofluorescence technique designated as ++++ (75 – 100 %), +++ (50 - 74.9 %), ++ (25 - 49.9 %), + (5 - 24.9 %) or - (< 5 %). CD40L-L cells and L cells were used as positive and negative control lines for CD40L detection. Daudi and L cells were used as positive and negative control lines for CD40 expression.

expression in normal breast epithelial cell line (HMEC) and normal lung fibroblast line (IMR-90). Expression levels in normal cell lines ranged from low (5.0 \pm 1.3%) for IMR-90 lung fibroblast line to negative (< 2.5%) for the HMEC breast epithelial line. Endogenous CD40L was expressed in low frequency (< 5%) in all breast cancer lines evaluated compared with > 95% of CD40L-positive cells in control CD40L- transfected

mouse fibroblast L cells ³⁰. Interestingly, one of two normal cell lines expressed low endogenous CD40L (IMR-90: $12 \pm 12.8\%$) (IMR90).

To determine if the cell lines expressed endogenous transcription factors that facilitate viral gene expression, we measured endogenous E2F-1 and HIF-1 α protein levels by immunoblot analysis. T47D and ZR-75-1 breast cancer cells expressed a high (+ / +++) endogenous level of HIF-1 α . With the exception of MCF-7, treatment with cobalt chloride (CoCl₂) (25 μ M, 24 hours) enhanced HIF-1 α levels in all breast cancer lines (T47D, BT-20, ZR-75-1) as well as the normal cell line (IMR-90) tested (Table 2.2). Hence, the treatment with CoCl₂ was used in our study to promote an HIF-1 α positive, viral permissive state.

Cellular E2F-1 potentially impacts viral gene expression through the activation of E2F-1 promoter incorporated in the E4 region. Western blot analysis showed that E2F-1 was over-expressed in all breast cancer cell lines tested. By comparison, E2F-1 expression was lower in the normal cells evaluated (Table 2.2), hence validating the premise that E2F-1 over expression is a common feature among malignant cells ^{100, 101} and appropriate as a conditional promoter for the viral permissive state. Subsequent studies were carried out with the T47D, MDA-MB-231, BT20 and ZR-75-1 breast cancer lines. These lines were selected on the basis of high CD40 expression, low CD40L expression, and an HIF-1 α ⁺ phenotype following hypoxic induction by CoCl₂. In accordance to their HIF-1 α ⁻ and E2F-1⁻ phenotype, the non-malignant IMR-90 cells were chosen as a negative control to define replicative selectivity and cytotoxicity.

Table 2.2: Immunophenotype of cancer and normal cell lines for viral permissive conditions.

Cell lines (Histology)	HIF-1 α expression			E2F-1 expression
	Status	No CoCl ₂	+ CoCl ₂	
<u>Breast cancer Lines</u>				
T47D (Ductal Carinoma)	Constitutive-Inducible	+++	++++	++++
ZR-75-1 (Ductal Carcinoma)	Inducible	+ / -	+ / ++	++++
BT20 (Adenocarcinoma)	Inducible	-	+	++++
MCF-7 (Adenocarcinoma)	Non Inducible	-	-	+
MDA-MB-231 (Adenocarcinoma)	ND	ND	ND	ND
<u>Normal Lines</u>				
IMR-90 (Lung fibroblast)	Inducible	-	+	-
HMEC (Mammary epithelial)	ND	ND	ND	ND

HIF-1 α and E2F-1 expression was determined by immunoblot analysis. Band intensities were normalized to β actin and designated as – (0-0.07), + (0.071-0.2), ++ (0.21-0.5), +++ (0.51-0.8), ++++ (>0.8), ND (not determined). Cells lines were defined as constitutive-inducible (endogenous HIF-1 α /increased HIF-1 α with CoCl₂), inducible (no endogenous HIF-1 α /increased HIF-1 α with CoCl₂) or non inducible (no endogenous HIF-1 α /no increase with CoCl₂) according to capacity to respond to CoCl₂ by HIF-1 α up-regulation.

ND: Not Determined

Transgene Expression in Breast Cancer Cell Lines Following Infection with Recombinant Adenovector (AdEHCD40L)

To compare adenoviral infectivity in various breast cancer lines, the level of early viral gene (E1A) expression was determined following treatment with the wild type adenovirus [multiplicity of infection (MOI) =1]. All breast cancer cells lines tested were

susceptible to adenoviral infection. $49.4 \pm 7.7\%$ of T47D cells and $44.7 \pm 7.4\%$ of MCF-7 cells expressed viral E1A, as compared with $38.8 \pm 4.9\%$ in ZR-75-1 and $23.9 \pm 12.5\%$ in BT-20 lines (Figure 2.2). Further, CD40L protein expression following infection with AdEHCD40L was determined in the viral permissive CD40⁺ (T47D) and CD40⁻ (ZR-751) breast cancer cells. 24% of T47D cells expressed CD40L following infection of MOI=1 up to MOI=10. There was an increase in CD40L expression following infection at the higher MOI of 50 (35.5%) or 100 (54.1%) (Figure 2.3A). Similarly, CD40L expression was observed in AdEHCD40L-infected ZR-75-1 cells, with a maximal expression of 85% of all cells at an MOI of 50 (Figure 2.3B). Peak level of CD40L transgene expression was observed on day 2 and sustained through day 4 post-infection (Figure 2.4). For ZR-75-1, a marked decrease in the % of CD40L⁺ cells was observed after 4 days post infection at an MOI ≥ 1 (Figure 2.4), which may reflect a selective loss of the virally infected subset from viral replication. These findings indicate that CD40L transgene expression is directly correlated with the infecting viral dose, with expression being maintained for up to 4 days in viral infected cells.

Effect of Cobalt Chloride on Viability and/or Transgene Expression of Breast Cancer Cells

The administration of cobalt chloride (CoCl₂) is a common approach for sustaining a hypoxic state in vitro, through prolongation of the half life of the transcription factor HIF-1 α ¹⁰². Hence, treatment with CoCl₂ allows us to achieve and/or optimize AdEHCD40L infectivity in vitro. The inducibility and regulation of the CD40L transgene expression was evaluated in breast cancer lines that were found to express low,

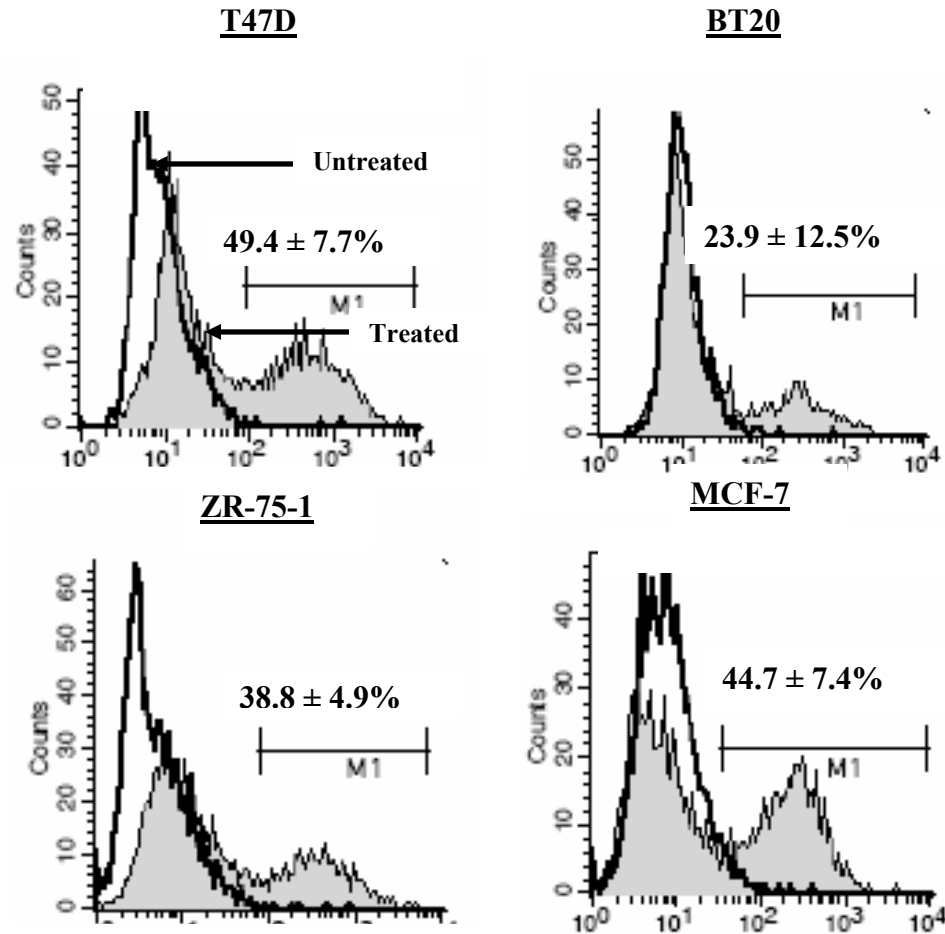


Figure 2.2: Viral E1A expression in breast cancer cells. Adv-WT (MOI=1) infected cells were evaluated at 48 hours post infection for viral E1A expression. Histogram plots represent average \pm SD from 3 separate experiments and represent treated cultures (grey) superimposed on untreated cultures (white)

constitutive (T47D, ZR-75-1) or no (BT-20, MCF-7) HIF-1 α expression. T47D displayed significantly increased CD40L expression with up-regulated HIF-1 α (T47D: 65.5 \pm 3.9% with increased HIF-1 α vs. 38.5 \pm 2.8 % under uninduced conditions, p = 0.007). Similarly ZR-75-1 (74.63 \pm 1.49% vs. 50.2 \pm 2.5%; p = 0.0001), BT20

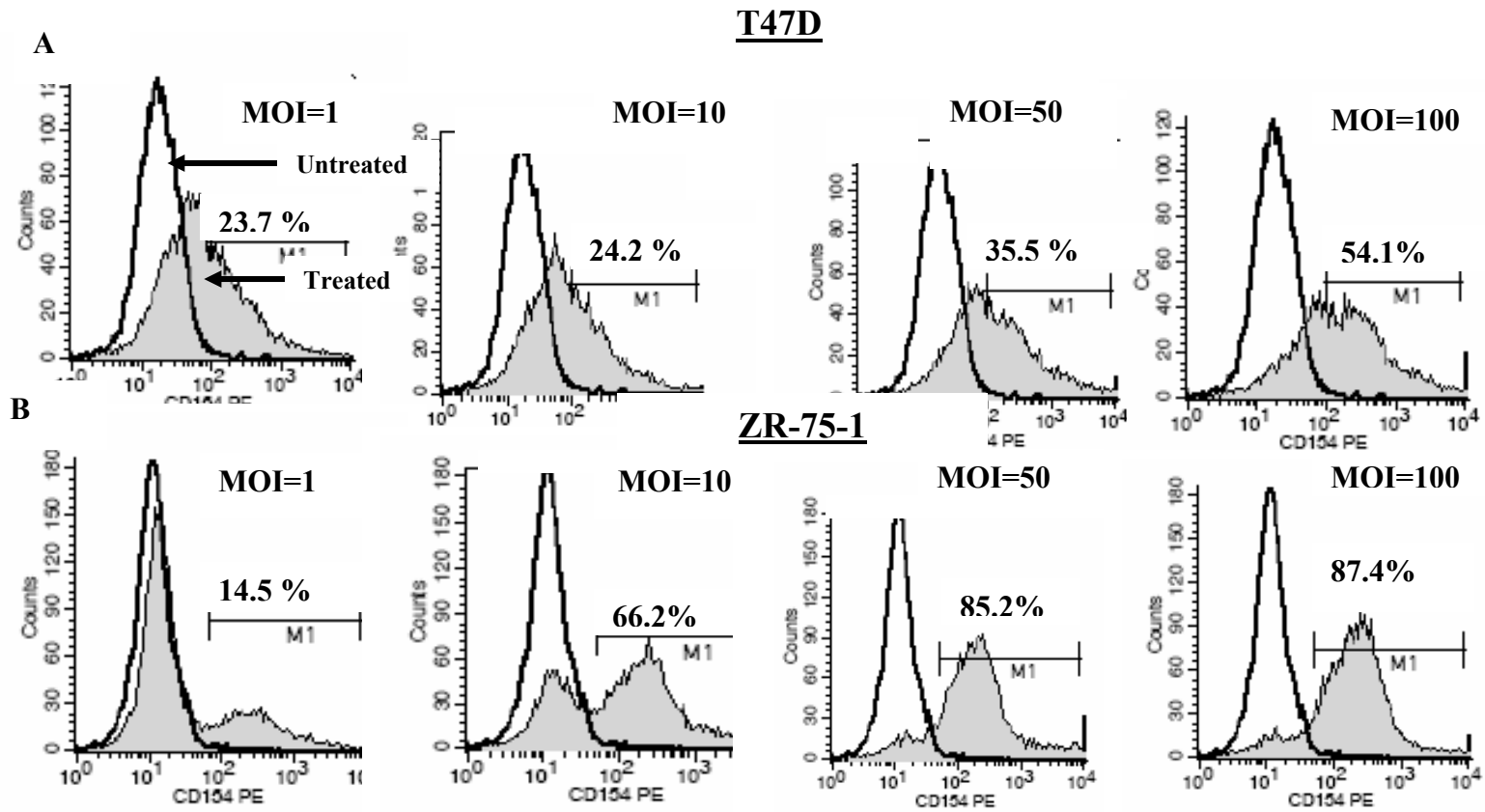


Figure 2.3: Flow cytometric analysis of CD40L protein following AdEHCD40L infection. T47D (A) and ZR-75-1 (B) AdEHCD40L (MOI=1-50) infected cultures were evaluated for CD40L protein following 72 Hrs post infection under non inducing conditions. Histogram plots represent treated cultures (grey) superimposed on untreated cultures (white).

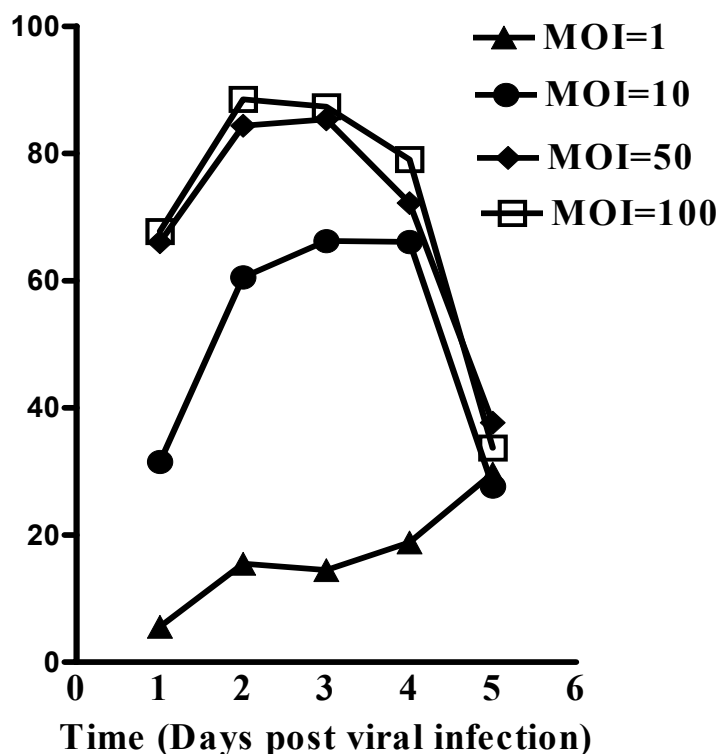


Figure 2.4: CD40L transgene expression in ZR-75-1 breast cancer cells. CD40L (CD154) transgene expression in AdEHCD40L (MOI=1) infected ZR-75-1 cells under non inducing conditions.

($43.2 \pm 14.9\%$ vs. $10.6 \pm 0.2\%$; $p = 0.03$) and MCF-7 ($23.5 \pm 1.76\%$ vs. $16.6 \pm 1.5\%$; $p = 0.003$) showed an increase in CD40L expression with increased HIF-1 α (Figure 2.5), illustrating a dependence of hypoxia for transgene expression. Further, studies were performed to characterize the impact of CoCl₂ and estradiol treatments on host cell viability using the (MTT) assay. MTT assay quantifies mitochondrial metabolic activity as a function of cell viability with a direct relationship between the absorbance and viability. The lowest effective concentration of CoCl₂ (25 μ M) produced an acceptable cytotoxicity of $< 15\%$ (Figure 2.6). Collectively, these findings indicate that CoCl₂

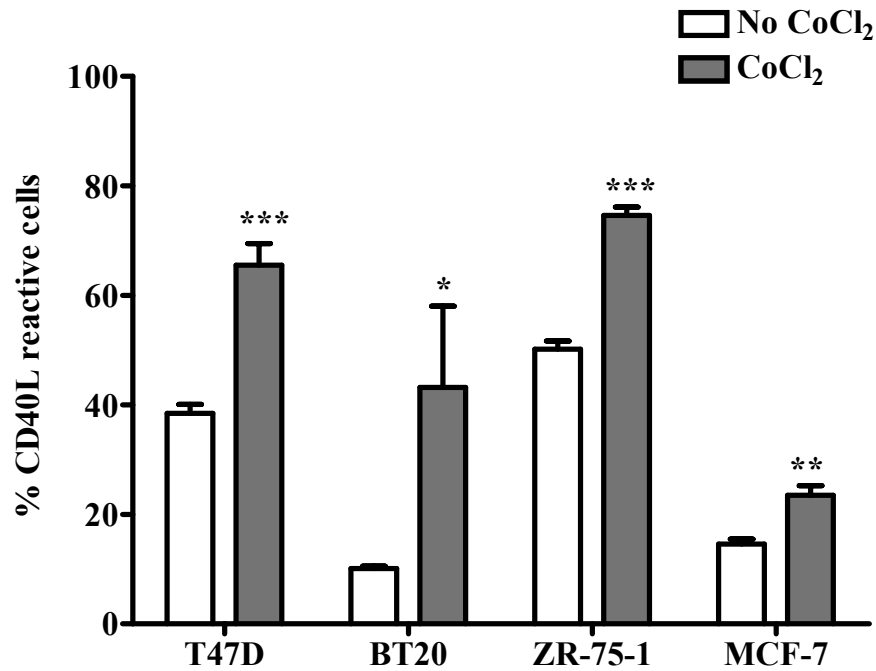


Figure 2.5: CD40L transgene expression in cancer cells on CoCl₂ induction. CD40L expression was evaluated in the presence and absence of CoCl₂ induction at 48 hours post infection. T47D, BT20, ZR-75-1 and MCF-7 breast cancer cells showed increased CD40L expression on induction. Mean \pm SD are based on 3 separate experiments. Statistical analysis was carried out using a 2 tailed t-test * $p < 0.05$; ** $p < 0.005$; *** $p < 0.0005$.

(25 μ M) can be used to induce a viral permissive state via stabilization or induction HIF-1 α protein expression¹⁰². This results in the up-regulation of the CD40L transgene indicating that the CD40L transgene expression can be modulated through HIF-1 α induction by CoCl₂ treatment.

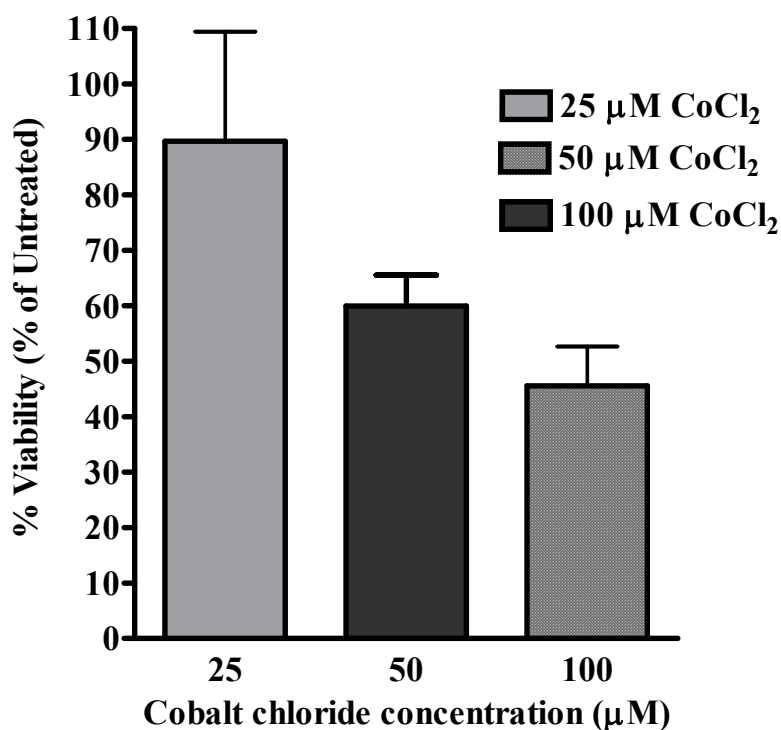
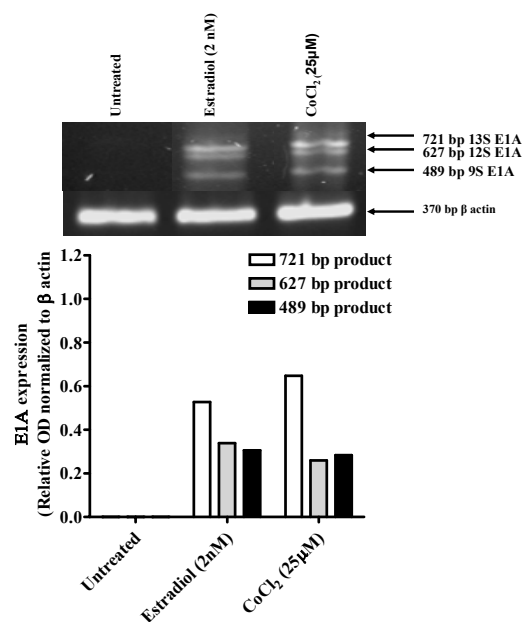


Figure 2.6: Effect of cobalt chloride on cell viability. Effect of cobalt chloride on cell viability of T47D cells was evaluated by MTT assay (24 hours). Values represent absorbance values (mean \pm SD) from 3 separate experiments.

Hypoxic Response Element is a More Potent Regulator of Viral Gene and Transgene Expression than the Estrogen Response Element

Both the hypoxic response element and estrogen response element are incorporated as promoter elements in the AdEH construct. We examined their relative effectiveness in regulating viral early gene E1A and CD40L transgene expression in AdEH infected cancer lines. Based on RT-PCR reactions using sequence specific primers, the CD40L message produced an amplification product of 683 bp. The E1A mRNA is expected to produce 3 amplification products of molecular sizes 489 bp, 627 bp

A



B

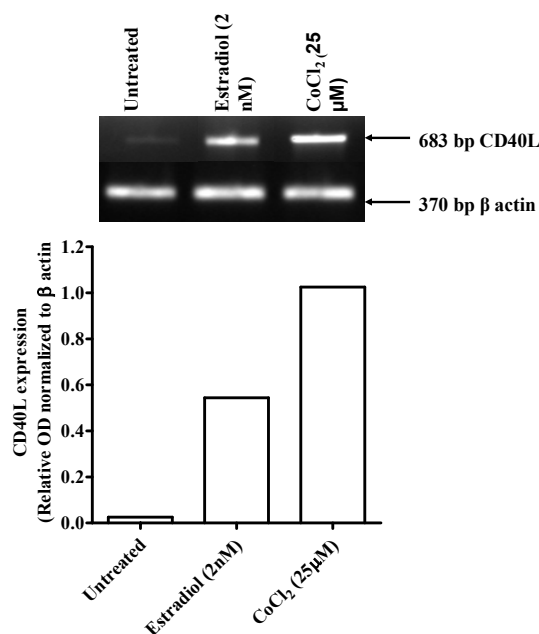


Figure 2.7: RT-PCR for viral E1A and CD40L. E1A (A) and CD40L (B) mRNA expression in ZR-75-1 breast cancer lines was validated under treatment with CoCl_2 or estradiol 12 hrs post AdEHCD40L treatment. β actin (370 bp) expression was determined as an internal reference control for the reaction, while deionized water was used as a negative control. Values represent absorbance values of band intensities normalized to β actin.

and 721 bp corresponding to differential spliced variants 13S, 12S, and 9S¹⁰³. E1A and CD40L transcripts were quantified by densitometric gel band analysis and were normalized to the β -actin amplification product which served as an internal control. Viral E1A and the CD40L mRNA transcripts were up-regulated in AdEHCD40L infected ZR-75-1 cell cultures by either estradiol or CoCl₂ treatment (Figure 2.7). Band intensities for CD40L was greater in the CoCl₂ treated (untreated: 0.03 vs. 1.03; 40.6 fold increase) compared to the estradiol treated cultures (untreated: 0.03 vs. 0.5; 21.5 fold increase) (Figure 2.7). These findings indicate that hypoxia induction by CoCl₂ is a more potent inducer of AdEH viral gene and CD40L transgene expression than estradiol, and is used for all further evaluations.

Discussion

CD40L has shown promise as a therapeutic agent for the treatment of various solid and hematological malignancies^{30, 32, 104}. Its anti-tumor activity in breast cancer was demonstrated in human xenografts models by us and others^{30, 86}. In this study, we have examined CD40L expression following delivery as a transgene in breast epithelial cancer cell lines. The human cDNA of CD40L has been cloned into an oncolytic adenovirus AdEH in order to deliver CD40L as a gene therapy agent. AdEH was previously shown to have selective oncolytic activity in breast HIF-1 α expressing cancer cells that over-express ER⁷⁰, hence demonstrating its applicability as a gene delivery agent that restricts viral replication and gene expression by transcriptional targeting. By cloning the human CD40L cDNA into the viral E3 region, transgene expression was governed by the endogenous late viral promoter, which was co-ordinately activated with viral replication

⁵¹. In addition, the E4 promoter of AdEHCD40L has been replaced by the E2F promoter which attenuates viral replication in E2F-1 deficient normal cells ¹⁰⁵. A panel of breast cancer and normal cell lines were evaluated for the expression of CD40, CD40L, and viral permissive conditions (HIF-1 α , E2F-1). Some cell lines expressed high endogenous levels of HIF-1 α (T47D and ZR-75-1). The insulin dependent requirement of these lines may account for their endogenous HIF-1 α activity, since HIF-1 is stabilized by insulin ¹⁰⁶⁻¹⁰⁸.

The CD40L mRNA and protein expression was regulated by hypoxia induction. However in MCF-7, while the HIF-1 α protein was not detected with CoCl₂ induction, we were still able to observe a small but significant up regulation of CD40L. This might be explained in part by the fact that HIF-1 α protein is rapidly degraded under normoxic conditions and short half life of the protein ¹⁰⁹⁻¹¹¹. Alternatively, in this particular cell line HIF-1 α may not be a determinant for viral permissive conditions. For ZR-75-1 cells, the viral permissive state of AdEH is dependent more on the hypoxic content (HIF-1 α) whereas estradiol modulation is relatively ineffective. These findings indicate that HRE is appropriate as a breast “specific” promoter for AdEH, since hypoxia is a common physiological feature of breast tumors and has been associated with aggressive diseases and pro-angiogenic activity ^{84, 98}.

In this study, we used CoCl₂ as an agent used to induce HIF-1 α ¹⁰². Effects of CoCl₂ treatment alone on cellular toxicity have been reported, although this phenomenon appeared to dependent on the host cell type. The induction of cell death was observed in mouse embryonic fibroblast and human cervical cancer (HeLa) cells, the same treatment resulted in survival and resistance to apoptosis in HepG2 cells ¹¹²⁻¹¹⁵. We observed a low

($\leq 15\%$) level of toxicity at the concentration of $\leq 25 \mu\text{M}$ CoCl_2 , which did not impact our experimental interpretations, hence allowing its use for HIF-1 α protein induction to achieve a viral permissive state in vitro.

In conclusion, we were able to show that the AdEHCD40L could selectively deliver CD40L to HIF-1 α expressing breast cancer cell lines, and hence an appropriate delivery agent for CD40L based gene therapy. The growth regulatory activity of AdEHCD40L was further examined in the next chapter.

CHAPTER THREE

Growth Regulatory Activities of AdEHCD40L

Non-replicative adenoviruses have been used to deliver CD40L to chronic lymphocytic leukemia and multiple myeloma cells and shown to enhance anti-tumor responses. Growth inhibition was achieved through immune activation and an increased sensitivity to Fas mediated apoptosis¹⁰⁴. By comparison, the growth regulatory impact of adenoviral delivery of CD40L remains unexplored in epithelial cancers. In this study, we have utilized the selective oncolytic adenovirus AdEH to deliver CD40L as a transgene. As described in chapter 2, oncolytic viruses are engineered to limit replication to cancer cells with defined genetic defects. Transgenes inserted into the viral early E1, E3 regions are expected to manifest their growth regulatory activity prior to the replicative process¹¹⁶⁻¹¹⁸. In addition, host cells are susceptible to the viral oncolytic process that also leads to the propagation of progeny to neighboring tumor cells, repeating the killing cycle. We hypothesize that the conditional expression of the CD40L transgene restricts its activity to the tumor micro-environment, thereby limiting the CD40L regulatory signal to cancer cells. Further, amplification of the initial viral input dose and sustained transgene expression through viral replication enhances the overall efficacy of the adenoviral gene delivery vector. Following the demonstration of selective viral and CD40L transgene expression in breast cancer cells (Chapter 2), we have determined the role of CD40L transgene expression in mediating growth inhibition.

This chapter describes our in vitro findings with CD40+ and CD40- breast cancer lines, based on comparative analysis with AdEHCD40L and AdEHNull, a non CD40L carrying AdEH construct.

Material and Methods

Cell lines and media have been previously described in chapter 2 in the material and methods section.

Viability Mitochondrial Assays

Cells in the logarithmic phase were inoculated in 96 well plates (BT20, T47D, ZR-75-1: 1×10^5 cells/ml; 100 μ l; MDA-MB-231: 5×10^5 cells/ml; 100 μ l) in their respective media. Cells were infected with either AdEHCD40L or control vectors (AdEHNull or Adv-WT) (MOI=1-100) in the presence/ absence of hypoxia (25 μ M). At varying time intervals cells were treated with MTT (R&D Systems, Minneapolis, MN) and % viability calculated as previously described in chapter 2 in the material and methods section.

Crystal Violet Staining for Cytopathic Toxicity

The adherent and viable population of cells can be stained by crystal violet staining and quantitated spectrophotometrically. Cancer cells (1×10^5 cells/ml; 100 μ l) in the logarithmic phase were inoculated in 96 well plates their respective supplements and incubated for 14 hours at 37°C, 5% CO₂ incubator. However to ensure the normal cells were quiescent they were plated to confluence (5×10^5 cells/ml; 100 μ l) in their

respective media. Cells were infected at an MOI=1 in the presence or absence of CoCl₂ (25 µM). Percentage viability was calculated as % of untreated cells based on an average of triplicate absorbance values obtained for each treatment group.

Viral Replication by Quantitative PCR

To determine the viral replicative activity and yield of infected cell cultures, 1 x 10⁵ cells/well were infected at an MOI=1. Cells and culture supernatants were collected separately immediately after infection (day 0) and at different time points post infection for 5 days. Total nucleic acids was extracted from 200 µl of culture supernatant or cell pellet resuspended in 200 µl distilled water using the QIAmp DNA blood kit (Qiagen, Valencia CA, USA). Purified deoxyribonucleic acid (DNA) was eluted in 50 µl with nuclease free water. Quantitative polymerase chain reaction (PCR) was performed as described by Gu et al ¹¹⁹ using the TaqMan® Universal PCR Master Mix (Applied Biosystems, Foster City, CA). Briefly 5 µl of sample was added to a 45 µl of PCR mix containing 1X PCR buffer, 25 mM MgCl₂, deoxynucleosides (10 mM A, 10 mM G, 10 mM C, 20 mM T), 10 pmol/µl of sense primer (5' GCTGGCGCAGAAGTATTCCA 3') and 10 pmol/µl of anti-sense primer (5' GTGCGGGTCTCATCGTACCT 3') (Sigma Aldrich, St Louis, MO) and 5 U/µl of Taq polymerase (Applied Biosystems). Reactions were run in duplicates or triplicates. The reactions were thermal cycled using the following conditions: 95°C, 5 minutes; 43 amplification rounds cycling between 95°C, 30 seconds, 60°C, 60 seconds on the ABI icycler (Biorad, Hercules, CA). Viral copies above a threshold cycle of 100 at a point in the exponential phase of amplification were taken for analysis and quantitated against a standard adenovirus reference (gene back

nucleotide number AY339865 (ATCC, Rockville, MD) serially diluted to obtain a range of 5×10^1 to 5×10^6 copies. The maximum sensitivity of the assay was 50 copies of adenoviral hexon, based on the fluorescent signal with probe labeled at the 5' end with 6-carboxytetramethylrhodamine (FAM) as the reporter dye and the 3' end labeled with 6-carboxyfluorescein (TAMRA) as the quencher (5'(6-FaM) ACCTTCCAGATCCGTCGA CCTGCA (Tamra) 3'). Samples that had less than 50 copies in the 25 μ l assay were considered negative for adenovirus hexon. Negative controls that contained only water was used to check for DNA contamination and had a threshold cycle of 100.

Soluble CD40L by ELISA

To determine the soluble CD40L in the culture supernatants of AdEHCD40L infected T47D cultures, supernatants were centrifuged at 300 g to remove cell debris. Soluble CD40L was detected by the high sensitivity human soluble CD40L ELISA kit (Bender Medsystems Inc, Burlingame, CA). Each sample was tested in triplicates according to the manufacturer's protocol. Briefly, 100 μ l of culture supernatant was mixed with 100 μ l of HRP-conjugated CD40L monoclonal antibody (MAb) (1:200 diluted according to the manufacturer's protocol). 150 μ l of the reaction mixture was transferred to a micro-well coated with CD40L MAb. The reactions were carried out on an orbital shaker (100 rpm, 2 hours, 25°C) with appropriate washing in between. 100 μ l of the substrate tetramethyl-benzidine (TMB) was added and the reaction carried out at 100 rpm for 25 minutes, 25°C with gentle shaking. The reactions were stopped by adding 100 μ l of stop solution and quantified by measuring the absorbance at 450 nm with a spectrophotometer (SPECTRAmax 340, Molecular devices corporation, Sunnyvale, CA).

The concentration of soluble CD40L was extrapolated from a standard curve. The standard curve was based on serially dilutions of a recombinant CD40L provided by the manufacturer ranging from 0.08 – 5 ng/ml.

Results

Growth Inhibitory Activity of AdEHCD40L

The anti-tumor activity of AdEHCD40L was evaluated in three CD40 positive breast cancer lines, T47D, BT20, MDA-MB-231, and a CD40 negative control cell line ZR-75-1 under viral permissive conditions by the MTT assay. To determine if the growth inhibitory responses with AdEHCD40L were attributed to the CD40L transgene or viral replication, a similar viral construct that lacks the CD40L transgene (AdEHNull) was used as control. AdEHCD40L (MOI = 1) produced markedly higher inhibition at 96 hours as compared to the AdEHNull construct in CD40+ cell lines (T47D: $58.4 \pm 5.0\%$ vs. $43.4 \pm 2.3\%$, $p < 0.05$; BT20: $41.5 \pm 3.3\%$ vs. $22.3 \pm 2.0\%$, $p < 0.05$; MDA-MB-231: $49.1 \pm 7.5\%$ vs. $28.1 \pm 4.6\%$, $p < 0.05$) (Figure 3.1). This enhanced anti-tumor response between the AdEHCD40L and AdEHNull was extended up to 144 hours. In contrast, the differential response between AdEHNull and AdEHCD40L was not observed in the CD40 negative line ZR-75-1, suggesting that viral oncolysis and CD40L-produced an additive growth inhibitory effect only in CD40+ cells.

Effective viral dose (ED_{50}), the viral dose that produced a 50% growth inhibition, was used as a reference to compare viral potency of each cell line. The ED_{50}

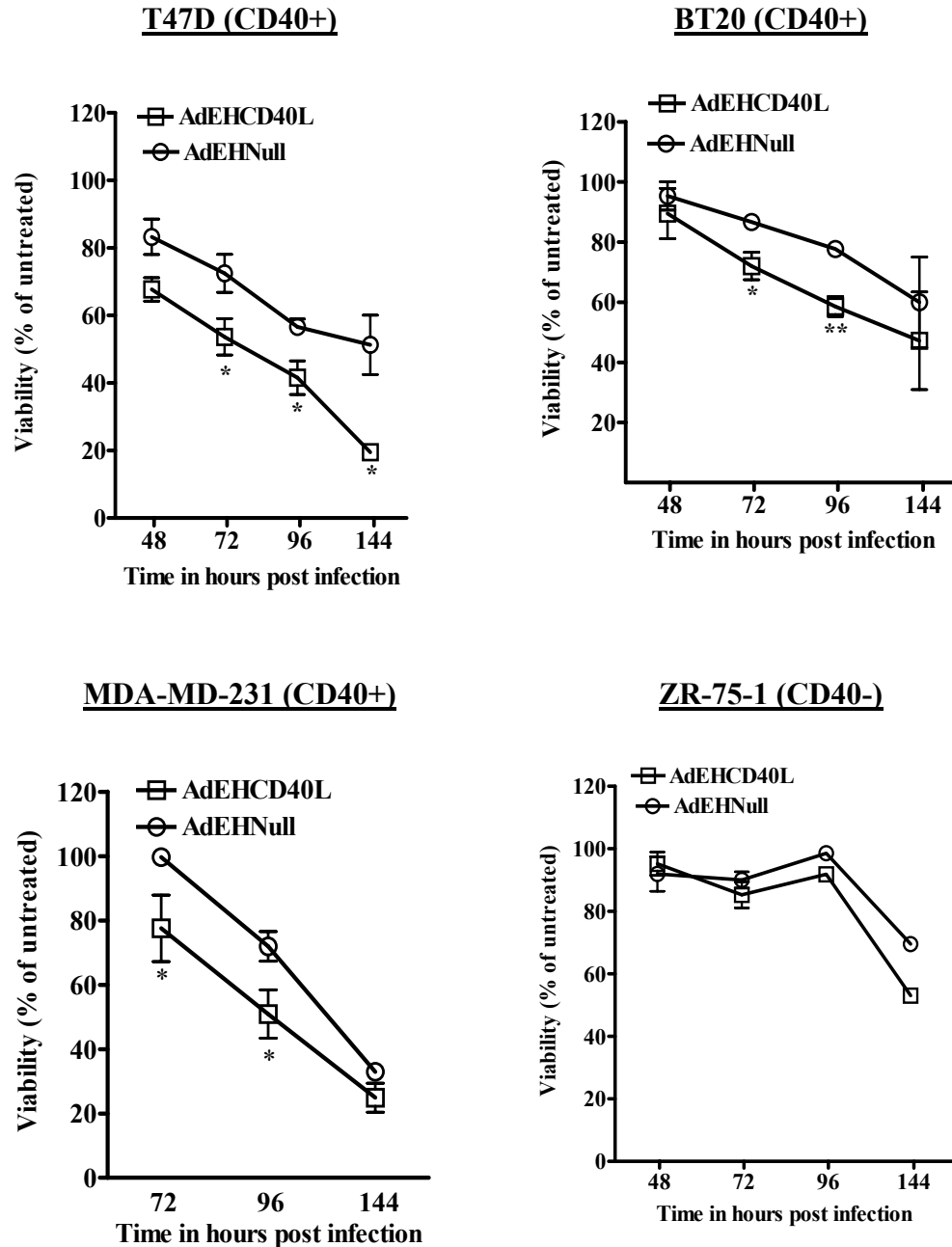


Figure 3.1: Time dependent growth regulatory outcome of AdEHCD40L. T47D, BT20, MDA-MB-231 and ZR-75-1 cells were infected with AdEHCD40L or AdEHNull (MOI=1) and monitored for cytotoxicity over 144 hours by MTT. Mean \pm SEM values were calculated as % of untreated cultures and based on 5 separate representative experiments. Statistical significance was based on a 2 tailed unpaired t-test, ** $p < 0.005$; * $p < 0.05$ and based on comparison's between AdEHCD40L vs. AdEHNull.

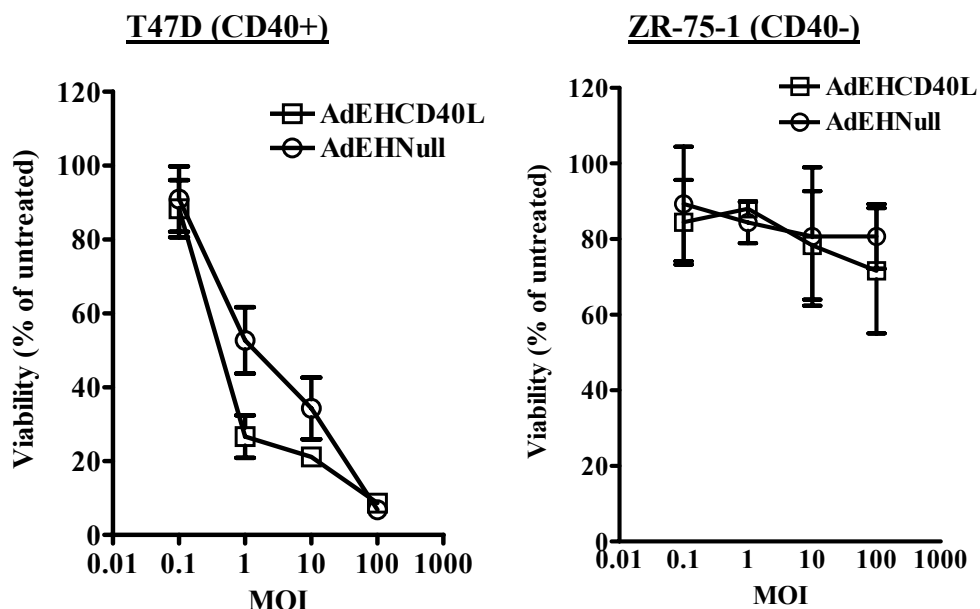


Figure 3.2: Relative antitumor efficacy of AdEHCD40L and AdEHNull. T47D and ZR-75-1 were infected with graded doses of AdEHCD40L and AdEHNull (MOI =1 -100). The % viability (Mean \pm SD) was calculated from 3 separate experiments. The ED₅₀ of the AdEHCD40L and parental construct (AdEHNull) was extrapolated by linear regression analysis.

value for T47D cells was determined to be MOI = 0.45 for the AdEHCD40L as compared with an MOI of 4 for the AdEHNull construct. Thus for T47D cells, AdEHCD40L was approximately 10 fold more effective in cell kill as compared with AdEHNull. In contrast the ED₅₀ could not be attained with ZR-75-1 even at an MOI =100 (Figure 3.2) demonstrating the resistance of this cell line to viral oncolysis. Dose response of AdEHCD40L was comparable to that of AdEH for this CD40- cell line.

Viral Replication of AdEHCD40L was Comparable to the Parental Construct AdEHNull

To determine if altered viral replicative activity contributes to the enhanced anti-tumor activity of AdEHCD40L, total viral yield was quantitated as a function of viral hexon DNA by the quantitative PCR technique in T47D-infected cultures. Comparable levels of the total viral hexon DNA was detected in both the recombinant AdEH vectors (AdEHCD40L and AdEHNull) as well as in the wild type (Adv-WT) infected cultures (AdEHCD40L: 3.3×10^3 vp; AdEHNull: 3×10^3 vp; Adv-WT: 5.2×10^3 vp at 96 hours; Figure 3.3). These findings indicate that both modified AdEH constructs have a comparable replicative activity as the wild type adenovirus in T47D breast cancer cell lines. Hence, incorporation of the CD40L transgene did not alter the replicative activity of the AdEH constructs and up-regulated viral replication is not the explanation for enhanced tumor cytotoxicity of AdEHCD40L.

Relative Efficacy of AdEHCD40L and the Recombinant CD40L Protein in T47D Cells

To compare the anti-tumor efficacy of the CD40L when introduced as a recombinant protein or a transgene, parallel treatments were carried out under pre-optimized conditions with the AdEHCD40L (MOI = 1) or the trimeric CD40L recombinant protein (1 μ g/ml, Alexis biochemicals, San Diego, CA)³⁰. The growth inhibitory response by AdEHCD40L was consistently more pronounced than that with the recombinant CD40L (rCD40L) over a period of 144 hours (80.5 ± 1.1 % vs. 17.8 ± 5.0 %, $p < 0.05$) (Figure 3.4). Treatments with AdEHNull were used to determine the growth inhibitory effect that was attributable to viral replication. This agent reduced 48.7 ± 8.8 % cell growth by 144 hours. Hence the CD40L transgene effect alone appears

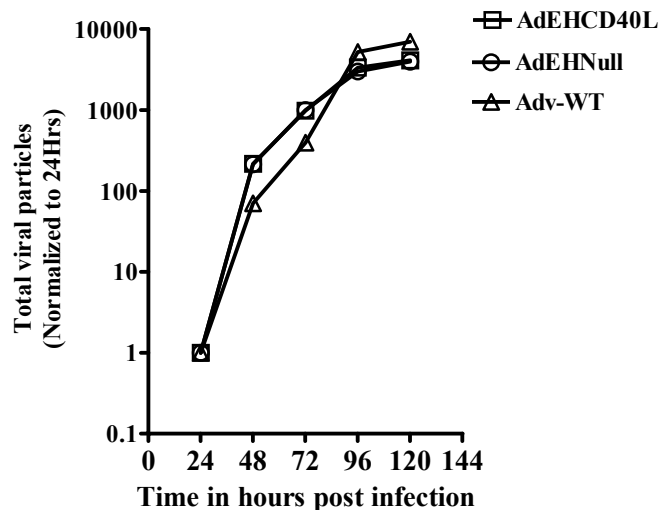


Figure 3.3: Viral replication of AdEHCD40L is comparable to the control construct. T47D cells were infected with AdEHCD40L, AdEHNull, Adv-WT (MOI = 1). The total viral particles in the culture supernatants and pellet of T47D infected cells (MOI = 1) was evaluated over 144 hours by quantitative PCR. Values were normalized to the respective vp contained at 24 hours for each treatment. Total viral hexon quantitated from the pellet and supernatant are based on triplicate reactions from a single experiment.

to generate a more pronounced anti-tumor effect (net of 41%) as compared with rCD40L, suggestive of a synergistic outcome with viral oncolysis.

AdEHCD40L was Attenuated in Viral Non Permissive Malignant and Non-Malignant Cell Lines

To validate the cancer selective activity of AdEH constructs, infectivity studies were carried out with malignant and non-malignant cell lines under viral non-permissive conditions. The cytopathic effect of recombinant virus to replicate and detach the adherent cells was evaluated by crystal violet staining. Whereas insertion of the CD40L

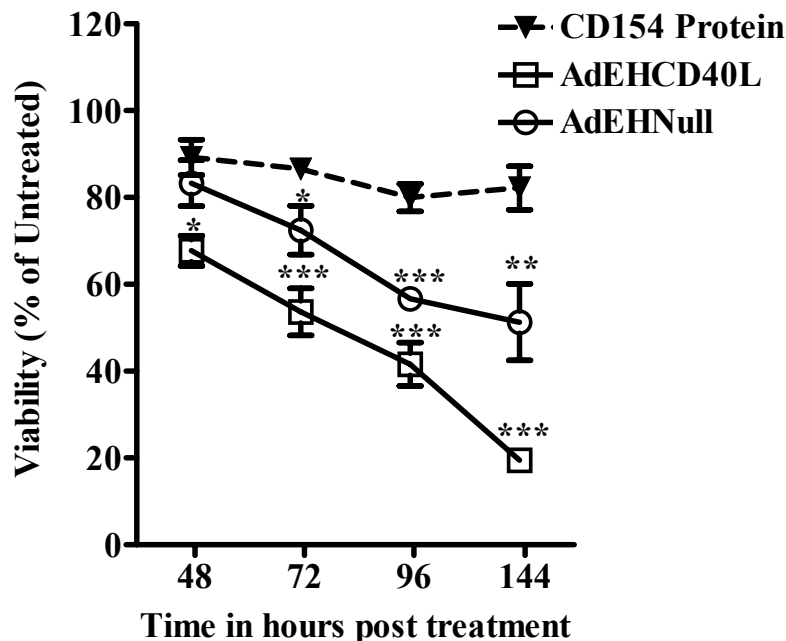


Figure 3.4: AdEHCD40L is more potent than the recombinant CD40L. Growth inhibitory activity was measured using the MTT assay. Mean \pm SEM values are representative of 5 separate independent experiments. Statistical significance was evaluated by the 2 tailed t-test (*, $p < 0.05$; **, $p < 0.005$; ***, $p < 0.005$)

transgene improved anti-tumor activity of AdEH (> 95% by AdEHCD40L vs. 50.6% by AdEHNull) in viral permissive T47D cells (Figure 3.5), both constructs remained attenuated in nonmalignant lung fibroblast (<5% growth inhibition by AdEHCD40L and AdEHNull). By comparison, Adv-WT produced 64.2% toxicity in T47D cells and 67.3% in IMR-90 (Figure 3.5). Evaluation of mitochondrial activity as a measurement of cell viability was used assessed to evaluate viral cytotoxicity in non-permissive BT20 cancer cell line. AdEHCD40L produced <12% growth inhibition (Figure 3.6), although CoCl_2

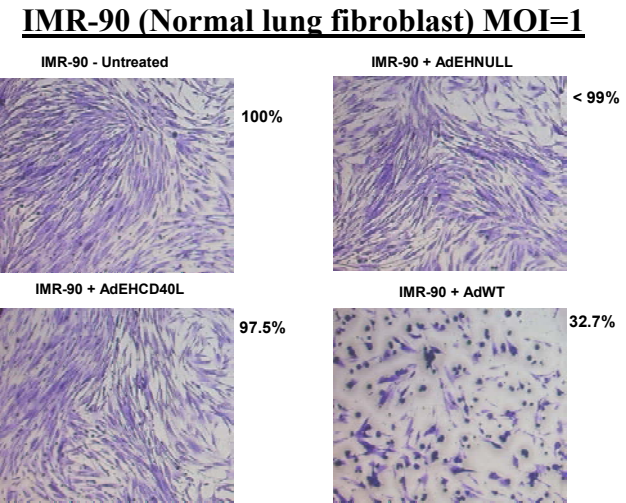
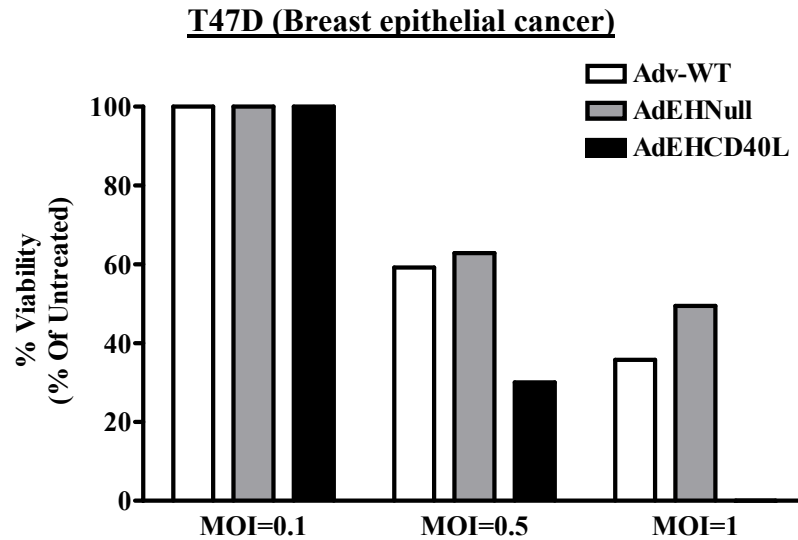


Figure 3.5: Crystal violet staining for cytopathic effect in non-malignant and malignant cell lines. Normal lung fibroblast (IMR-90) and cancer (T47D) cell lines were infected with graded doses of AdEHCD40L and the control virus (AdEHNull and Adv-WT). Cells (T47D: 1×10^4 ; IMR-90: 5×10^4) were stained with crystal violet when CPE was observed in 50 - 60 % of the Adv-WT infected cultures (day 3 for T47D and day 4 for IMR-90). % viability was calculated as % of untreated cultures. Values represented are average from 2 separate experiments each done in triplicates.

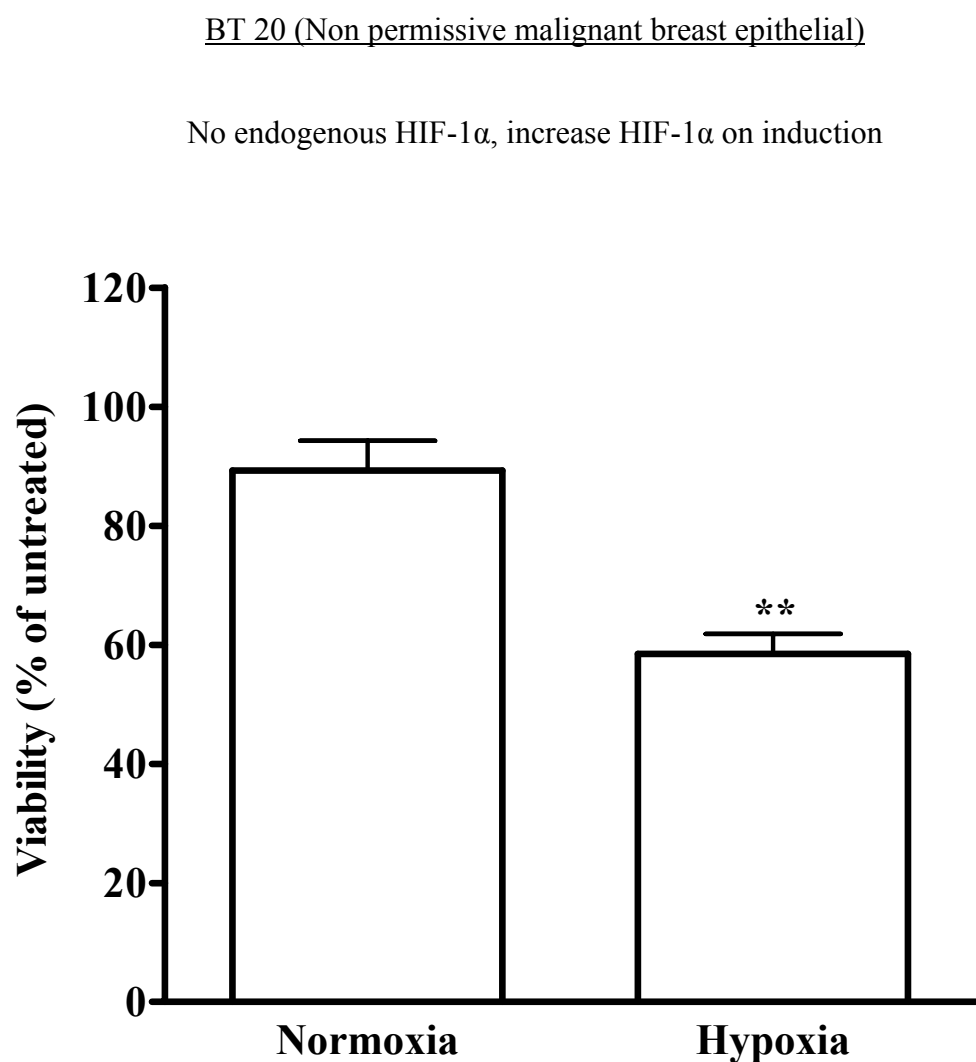
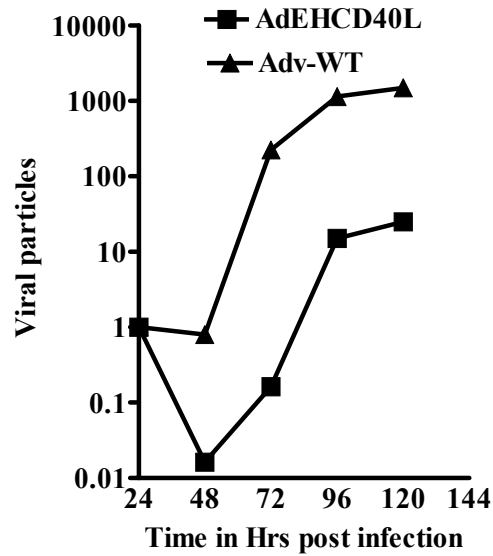
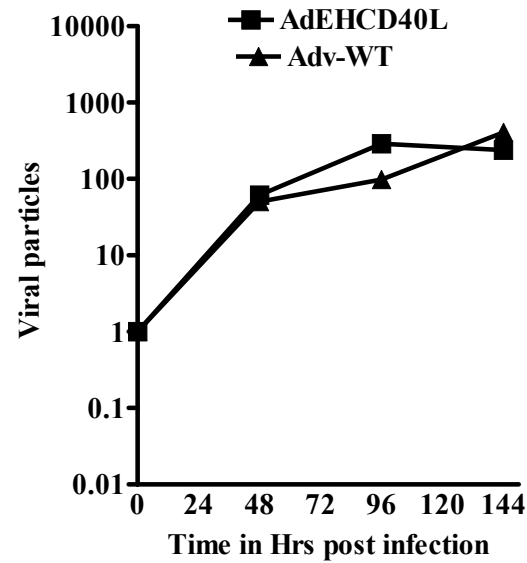


Figure 3.6: AdEHCD40L attenuated in non-permissive BT20 cells. BT20 cells were infected with AdEHCD40L (MOI = 1) under non-inducing and inducing conditions. % viability was measured by the MTT assay. Mean \pm SEM values were calculated as % of untreated and based on 5 separate representative experiments. Statistical significance was based on a 2 tailed unpaired t-test, ** $p < 0.005$.

Non malignant lung Fibroblast
(IMR-90) –Non Permissive



Non malignant breast epithelium
(HMEC)- Permissive



Breast epithelial cancer (T47D)-
Permissive

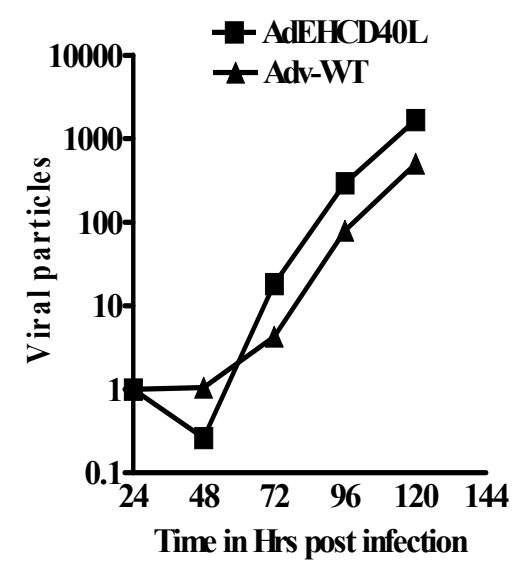


Figure 3.7: Viral replication in non-malignant and malignant cell lines. Viral burst assay in non malignant lung fibroblast (IMR-90), epithelial (HMEC) and cancer (T47D) cell lines. Number of viral particles released into the culture supernatants was quantified by PCR and normalized to either total viral particles at 24 hours (IMR-90, T47D) or Day 0 (HMEC).

induction promoted this growth inhibitory outcome (41.5 %) These findings suggest that AdEHCD40L is attenuated in non-malignant and non-permissive cell lines and is cytotoxic only in hypoxic permissive conditions

The cytotoxicity activity of AdEHCD40L in viral non-permissive cells correlated with viral yield determinations. Viral replication of AdEHCD40L was attenuated by > 1000 fold in IMR-90 when compared to Adv-WT, reaching its maximum at 96 hours post infection (Figure 3.7). In contrast, viral replicative activity of AdEHCD40L was comparable to Adv-WT in permissive malignant (T47D) and non-malignant cell lines that express endogenous HIF-1 α (Figure 3.7). Collectively, we demonstrated that the cytotoxicity and viral replicative activity of the AdEHCD40L construct were dependent on the viral permissive state of the cell line

Soluble CD40L Levels in Cell Culture Supernatants of AdEHCD40L Treated Cultures

CD40L manifests in different isoforms that result from alternative splicing during transcription, or cleaved by metalloproteases on the cell membrane and subsequently released as a soluble form¹²⁰. These events may lead to the release of soluble CD40L (sCD40L) which in turn participates in cancer growth regulation. We have quantified sCD40L level by colorimetric ELISA analysis in AdEHCD40L infected (MOI=1) T47D cultures. The detected concentration of soluble CD40L was above the sensitivity detection limit of 0.005 ng/ml. and varied on CoCl₂ induction, ranging from 0.18 ± 0.02 and 0.3 ± 0.15 ng/ml at 72 hours and 96 hours, respectively (Table 3.1). Nevertheless, the level of soluble CD40L was markedly below the effective growth inhibitory dose and likely to minimally contribute to the growth inhibitory outcome.

Table 3.1: Quantification of soluble CD40L by ELISA

Time Tested	CD40L concentration (Mean \pm SD; ng/ml)	
	No CoCl ₂	+ CoCl ₂
24 hours	< 0.005	< 0.005
48 hours	< 0.005	< 0.005
72 hours	0.18 \pm 0.02	< 0.005
96 hours	0.33 \pm 0.15	< 0.005
144 hours	0.13 \pm 0.02	0.11 \pm 0.01

Discussion

The capacity of recombinant CD40L to modulate growth in solid cancer has been described in a number of studies¹²¹⁻¹²³. We previously reported that recombinant CD40L inhibited the growth of CD40 positive breast cancer cell lines³⁰. To enhance the overall anti-tumor efficacy of current delivery vehicles, we have utilized a conditional replicative adenovirus for restricted delivery of CD40L to breast cancer cells.

In this study, anti-tumor response to CD40 positive lines (T47D, BT20, and MDA-MB- 231) was markedly enhanced by the presence of the CD40L transgene under viral permissive conditions, when compared to AdEH lacking the CD40L transgene. This additive response was not observed in the CD40 negative line ZR-75-1, indicating that cytotoxicity represented the combined outcome of viral mediated cytolytic activity

and CD40L toxicity. However, blocking studies against CD40L will allow us to further establish the role of CD40L in this enhanced cytotoxic phenomenon. Though we observed that AdEHCD40L-infected ZR-75-1 expressed higher levels of CD40L than T47D (Chapter 2, figure 2.9), the ED₅₀ value could not be attained in ZR-75-1 cells even at an MOI = 100. These findings suggest that ZR-75-1 cells may be susceptible to viral infection and resistant to the subsequent viral oncolytic process^{52, 124}. The underlying mechanism of resistance needs to be further investigated

The advantage of using CD40L as a transgene with a conditional replicative adenovirus, was further validated by comparison of cytotoxic response between recombinant CD40L and CD40L transgene. We were able to show that delivery of CD40L with a replicative adenovirus led to a more pronounced CD40L dependent cytotoxic effect when compared to the recombinant CD40L protein.

Selectivity is an important aspect of oncolytic adenoviral therapy. We demonstrated that the viral replication of AdEHCD40L was comparable to the Adv-WT in HIF-1 α expressing lines (HMEC and T47D). In contrast, AdEHCD40L was attenuated in HIF-1 α negative normal lung fibroblast cells with reduced growth inhibitory impact. These findings affirm the applicability of AdEH for CD40L transgene delivery to HIF-1 α expressing cancer cells.

Downstream mediators of the CD40-CD40L pathway like NF κ B and PI3kinase^{125, 126}, have been known to be affected by viral gene expression during the adenovirus infection process. Conversely, perturbation of cellular signaling by CD40L may interfere with the viral replicative process. Findings of viral yield demonstrated that CD40L incorporation did not affect viral replication, with recovery of AdEHCD40L, comparable

to AdEHNull and the Adv-WT, in viral permissive T47D cells. Since insertion of CD40L did not promote viral replication, it is also unlikely that the increased anti-tumor efficacy of AdEHCD40L was due to enhanced viral replication.

CD40L may be expressed either as a membrane bound ligand or as a soluble cleaved product. We observed low levels of soluble CD40L in AdEHCD40L treated T47D cells. Though we cannot extrapolate our current findings of soluble CD40L into its patho-physiological relevance, the levels of detectable soluble CD40L fall markedly below the threshold for cancer growth modulation which we previously determined to be $\geq 1 \mu\text{g/ml}$ ³⁰.

Collectively, our studies demonstrated that the CD40L transgene acted in concert with viral oncolysis to suppress cancer growth. Nevertheless, the incorporation of the transgene did not markedly alter viral replicative activity of the parental AdEH construct. Importantly, AdEHCD40L has limited cytotoxic activity in non-permissive cells. The applicability of AdEHCD40L for the experimental treatment of breast cancer will be further validated in severe combined immunodeficiency (SCID) mice with human xenografts models, together with studies that seek a better understanding of its mechanisms of action.

CHAPTER FOUR

In Vivo Growth Regulatory Activities of AdEHCD40L

Our in vitro findings suggest that AdEHCD40L can inhibit the growth of human breast cancer cell lines and manifests an additive response that can be attributed to the cytotoxic effects of CD40L and adenoviral oncolysis. The enhanced anti-tumor efficacy of AdEHCD40L was increased in HIF-1 α + cells in vitro. Limited data is available on the HIF-1 α protein expression of breast cancer tumors established in mice. Cho et al demonstrated that MDA-MB-435 xenografts established in mice express the HIF-1 α protein which regulated hypoxia responsive promoters¹²⁷.

To determine the efficacy of AdEHCD40L in vivo, a severe combined immunodeficient (SCID) xenograft model was used. SCID mice lack functional B and T cells due to the lack of re-arrangement of genes encoding for the T cell receptor and those encoding for the immunoglobulin^{128, 129}. The ability of this model to sustain human tumors cells has been well documented^{130, 131}. Though SCID mice have natural killer cells that might contribute to anti-tumor activity, it has served as a preliminary model to evaluate the direct growth inhibitory impact of CD40L on CD40 positive breast tumors^{30, 86}. Concerns with toxicity issues associated with replicative adenovirus warrants validation of the distribution patterns and maximum tolerated dose of AdEHCD40L. In this chapter, we have studied the efficacy of AdEHCD40L on human breast cancer xenografts established in SCID mice. Additionally, the biodistribution and maximum tolerated dose was evaluated in an immunocompetant Balb/c mice model.

Material and Methods

Biodistribution and Maximum Tolerated Dose in Balb/c Mice

The biodistribution and maximum tolerated dose (MTD) was evaluated in immunocompetant female BALB/c mice (Harlan Sprague Dawley, Indianapolis, IN) following tail vein injections of AdEHCD40L. The scheme for evaluating the biodistribution of AdEHCD40L is outlined in figure 4.1. To determine the biodistribution, a single intravenous injection (100 μ l) of graded doses (2×10^9 pfu, 2×10^8 pfu, 1×10^7 pfu) of AdEHCD40L (3 mice per group) was administered to the mice. Adv-WT (2×10^9 pfu) was administered as a control for the intravenous injections while mock or PBS controls were used as negative controls (2 mice per group). The mice were monitored daily for overt toxicity (loss of >25% body weight, death) for 14 days. Animals were euthanized at the end of the study by cervical dislocation following anesthesia by isoflurane vapor inhalation.

To determine the biodistribution of the virus in the normal organs of mice, animals were euthanized with isoflurane inhalation at 12 hours, 7 days and 14 days post injection. 10-50 mg of tissues (liver, spleen, lung) obtained from euthanized mice was washed twice in 1X PBS, quick frozen in ethanol dry ice mixture and stored at -85°C . Serum samples were obtained by centrifugation of whole blood and stored at -20°C . Tissues were weighed prior to the extraction of total nucleic acid. Total nucleic acids were extracted using the QIAamp DNA minikit (Qiagen, Valencia CA, USA). Quantitative PCR was performed as described in chapter 3.

Similarly, to determine the maximum tolerated dose, a single intravenous injection (100 μ l) of graded doses (2×10^9 pfu, 2×10^8 pfu, 1×10^7 pfu) of AdEHCD40L

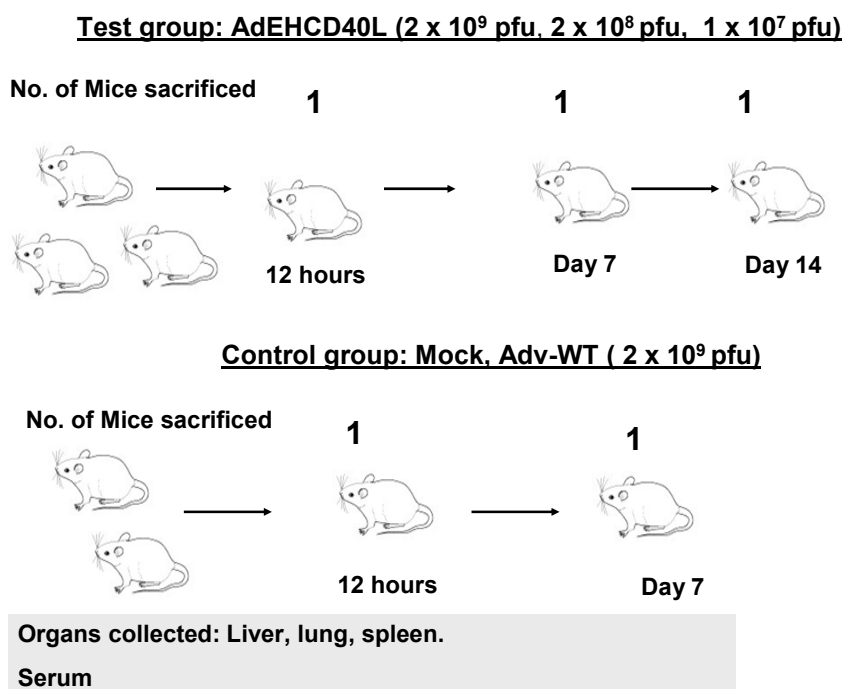


Figure 4.1: Schematic representation of biodistribution and maximum tolerated dose experimental design. Female BALB/c mice were given a single intravenous tail vein injection with varying doses (1 x 10⁷, 2 x 10⁸, 2 x 10⁹ pfu) of AdEHCD40L or PBS (mock). Adv-WT was used as a control for injections. Animals were sacrificed at varying time points. The mice injected with AdEHCD40L or Adv-WT (2 x 10⁹ pfu) did not survive beyond 4 and 7 days respectively. The serum and organs were analyzed for viral hexon by quantitative PCR. Mice were monitored for up to 14 days for signs of overt toxicity.

(3 mice per group) was administered to the mice. Adv-WT (2 x 10⁹ pfu) was administered as a control for the intravenous injections, while mock or PBS controls were used as negative controls (2 mice per group). The mice were monitored daily for overt toxicity (loss of >25% body weight, death) for 14 days. Animals were euthanized at the end of the study by cervical dislocation following anesthesia by isofluorane vapor inhalation.

Anti-Tumorigenic T47D Model

The anti-tumor activity of AdEHCD40L was examined in vivo using a T47D xenograft model in SCID mice (CB17/IcrHsd-scid, Harlan Sprague Dawley). Animals were fed on a high protein diet. All protocols were reviewed and approved by the institutional animal care and use committee at Baylor Research Institute. T47D is an ER+ cell line that establishes tumors in mice that have estradiol supplements¹³². A week prior to implantation of cells, 0.72 mg/60 day sustained release 17- β estradiol pellet (Innovative research of America, Sarasota, Florida) was injected into the lateral side of the neck between the ear and the shoulder using a 10 gauge precision trochar (Innovative research of America). T47D cells were seeded in a T-225 cm² culture flask (1x10⁷ cells/flask) in RPMI 1640 with 2% FBS and insulin (9 μ g/ml). Cells were either mock treated or infected with AdEHCD40L, AdEHNull at an MOI=1 and cultured for 48 hours. Trypsinized cells were washed twice with 1X PBS and re-suspended with sterile RPMI 1640 at a final concentration of 2 x 10⁷ cells/ml. Cells were mixed with matrigel (BD Biosciences, Bedford, MA) in a 1:2 ratio to get a final cell concentration of 1x10⁷ cells/ml. The suspension was drawn into a 1ml syringe with a 25 gauge needle that had previously kept on ice. 100 μ l of cell matrigel suspension was injected into the left flank of each mouse. Control mice (2 per group) with estradiol pellet and cells only were also monitored. The mice were checked twice a week and tumors measured with a vernier caliper for up to a period of 30 days post cell inoculation. Mean tumor diameter (D) was determined as the geometric mean $[D = (D1D2)^{1/2}]$ of two perpendicular measurements $[D1, D2]$ ³⁰. Differences in primary tumor xenograft size were compared statistically by the 2 tailed unpaired t-test. Animals were euthanized by cervical dislocation following

anesthesia by isoflurane vapor inhalation and checked for evidence of metastatic nodules in the lungs, liver, and bone marrow. The tumors were fixed in formalin for histological evaluation.

Intra-Tumoral Model for MDA-MB-231

Subcutaneous breast carcinoma cell line (MDA-MB-231) xenografts were established by injecting 3×10^7 cells in 100 μ l of cell suspension with matrigel in a 1:2 ratio into the left flank of CB17/IcrHsd SCID mice (Harlan Sprague Dawley, Indianapolis, IN). After tumor emergence (approximately 7-10 days after inoculation), animals received a single intratumoral injection (100 μ l) of either media only, AdEHCD40L (2×10^7 pfu, 5×10^7 pfu) or AdEHNull (2×10^7 pfu, 5×10^7 pfu). This injection was given daily for 5 consecutive days. The tumors were monitored as described for T47D. Animals were euthanized by cervical dislocation following anesthesia by isoflurane vapor inhalation and checked for evidence of metastatic nodules in the lungs, liver, and bone marrow.

Immunohistochemical Staining of HIF-1 α

Formalin fixed, paraffin embedded T47D xenografts sectioned slides were stained for the presence of the hypoxic marker HIF-1 α . Cells were stained as previously described¹³³. Briefly, slides were deparaffinized in xylene and graded alcohols. Antigen retrieval was carried out in 0.01 M citrate buffer in the microwave (Target Retrieval Solution, pH 6.0; Dako, Carpinteria, CA, USA). HIF-1 α , expression was determined using the avidin–biotin-complexed immunoperoxidase reaction (DAB Detection Kit;

Ventana Medical Systems, Tucson, AZ, USA) following initial incubation with monoclonal mouse anti-human HIF-1 α 67-sup antibody (1:1000; Novus biologicals, Littleton, CO), using the Ventana 320ES System (Ventana Medical Systems). The reaction was compared with an IgG2b isotypic antibody control (BD Pharmingen, San Jose, CA) stained slide. Human tonsils and infiltrating lobular breast carcinoma's were stained and used as negative and positive controls. The HIF-1 α positive slides were distinguished by the histological criteria of a pathologist.

Results

Maximum Tolerated Dose and Biodistribution of AdEHCD40L

The maximum tolerated dose of AdEHCD40L was determined in an immunocompetant Balb/c model following a single intravenous injection. The injected mice survived the dose of 2×10^8 pfu (1.5×10^{10} vp) over a period of 14 days with no overt signs of toxicity. (Table 4.1). By comparison, animals that received 2×10^9 pfu, of Adv-WT or AdEHCD40L expired by day 3 and day 7, respectively post viral injections. The maximum tolerate dose of the AdEHCD40L was therefore determined as 2×10^8 pfu.

Biodistribution of AdEHCD40L in Balb/c mice was determined by real time PCR quantification of viral hexon DNA following tail vein injection, and was found to be similar to that previously observed with other adenoviral constructs¹³⁴. The highest proportion of viral particles was detected in the liver of the mice over the dose range tested (2×10^9 pfu/ 1.5×10^{11} vp: 1.3×10^7 vp/mg tissue; 1×10^7 pfu/ 7.3×10^8 vp: 7.3×10^4 vp/mg tissue) at 12 hours post infection (Figure 4.2). Viral load in the liver increased with time for animals that received the lower dose of 1×10^7 pfu (12 hours: 2.5×10^4

Table 4.1: Determination of Maximum tolerate dose (MTD) of AdEHCD40L in vivo

Days post injection	No. Alive/ Total animal injected @ viral dose (pfu)			
	Mock	1 x 10 ⁷ pfu	2 x 10 ⁸ pfu	2 x 10 ⁹ pfu
1	2/2	3/3	3/3	3/3
7	2/2	2/2	2/2	0/2
14	0/0	1/1	1/1	0/2

vp/mg tissue, day 7: 1.5×10^5 vp/mg tissue). Viral particles were also be detected in the spleen and lung of mice that were injected with treated $\geq 2 \times 10^8$ pfu, day 7. Circulating virus was detected in serum following injection of $\geq 2 \times 10^8$ pfu, but not in mice that received a lower viral dose (1×10^7 pfu). Interestingly, by day 14, the vector was below the detection limit at all doses tested in the liver, spleen, lung and serum (Figure 4.2, 4.3).

Pre-Treatment of T47D Cells with AdEHCD40L Alter Growth Properties in SCID Mice

The incorporation of the hypoxic response element and estrogen response element is expected to limit AdEHCD40L and AdEHNull replication to estrogen expressing and hypoxic conditions. To determine the hypoxic status of the T47D human xenografts, immunohistochemical analysis was carried out using a HIF-1 α specific primary antibody. We found that the entire tumor reacted strongly for the HIF-1 α (+++) reactive antibody. HIF-1 α expression was independent of blood vessel proximity (Figure 4.4), confirming viral permissibility of breast cancer xenografts.

The anti-tumor efficacy of AdEHCD40L was further evaluated with breast cancer xenografts established in CB-17/Icr-Hsd SCID female mice. Initial studies were

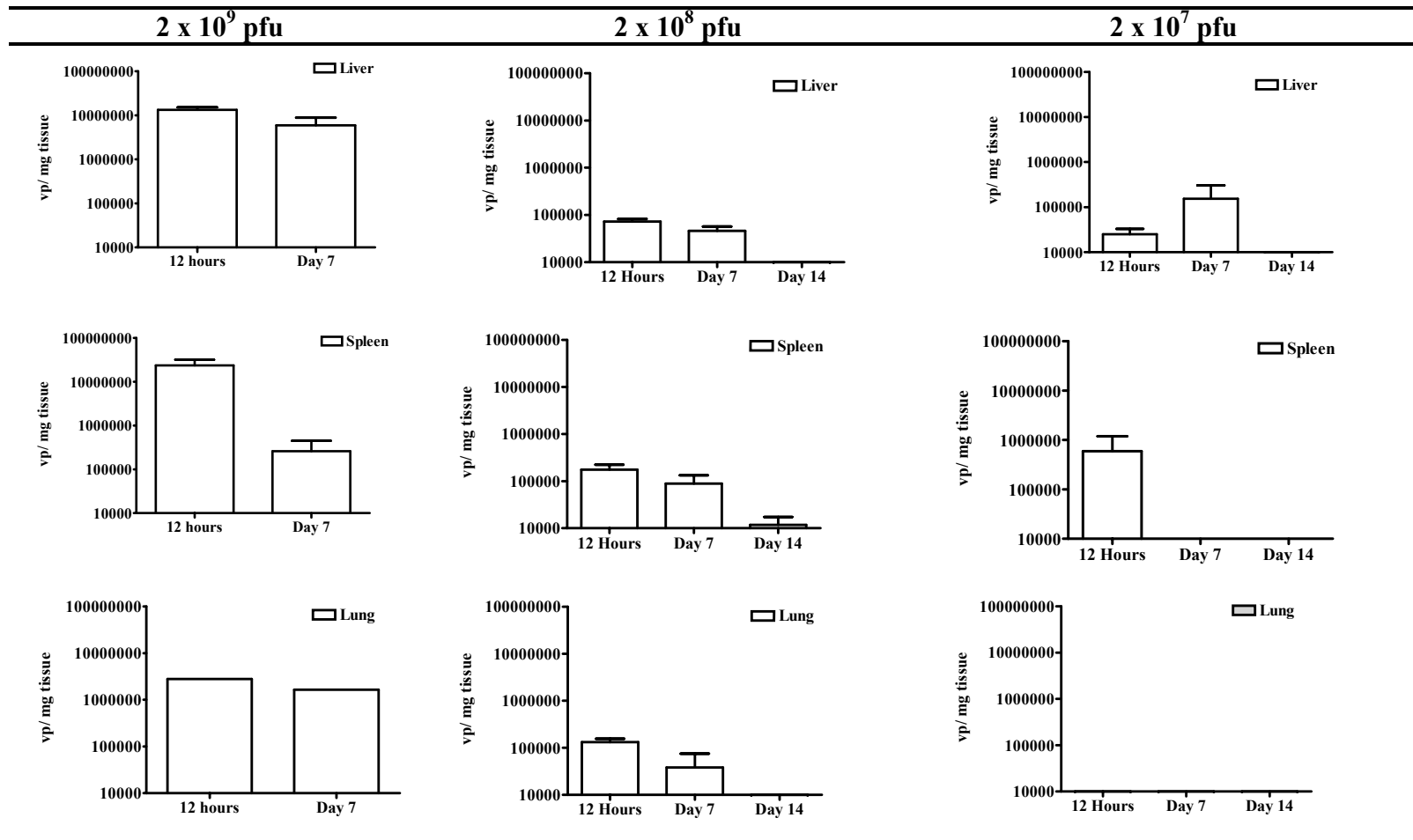


Figure 4.2: Biodistribution of AdEHCD40L in organs of female Balb/c mice. 4-5 weeks old Balb/c mice were injected intravenously with 1×10^7 pfu, 2×10^8 pfu and 2×10^9 pfu. Number of viral particles in the tissues was determined by qPCR and calculated per mg of tissue. Mean \pm range are based on values 2 separate extractions from a single organ and a single experiment

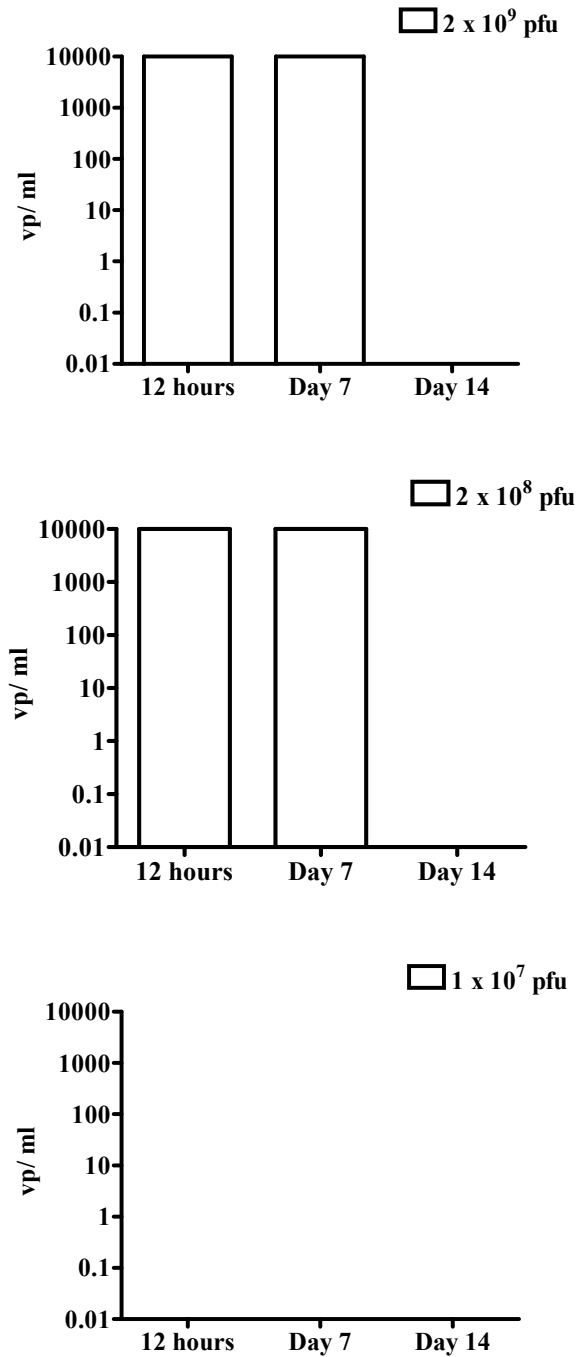


Figure 4.3: Biodistribution of AdEHCD40L in serum of female Balb/c mice. 4-5 weeks old female Balb/c mice were injected intravenously with 1×10^7 pfu, 2×10^8 pfu and 2×10^9 pfu. Number of viral particles was determined by qPCR and calculated per ml of sample. Mean \pm range are based on values 2 separate extractions from a single organ and a single experiment.

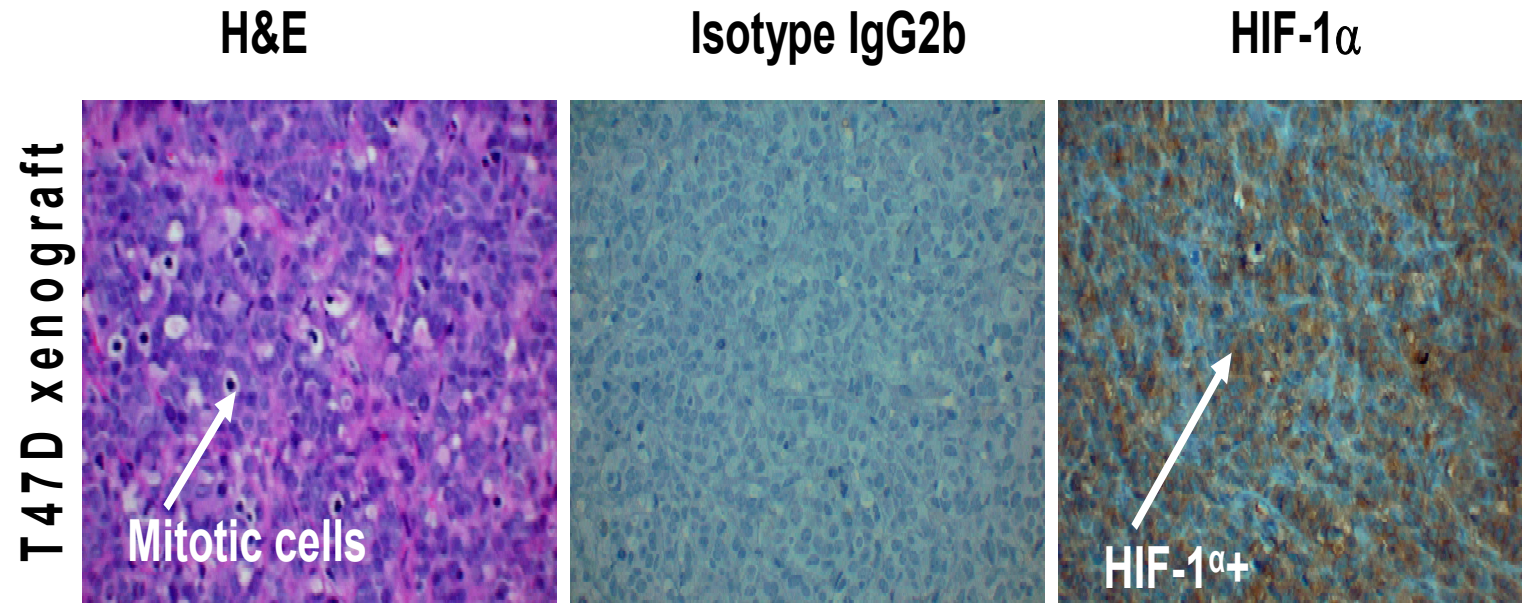
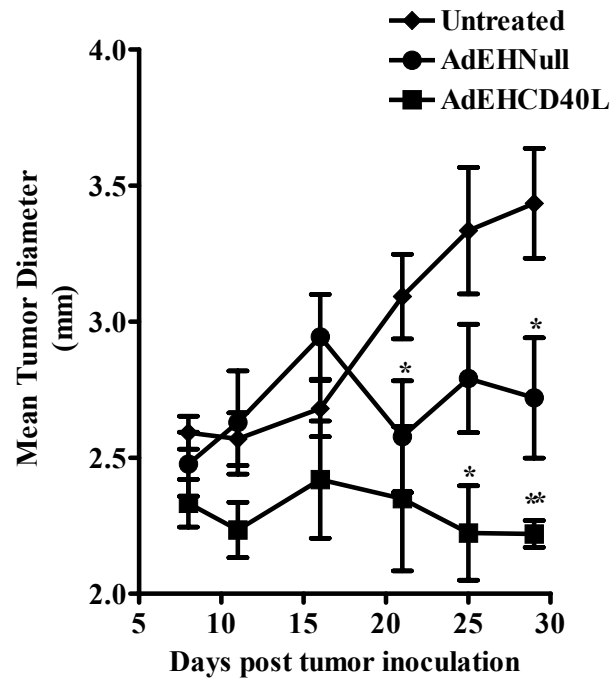


Figure 4.4: H&E and HIF-1 α staining of T47D xenografts. T47D xenografts were evaluated histologically for hypoxic marker HIF-1 α against an isotypic control. The mitotic actively dividing cells were detected in the H&E stained xenograft sections.

performed using T47D cells, an estrogen receptor positive cell line that requires estradiol for the growth in vivo. Mice implanted with sustained release estrogen pellets were injected with pre-treated T47D cells (AdEHCD40L, MOI=1; AdEHNull, MOI=1, or PBS) and tumor growth was monitored. A statistical significant reduction in the mean tumor diameter was observed between the treated (AdEHCD40L and AdEHNull) and untreated group (Untreated: 3.4 ± 0.2 vs. AdEHCD40L: 2.2 ± 0.05 ; $p < 0.005$, Untreated: 3.4 ± 0.2 vs. AdEHNull: 2.7 ± 0.2 ; $p < 0.05$) (Figure 4.5A). Further, the mean tumor diameter of AdEHCD40L treated tumors was markedly smaller than AdEHNull treated tumors at day 29 post inoculation ($p < 0.05$). These findings suggest that insertion of the CD40L into the AdEH backbone potentiated the anti-tumorigenic activity of AdEH on the growth of T47D xenografts. The proportion of mice that survived through the end of the experiment was 75 % (untreated), 62.5 % (AdEHNull) and 37.5 % (AdEHCD40L) (Figure 4.5B). It appears unlikely that viral treatment was the cause of lethality due to the following reasons namely; the maximum tolerated dose (MTD) was 2×10^8 pfu in Balb/c mice, as compared with 1×10^7 pfu injected tumor xenografts. Further, following consultation with a veterinarian, we speculate that the mice died of estradiol toxicity but not the virus treatment. In context of our experiment, one possible explanation is that estradiol if not taken up by the tumor xenografts is likely to generate systemic toxicity through reduction of appetite and loss of weight¹³⁵. To confirm our findings, current studies are ongoing to determine the high lethality rate in mice implanted with estradiol alone.

A



B

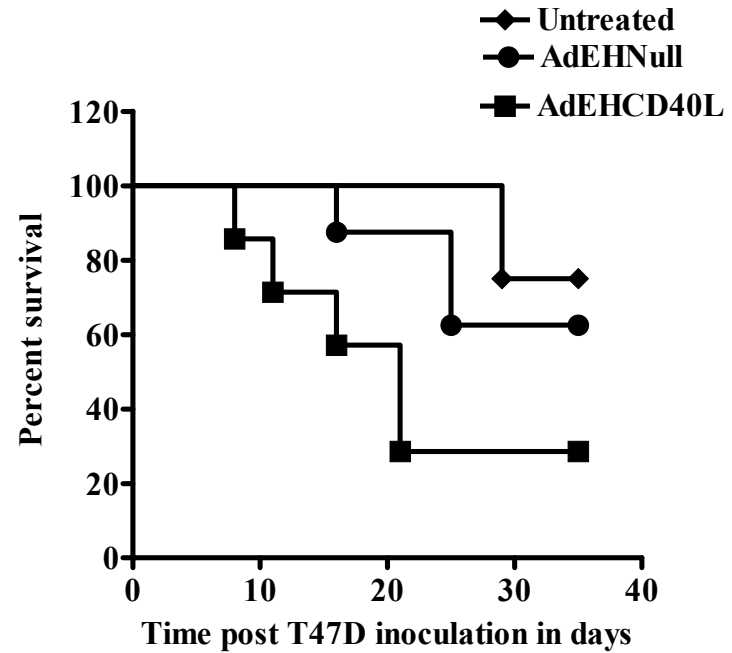


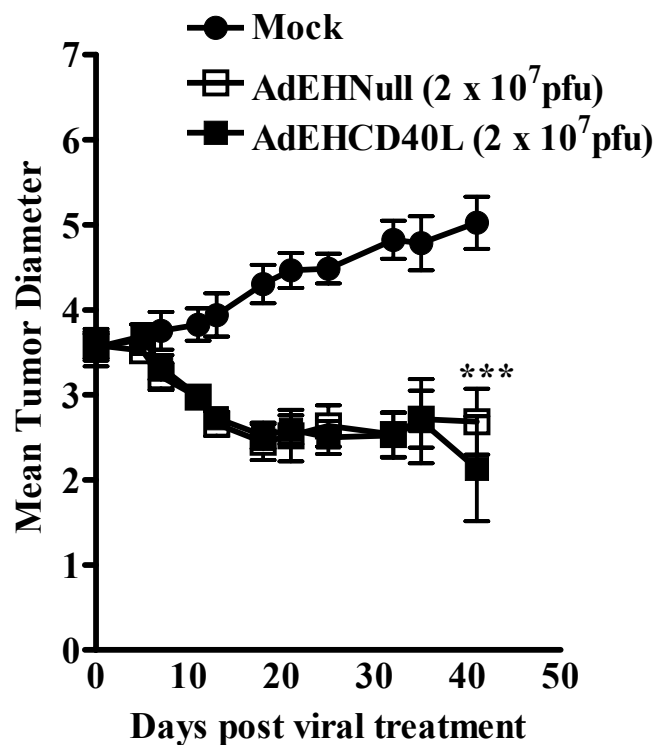
Figure 4.5: AdEHCD40L evaluation in T47D SCID xenograft. (A) T47D breast cancer xenografts were established in SCID mice following in vitro treatment with AdEHCD40L (MOI=1) or AdEHNull (MOI=1) for 48 hours. Mean tumor diameter was monitored from day of inoculation of cells (day 0) over 30 days. Tumor diameter at any given time point was calculated as the geometric mean of two perpendicular vernier caliper measurements. SEMs were $\leq 25\%$ of mean value. Statistical significance was determined by Student's t test as compared with the untreated mean (*, $p < 0.05$; **, $p < 0.005$). (B) Percentage of mice surviving was plotted overtime for each treatment group.

Anti-Tumor Efficacy of AdEHCD40L in a Subcutaneous Breast Cancer (MDA-MB-231) SCID Xenografts Model

To obviate the impact from estradiol implantation, we sought an alternative, estradiol-independent human breast cancer xenograft model to confirm the in vivo anti-tumor activity of AdEHCD40L. The MDA-MB-231 breast cancer line was used for xenografts induction and evaluation of the anti-tumor efficacy of AdEHCD40L. The pre-established, palpable MDA-MB-231 tumors were injected for 5 consecutive days with either a single intra-tumoral injection of AdEHCD40L, AdEHNull (2×10^7 or 5×10^7 pfu) or PBS. The dosing schedule was based on previous findings that multiple dosing with adenoviral vectors can produce a more pronounced anti-tumor outcome¹³⁶. At a dose of 2×10^7 pfu, both the AdEHCD40L and AdEHNull caused a 58% and 46% reduction in tumor growth, respectively, at 41 days post treatment. Increasing the viral dose to 5×10^7 pfu did not further enhance the anti-tumor response of either AdEHCD40L or AdEHNull (Figure 4.6). Both AdEHCD40L and AdEHNull significantly reduced xenografts growth, as compared with untreated tumors at day 7 post treatment (Figure 4.4). However, tumor reduction by AdEHCD40L did not differ significantly from that by AdEHNull at 2×10^7 pfu and 5×10^7 pfu (Figure 4.6).

Based on the formulae that 1 mm of tumor diameter equals to 1×10^6 cells¹³⁷, the injected dose of 2×10^7 is equivalent to an MOI = 6 and the dose of 5×10^7 pfu is equivalent to an MOI = 16.6. Previous in vitro studies (Chapter 3) suggested that the potentiating effect of the CD40L transgene occurred at a low MOI of \leq MOI = 1 (Figure 3.1, 3.2). Therefore, a significant elevated anti-tumor response by AdEHCD40L and AdEHNull may be anticipated at a lower viral dose, although may not be evident at MOI of ≥ 5 . We are currently evaluating the anti-tumor activity with two lower doses of the

A



B

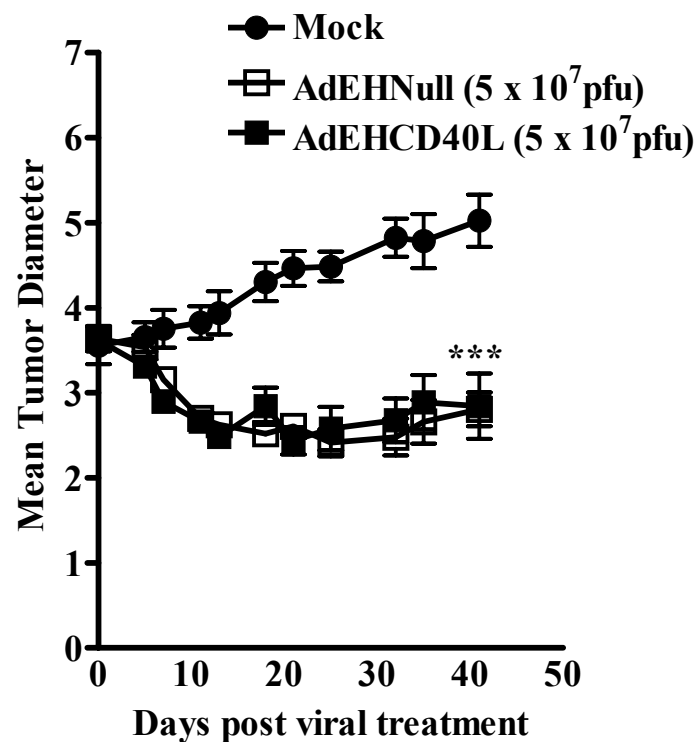


Figure 4.6: Anti-tumor responses of AdEHCD40L in MDA-MB-231. Pre-established MDA-MB-231 subcutaneous tumors were treated with 2 x 10⁷ pfu (A), 5 x 10⁷ pfu (B) and tumors monitored overtime. PBS injected tumors were the control group. Mean tumor diameter was monitored over time post viral treatment (0 Day, 1st injection). Tumor diameter at any given time point was calculated as the geometric mean of two perpendicular vernier caliper measurements. SEMs were $\leq 25\%$ of mean value. Statistical significance was determined by Student's t test as compared with the untreated mean (***, $p < 0.0005$).

virus (MOI = 0.1 and MOI = 1). Collectively, we demonstrated that MDA-MB-231 is extremely sensitive to adenovirus infection. At doses of 2×10^7 and 5×10^7 pfu both AdEHCD40L and AdEHNull caused a 40 -58% reduction in the tumor burden.

Discussion

Due to the lack of B and T cells in SCID mice, these mice best accommodate the growth of foreign human cancer cells and are appropriate for studying the immune independent interaction between a therapy agent and the targeted cancer cells. Our previous findings described in chapters 2-4, suggests that AdEHCD40L can enhance anti-tumor activities in human breast cancer cell lines in vitro. We observed a similar ability of AdEHCD40L to inhibit T47D xenografts. However, we observed a significant reduction in the survival of mice that might be attributable to estradiol, though measurements of estradiol levels in mice serum would help validate this speculation.

Further, we also were able to demonstrate that in an ER negative MDA-MB-231 xenograft model, both AdEHCD40L and AdEHNull caused a 44 – 58% reduction in the tumor load. The anti-tumor efficacy of AdEHCD40L is dose dependent and is observable at an $\text{MOI} \leq 1$ in vitro. Further studies at lower viral doses would help defining enhanced efficacy of AdEHCD40L in vivo. Alternatively, the enhanced anti-tumor activity of AdEHCD40L is observable in rapidly growing tumors. Injections of AdEHCD40L and AdEHNull performed when tumors are larger and in the logarithmic phase of growth might help validated enhanced anti-tumor activity of AdEHCD40L. In keeping with the ability of CD40L to enhance immune responses when delivered as a transgene¹³⁸, AdEHCD40L would be an advantage for breast cancer therapy. Studies in

syngeneic mice models would help further validate the advantage of using AdEHCD40L for the treatment of breast cancer.

Owing to the lack of more appropriate animal models, mice have been considered appropriate preclinical model for examining toxicity and persistence of the human adenovirus¹³⁹. The maximum tolerated dose of AdEHCD40L in Balb/c mice was comparable to that of other oncolytic adenovirus¹³¹. The AdEHCD40L injected mice were monitored over 14 days and organs analyzed at 12 hours and 7 days post treatment based on previous reports¹⁴⁰. The biodistribution studies with AdEHCD40L showed that distribution of virus in the normal organs of mice was dose dependent with equivalent levels of virus in the liver, spleen, and lung at higher doses while at lower doses the virus was mainly found in the liver. Green et al demonstrated a similar phenomenon with a replication deficient adenovirus where the spleen and lung showed a significant effect on biodistribution when liver failed to mediate the clearance of viruses¹⁴¹. Though the mice displayed no overt toxicities at 2×10^8 pfu as monitored by the loss of body weight and other signs of toxicity, evaluation of liver enzymes might further validate that AdEHCD40L dose dependent increase did not affect the liver function. Interestingly, AdEHCD40L persisted in the serum for 7 days at viral doses of 2×10^8 pfu (1.5×10^{10} vp) and above. This might partly be explained by the findings by others, that higher doses result in viral persistence in plasma for both virus reflecting the saturation of kupffer cells¹⁴¹. Alternatively, $1-2 \times 10^{10}$ vp has been suggested as a threshold for the uptake by kupffer cells in the liver¹⁴² which falls in the range of the amount of AdEHCD40L administered (1.5×10^{10} - 1.5×10^{11} vp).

Collectively, we demonstrated that AdEHCD40L has a MTD and biodistribution similar to other oncolytic adenovirus and can inhibit the growth of breast cancer xenografts in SCID mice, suggesting that AdEHCD40L maybe used as a potential experimental treatment approach for human breast cancer.

CHAPTER FIVE

Tumor Growth Inhibitory Mechanisms of AdEHCD40L

CD40 ligation has diverse outcomes ranging from the stimulation of cell growth to cell cycle blockade and apoptotic induction^{26, 30, 47}. Though the CD40 molecule lacks intrinsic enzymatic activity, it mediates its biological outcome through the recruitment of adaptor proteins like TRAF (tumor necrosis factor receptor associated factor) to promote the signal transduction. Depending on the differentiation state of cells, strength and the duration of CD40L interaction with CD40, different TRAF adaptor molecules are recruited to the CD40 cytoplasmic tail that ultimately activate unique signal transduction pathways including JNK (c-jun N-terminal kinase also known as stress activated protein kinase or SAPK), Erk (extracellular signal regulated mitogen activated protein kinase), p38 MAPK (mitogen activated protein kinase), NFkB (nuclear factor-kappa B), and PI3Kinase (phosphatidylinositol-3 kinase) (Figure 5.1). In B cells, TRAF 3 was shown to mediate activation of p38 MAPK, JNK, cytokine secretion, and immunoglobulin production following ligation of CD40¹⁴³, while TRAF 6 was required for the affinity maturation¹⁴⁴. This suggests that unique TRAF mediators differentially regulate B cell physiological outcome. The MAPK transcription factor p38 can mediate pro-apoptotic or anti-apoptotic responses¹⁴⁵⁻¹⁴⁷.

Differential activation of NFkB and the activation protein-1(AP-1) dictates survival outcome in intra-hepatic endothelial and epithelial cells (Table 1.2)¹⁴⁸. In

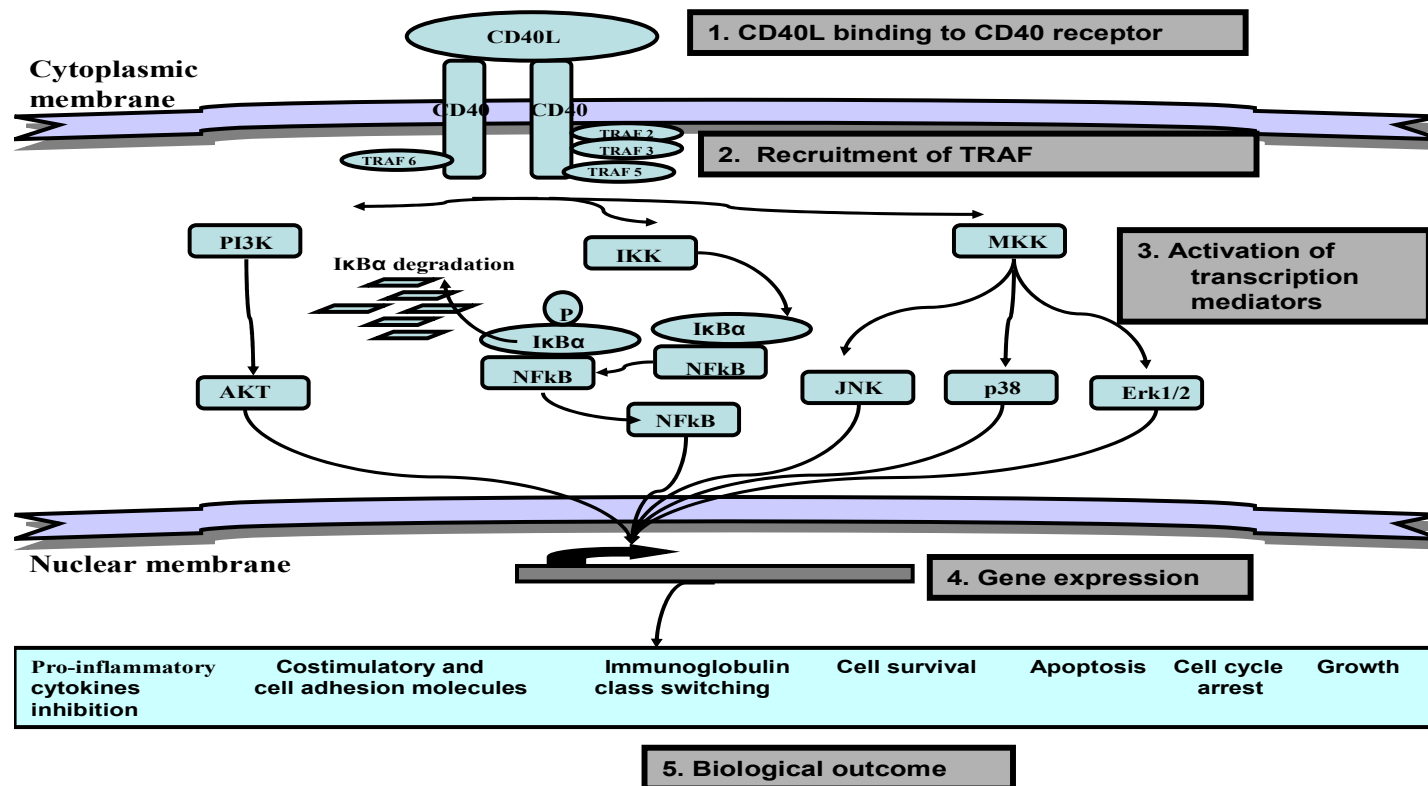


Figure 5.1: Schematic of CD40-CD40L signaling pathways. CD40 exists as monomers or homodimers/trimers. Their cytoplasmic domains lack intrinsic kinase activity. TRAF's are adaptor molecules that recruit various proteins into the signaling complex. TRAF 2, 3 and 6 can act directly with the cytoplasmic tail of CD40, while TRAF1 and TRAF5 act indirectly through formation of hetero-oligomers with TRAF2 and TRAF3. Depending on the various TRAF and protein complexes recruited, one or more of the transcription factors (PI3Kinase, NF κ B, JNK, p38 or Erk1/2) are activated. This in turn activates the transcription of various genes that ultimately dictate the biological outcome of the cell.

epithelial cancers, blocking either NF κ B or PI3Kinase has sensitized cells to growth inhibition by CD40L^{148, 149}. In contrast, in ovarian cancer, growth inhibition occurred independently of the NF κ B activation and apoptotic events⁴⁷.

Previously, our studies on T47D breast cancer with the recombinant CD40L showed that the decrease in cell proliferation of breast cancer cells was mediated by the up regulation of pro-apoptotic Bax, suggesting contribution of Bcl-2 family members to the growth inhibitory outcome. Additional reports by others indicate that the presence of interferon gamma (IFN γ) can further augment growth inhibition in breast cancer by recombinant CD40L. This activity was accompanied by Fas up regulation which sensitized cells to Fas mediated apoptosis^{86, 87}. Collectively, these findings demonstrate that CD40L-induced biological outcomes are cell-dependent and diverse, and need to be properly defined. With the use of an oncolytic virus as a delivery agent, perturbations of additional growth regulatory pathways can be expected. It is, therefore, necessary to characterize the cellular and molecular outcomes of AdEHCD40L treatment of breast cancer cells.

Previously, p38, PI3Kinase, and NF κ B have also been shown to be involved in adenoviral induced alteration in host cell signaling pathways. Adenovirus affect NF κ B and MAPK signaling pathways in normal vascular smooth muscle, endothelial, and dendritic cells^{125, 150, 151}, although limited information is available regarding activation of these pathways in cancer cells¹⁵². The viral E4 genes also have been shown to activate PI3Kinase¹²⁶ while p38 activation may be involved during adenoviral entry into the cell

This chapter examines the cellular and molecular mechanisms involved in the enhanced CD40L mediated tumor cytotoxicity observed in AdEHCD40L infected breast cancer cells. We evaluated the impact of AdEHCD40L on cell cycle regulation, apoptosis and the phosphorylation state of transcription factors downstream of the CD40 signaling pathway. Additionally, we explored the impact of AdEHCD40L infection on chemokine and cytokine regulation

Material and Methods

Annexin/PI Staining

In early stages of apoptosis, cells translocate the membrane phospholipid, phosphatidylserine to the outer leaflet of the plasma membrane where it can be detected by its high-affinity binding to annexin V, a calcium dependent phospholipid binding protein. Prolonged apoptosis can cause cell death that can be identified by staining positive for the vital dye, propidium iodide (PI). Therefore, apoptotic activity was measured by annexin V and PI staining. T47D cells (5×10^5 cells/well) were seeded in a 6 well plate and allowed to adhere overnight. Cells were then infected with AdEHCD40L, AdEHNull or Adv-WT at an MOI=1 in the presence of inducing conditions as previously described in chapter 2. At different time points, cells were trypsinized, washed twice with cold PBS and resuspended to 1×10^6 cells/ml. Cells (1×10^5 cells; 100 μ l) were then stained with 1 μ l of prediluted fluorescein labeled annexin V (BD pharmingen) and 2 μ l of PI (20 μ g/ml, Sigma, St Louis, MO) and incubated for 15 minutes at room temperature in the dark. Binding buffer (300 μ l) was added to each sample prior to two color fluorescence analysis (Becton Dickinson, FACScan). Treatment

with a Fas (1 $\mu\text{g/ml}$, 100 μl ; Beckman coulter, Marseille, France) was used as positive control for annexin V detection while untreated cultures were the negative control. The percentage of annexin-PI⁻ (live), annexin+PI⁻ (early apoptotic), annexin+PI⁺ (late apoptotic), and annexin-PI⁺ (necrotic) cells was determined based on 5000 events and analyzed with the CELLQuest software analysis (Becton Dickinson).

Cell Cycle Analysis

T47D or ZR-75-1 cells (5×10^5 cells/well) were infected with either AdEHCD40L or the control virus (AdEHNull) at an MOI=1 in the absence or presence of CoCl₂ (25 μM). At 48, 72, 96, and 144 hours post infection, cells were collected and the DNA content was determined by PI staining by flow cytometric analysis as previously described¹⁵⁴. Briefly, cells were fixed in 80% ethanol in 1X PBS overnight at -80°C. Cells (1×10^6) were stained with 1 ml of 1X PBS containing PI (40 $\mu\text{g/ml}$, Sigma) and RNase A (100 $\mu\text{g/ml}$, Qiagen) at 37°C for 30 minutes. Flow cytometric analysis was carried out by sampling 20,000 events (FACScan, Becton Dickinson). Cell cycle distribution was analyzed with the Verity cell cycle analysis software (Verity Inc, Topsham, ME).

Western Blot

To determine the involvement of transcription factors commonly associated with the CD40-CD40L signaling pathways (ErK, p38 MAPK, JNK, PI3Kinase, NFkB), immunoblot analysis was carried out following infection of T47D cells with the recombinant AdEH viral constructs. T47D cells (1×10^7) were initially treated with

AdEHCD40L, AdEHNull, Adv-WT (MOI=1) or recombinant CD40L (1 µg/ml, Alexis, San Diego, CA) under non-inducing conditions. Whole cell protein was extracted and western blot performed as previously described in chapter 2 in the material and methods section.

Membranes were treated with either a phospho specific rabbit anti-human SAPK/JNK, p38 MAPK [Thr (threonine) 180/Tyr (tyrosine)182], phospho p44/p42 MAP kinase (Thr 202/Tyr 204), AKT (Ser 473) or mouse phospho specific IκBα (Inhibitor of NF-kappaB) [Ser (serine) 32/36] or p21^{Waf1/Cip-1} (1:1000, Cell signaling technologies, Danvers, MA) primary antibodies. The total protein was detected using the respective total rabbit anti-human SAPK/JNK, p38 MAPK, p42/p44 MAP kinases, AKT, IκBα (1:1000, Cell signaling technologies, Danvers, MA) or β tubulin (1:100, Santa Cruz biotechnology, Santa Cruz, CA) primary antibodies (overnight, 4°C), followed by incubation with a goat anti-rabbit or goat anti-mouse horseradish peroxidase (HRP) conjugated secondary antibody (1:2000, Santa Cruz biotechnology, Santa Cruz, CA) for 1 hour with appropriate washings (1X PBS, 0.1% Tween 20). The reaction was developed by enhanced chemiluminescence (ECL plus detection kit, GE healthcare, Piscataway, NJ) as per manufacturer's specifications, and visualized by autoradiography using Kodak scientific imaging film (Perkin Elmer, Wellesley, MA). Bands were quantified by densitometric analysis using the Alphamanager 2000D and Scion Image Software.

Biological Activity of NFκB

To determine the impact of NFκB on the growth inhibition, blocking studies were performed using the IκB kinase inhibitor peptide (Cell signaling biotechnology) that

blocks I κ B phosphorylation. T47D cells (1×10^5 , 100 μ l) were treated with AdEHCD40L, the control virus AdEHNull, and Adv-WT (MOI=1) under non-inducing conditions. Following infections, cells were treated with graded concentrations of the I κ B kinase inhibitor peptide (1 μ g/ml, 5 μ g/ml, 10 μ g/ml). At 96 hours post infection, the metabolic activity which is an indirect measure of cell viability was assessed. Values were calculated as % untreated using the untreated cultures with the respective concentrations of inhibitor as a reference.

Multiplex Cytokine Analysis

CD40-CD40L interactions are known to stimulate cytokines and chemokines production in cancer cells ¹⁵⁵. In order to determine if AdEHCD40L treated T47D cultures enhance cytokine secretion that could impact the growth inhibition, multiplex luminex proteonomics analysis was done on cultures supernatants of T47D treated cells. T47D (1×10^5 cells, 100 μ l) were treated with AdEHCD40L and control viruses AdEHNull and Adv-WT (MOI=1). Recombinant CD40L (1 μ g/ml, 100 μ l; Alexis, San Diego CA) was used as a control for CD40L mediated responses. Chemokines and cytokines [Interleukin (IL) -1 α , IL-1 β , IL-6, IL-8, IL-10, IL-12p40, granulocyte macrophage colony stimulating factor (GM-CSF), tumor necrosis factor (TNF) α , RANTES (Regulated on Activation Normal T Cell Expressed and Secreted), MIP-1 α (macrophage inflammatory protein-1 alpha), interferon (IFN) α and vascular endothelial growth factor (VEGF)] known to be related to breast cancer pathogenesis or mediated by CD40L or adenovirus were evaluated by Luminex (Biosource). Samples were tested in duplicates according to the manufacturer's protocol.

Results

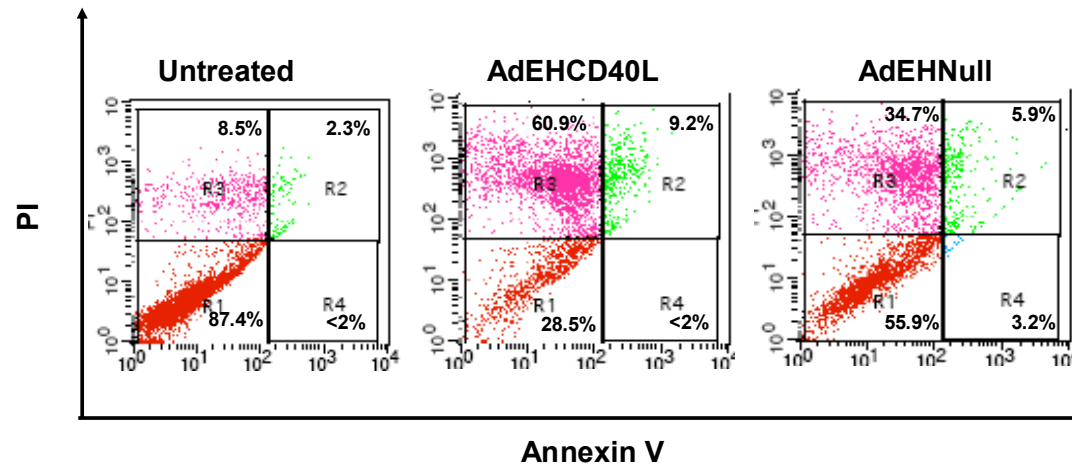
AdEHCD40L Induces Apoptosis and Necrosis in T47D Cells

To characterize the tumor growth inhibitory mechanisms of AdEHCD40L, apoptotic analysis was carried out with AdEHCD40L infected T47D cells at 144 hours post infection, when maximal growth inhibition was observed (Figure 3.1, chapter 3). The percentage of apoptotic (annexin V reactive) and necrotic (PI reactive) cells were quantified using the two color fluorescence flow cytometric assay. Cells are classified as viable (annexin- PI-), early apoptotic (annexin+ PI-), late apoptotic (annexin+ PI+), and necrotic (annexin- PI+).

We observed a significant decreased in the percentage of Annexin- PI- cells (71.5%) as compared to the treatment with the parental construct AdEHNull (44.1%) under viral permissive conditions (Figure 5.2). There was an increase in the annexin V+ apoptotic fraction among the virus treated cells (10.7%, 9.1%) as compared to the untreated cultures (4.1%) (Figure 5.2). However, no significant difference was found between the AdEHCD40L and parental (AdEHNull) virus. Nonetheless, AdEHCD40L treated cultures contained markedly higher levels (60.9%) of annexin- PI+ cells as compared to the AdEHNull treated cultures (34.7%), reflecting a higher level of cytotoxicity.

Virus Induced Cell Cycle Arrest

Cells at different cell cycle phases are distinguished by their DNA content into sub-G₀ (< 2n DNA), G₀/G₁, S (2n DNA) and G₂/M (4n DNA). Infection by adenovirus



Treatment	% of Total Cells			
	Viable Cells	Non-Viable Cells		
		Annexin+/ PI-	Annexin+/PI+	Annexin-/PI+
Untreated	87.41 ± 3.9	1.8 ± 1.5	2.3 ± 0.6	8.5 ± 1.7
AdEHCD40L	28.5 ± 1.8	2.3 ± 2.4	8.4 ± 8.0	60.9 ± 8.5
AdEHNull	55.9 ± 7.3	3.2 ± 3.4	5.9 ± 7.2	34.7 ± 2.9

Figure 5.2: Annexin V/ PI staining of T47D infected cultures. AdEHCD40L (MOI=1) treated cultures showed reduced viable cells (29% Ann-PI- cells) as compared with treatment by the parental AdEHNull construct (56%) at 144 hours post infection under HIF-1 α inducing conditions. Values represent mean \pm SD values from 3 separate experiments. The positive Fas control produced 3.9 \pm 0.7% (Annexin+ PI-) and 22.1 \pm 3.3% (Annexin+ PI+) under similar conditions (48 hours).

or CD40 ligation have both been shown to affect cell cycling which in turn impacts cell growth. Tamoxifen, a well established inducer of G₀/G₁ arrest in breast cancer cells was used as positive control for the assay. The majority of the untreated cells accumulated in the G₀/G₁ phase (90.2% at 144 hours). By comparison, the CD40L carrying AdEH vector caused equal accumulations of cells in G₂/M (25.7%) and S (32.8%) phases while AdEHNull infection produced mostly an S phase (58.6%) arrest. (Figure 5.3A). The total distribution of G₀/G₁ + S + G₂M cells were markedly decreased in both AdEHNull and AdEHCD40L treatment groups that corresponded to an increase in the sub-G₀ fraction (Untreated, 1.5%; AdEHCD40L, 36.8%; AdEHNull, 21.6%). The sub-G₀ fraction, indicative of cells with < 2n DNA content, is commonly considered to be representative of apoptotic cells.

Upon treatment with CoCl₂ to further upregulate HIF-1 α expression, S phase accumulation was evident as early as 48 hours with AdEHCD40L and AdEHNull treatments (AdEHCD40L: 72.1%; AdEHNull: 53.3%). This S phase arrest was sustained up to 144 hours (Figure 5.3B). By comparison, cell cycle distribution in the untreated culture was mostly unaltered by CoCl₂ treatment (83.4% in G₀/G₁). AdEHCD40L similarly exhibited a higher proportion (14%) of sub G₀/G₁ apoptotic cells as compared with AdEHNull (0.7%).

Cell cycle distribution analysis of untreated, CD40 negative ZR-75-1 breast cancer cells showed that majority of the cells accumulated at G₀/G₁ phase. Following AdEHNull treatment, 80% of cells remained at G₀/G₁ (80%) whereas the AdEHCD40L treatment resulted in accumulations in G₀/G₁ as well as the S phase (G₀/G₁: 49% vs. S: 42%) (Figure 5.3C). Collectively, we demonstrated that the adenovirus perturbs the cell

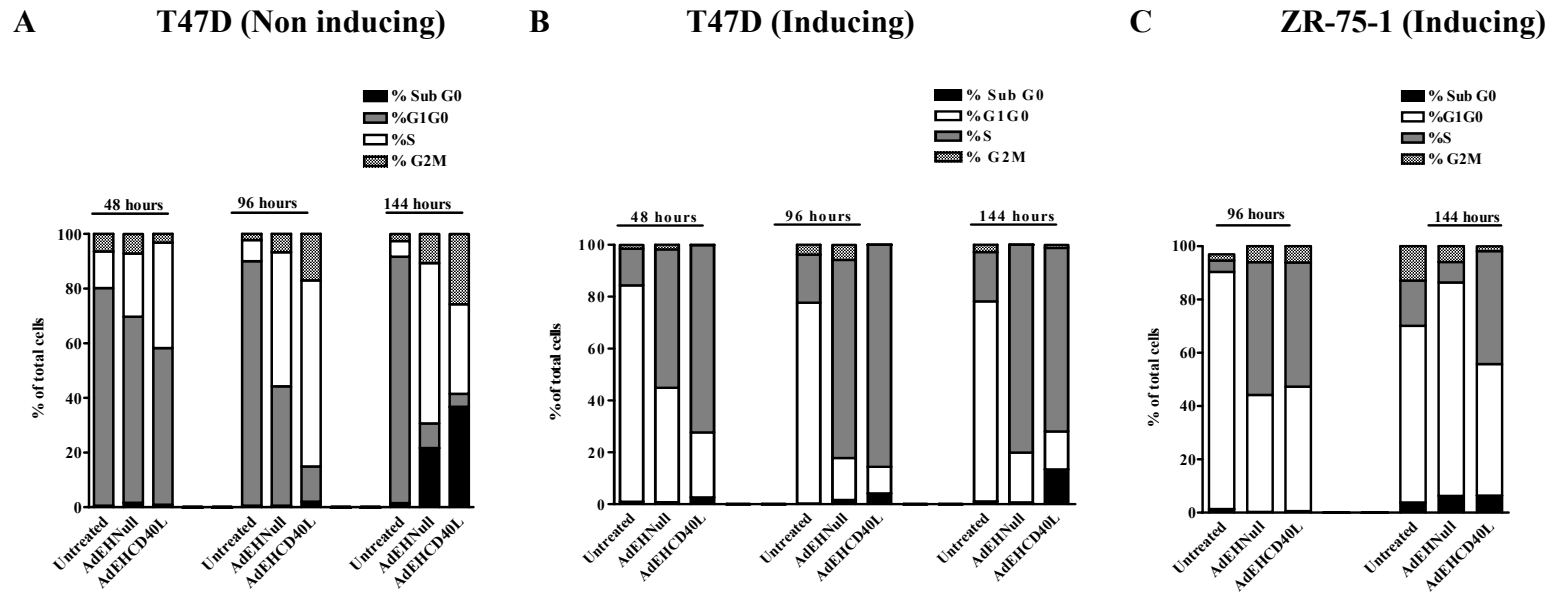


Figure 5.3: Cell cycle analysis. T47D and ZR-75-1 cells were infected with AdEHCD40L and AdEHNull (MOI = 1), under non-inducing and HIF-1 α inducing conditions. At graded intervals, cells were analyzed after propidium iodide staining for cell cycle distribution. Values represent percentage of total cells with a total of cycling and non cycling population equaling to 100%. Mean values are obtained from 3 independent experiments.

cycle resulting in an S phase accumulation. An increase in sub G₀ fraction of cells could be observed only in the CD40 positive cell lines.

NFkB Down-Regulation by AdEHCD40L

To further understand and characterize the mechanism of CD40L mediated growth inhibition, western blot analysis was performed to identify the involvement of signal transduction intermediates. PI3Kinase, p38, Erk, JNK and NFkB activation have been linked to CD40L and adenoviral perturbations. p42/p44 and AKT (also known as protein kinase B), downstream components of Erk and AKT signaling pathways, respectively, were evaluated. The phosphorylation status of proteins was used as an indicator of protein activation. Parallel studies were carried out with the AdEHNull and Adv-WT, in order to distinguish the pathways activated by CD40L vs. viral proteins. In addition, treatment with the recombinant CD40L protein was used as a positive control to validate CD40L mediated responses.

Based on studies with T47D cells, which maintains a viral permissive state in the absence of CoCl₂, we observed that the phosphorylation of p38 was not markedly affected by AdEHCD40L and AdEHNull. However, the phosphorylated form of p38 was down-regulated by the recombinant protein. By comparison, p42/p44 MAPK mediator was markedly increased by AdEHCD40L, AdEHNull, and Adv-WT (Figure 5.4). These changes were only evident at 24 hours and but not at 72 hours, suggesting that transient p42/p44 activation was primarily a viral mediated event. Similarly, we observed a parallel activation of AKT, a downstream mediator of the PI3Kinase by both AdEHCD40L and the control virus AdEHNull, while the recombinant protein did not alter the phosphorylated AKT level (Figure 5.5A, B).

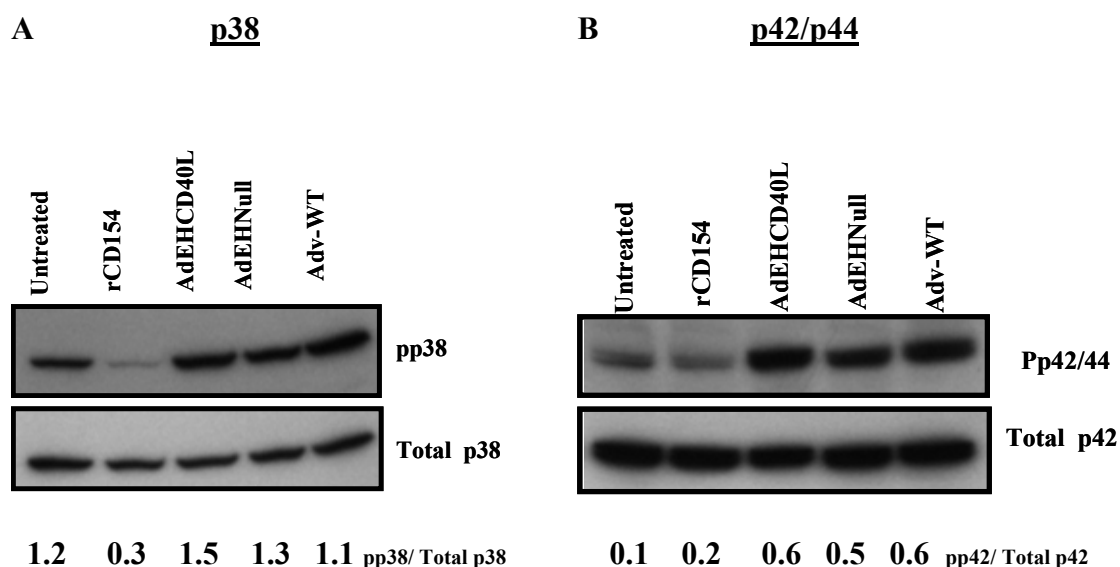


Figure 5.4: Western blot analysis for p38 and p42/p44: T47D cultures were infected with either AdEHCD40L or the control viruses AdEHNull or Adv-WT (MOI=1) under non inducing conditions. At 24 hours protein were extracted and subjected to western blot analysis. Membranes were probed for the phosphorylated forms of p38 (A) or p42 (B) protein, stripped and re-probed for the total protein levels. The bands were quantitated by Scion imagine analysis. The phosphorylated protein levels were normalized to the total protein levels. Values represented are based on the average normalized phosphorylated band intensities of 3 separate experiments.

This activation was observed at 24 hours and was sustained to 72 hours post infection, suggesting AKT activation is primarily virally mediated

The mobilization of NFkB by IκBα phosphorylation is one of the best known events of CD40 activation. IκBα localizes in the cytoplasm, complexes with NFkB keeping NFkB in an inactive state. The phosphorylation of IκBα releases NFkB from its inactive status, leading to its localization to the nucleus. IκBα phosphorylation status is therefore an indirect measurement of NFkB activity. We quantified IκBα phosphorylation in T47D cultures following AdEHCD40L and AdEHNull treatments. Phosphorylated IκBα levels were down-regulated by both AdEHCD40L and AdEHNull

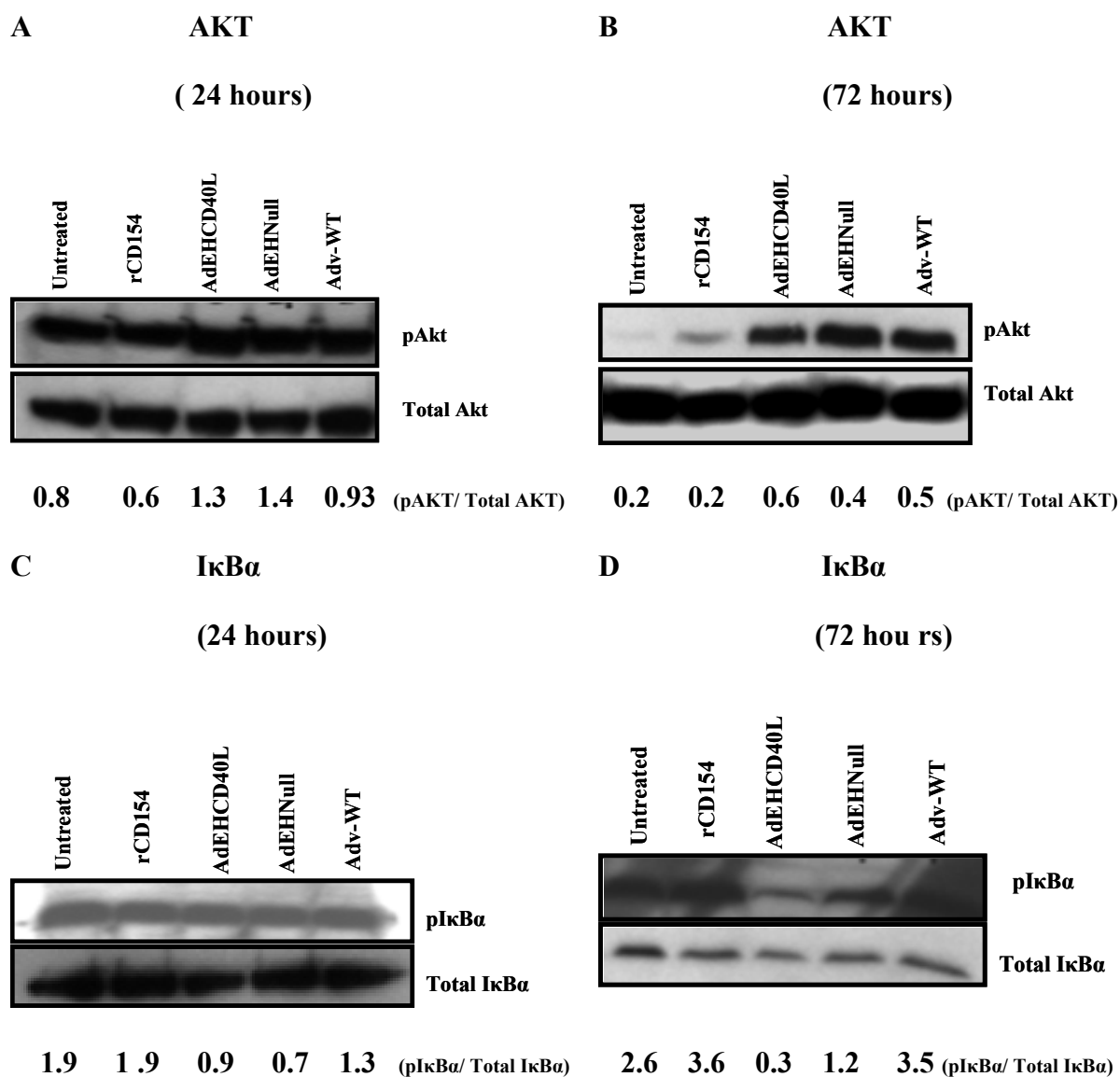


Figure 5.5: Western blot analysis for AKT and IκBα: T47D cultures were infected with either AdEHCD40L or the control viruses AdEHNull or Adv-WT (MOI=1) under non inducing conditions. At either 24 hours (A, C) or 72 hours (B, D) protein were extracted and subjected to western blot analysis. Membranes were probed for the phosphorylated forms of AKT (A, B) or IKK (C, D) proteins, stripped and reprobed for the total protein levels. The bands were quantitated by Scion imagine analysis. The phosphorylated protein levels were normalized to the total protein levels. Values represented are based on the average normalized phosphorylated band intensities of 3 separate experiments.

at 72 hours (Figure 5.5D) but were markedly more decreased in AdEHCD40L treated cells. By comparison, the recombinant protein up-regulated the I κ B α protein. This suggests that I κ B α is down-regulated differentially by AdEHCD40L.

p21^{Waf1/Cip-1} (cyclin dependent kinase inhibitor-1) is an inhibitor of cell cycle progression that acts in an NF κ B dependent manner¹⁵⁶⁻¹⁵⁸. In association with a broad range of cyclin-cdk (cyclin dependent kinase) complexes, over expression of p21^{Waf1/Cip-1} blocks the cell cycle progression through G₀ /G₁, G₂M or S arrest and inhibits the proliferating cell nuclear antigen, a subunit of DNA polymerase¹⁵⁹⁻¹⁶¹. We have measured the levels of p21^{Waf1/Cip-1} following the treatment of AdEHCD40L, the control viruses (AdEHNull and Adv-WT), as well as the recombinant CD40L protein. AdEHCD40L and recombinant CD40L did not affect the levels of p21^{Waf1/Cip-1} (Figure 5.6). In contrast, control viruses, AdEHNull and Adv-WT increased p21^{Waf1/Cip-1} levels, indicating AdEHCD40L exerted a unique and differential effect on p21^{Waf1/Cip-1}.

Biological Activity of NF κ B

In order to characterize the involvement of NF κ B inhibition on the growth regulatory activity of AdEHCD40L, blocking studies were performed with T47D cells. An I κ B kinase (IKK) inhibitor peptide that has been shown to blocks I κ B phosphorylation was used¹⁶².

Treatment with the inhibitor did not produce an additive growth inhibitory outcome in AdEHCD40L cultures but augmented the viral cytotoxic effects in AdEHNull and Adv-WT treated cultures (Figure 5.7). These findings provide indirect evidence that the CD40L transgene utilized I κ B α phosphorylation blockage to attain the growth inhibitory outcome above and beyond the viral cytotoxic effects.

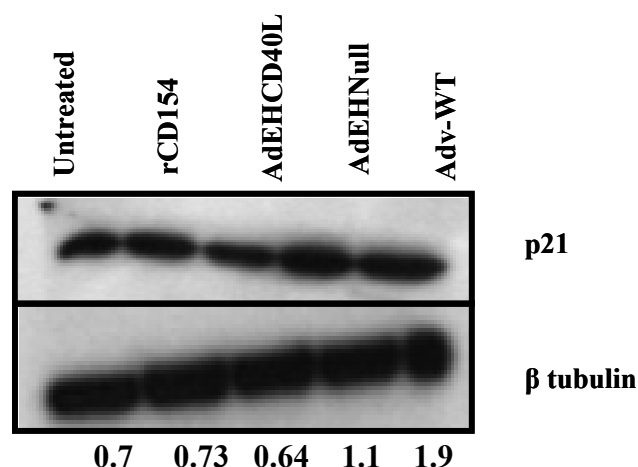


Figure 5.6: Western blot analysis for cell cycle regulator p21^{waf1/cip-1}: T47D cultures were infected with either AdEHCD40L or the control viruses AdEHNull or Adv-WT (MOI=1) under non inducing conditions. At 24 hours protein were extracted and subjected to western blot analysis. Membranes were probed for p21 protein, stripped and reprobed for the housekeeping protein β tubulin. The bands were quantitated by Scion image analysis. The p21 protein levels were normalized to β tubulin. Values represented are normalized band intensities based on a single experiment.

Collectively, we demonstrated that, 1) MAPK p42/p44 and AKT are activated by AdEHCD40L as well as the control viruses and likely reflect viral mediated effects (Table 5.1). Only AKT activation is sustained up to 72 hours. 2) AdEHCD40L uniquely down-regulated I κ B α that was not observed by AdEHNull or Adv-WT. 3) The recombinant CD40L activated the NF κ B pathway, but down-regulated the p38/MAPK pathway. 4) p21^{waf1/cip1} was up-regulated by AdEHNull and Adv-WT and not by AdEHCD40L. These findings indicate that the growth inhibitory activities observed by the CD40L transgene were accompanied by a unique down-regulation of I κ B α phosphorylation at 72 hours post infection (Figure 5.5D).

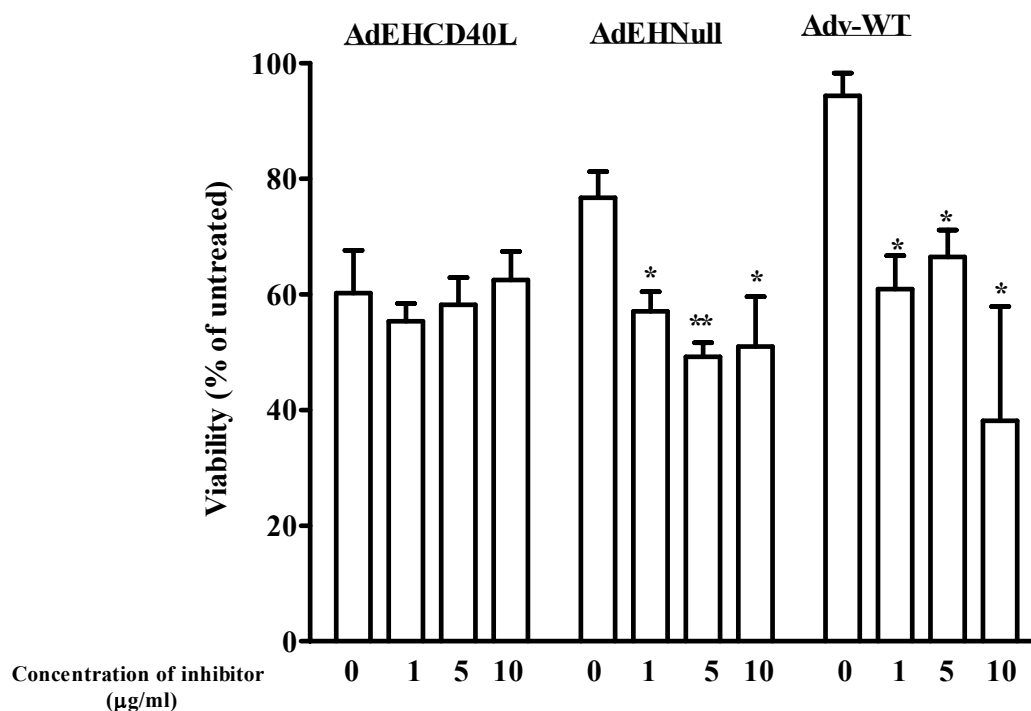


Figure 5.7: Effect of blocking $\text{I}\kappa\text{B}\alpha$ phosphorylation on growth regulation. T47D cells were infected with AdEHCD40L, AdEHNull or Adv-WT (MOI=1) under non inducing conditions. Following infections cells were treated with graded concentrations of $\text{I}\kappa\text{B}\alpha$ inhibitor peptide (1 $\mu\text{g/ml}$, 5 $\mu\text{g/ml}$, 10 $\mu\text{g/ml}$). At 96 hours post infection, the metabolic activity an indirect measure of cell viability was performed. Values were calculated as % untreated using the untreated cultures with the respective concentrations of inhibitor as a reference and are representative of a single experiment, run in triplicates. Statistical comparisons were made by comparing the respective virally infected cultures in the presence/absence of inhibitor to the untreated cultures in the presence/absence of the inhibitor. P value was determined using the 2-tailed unpaired t-test (* $p < 0.05$; ** $p < 0.005$).

Table: 5.1: Western blot analysis of transcription mediators

Transcription Mediators	Time in hours (Relative band intensities of phosphorylation protein/ total protein)									
	Untreated		Recombinant CD40L		AdEHCD40L		AdEHNull		Adv-WT	
	24	72	24	72	24	72	24	72	24	72
P38	1.2	BD	0.3	BD	1.5	BD	1.3	BD	1.1	BD
P42/p44	0.1	BD	0.2	BD	0.6	BD	0.5	BD	0.6	BD
AKT	0.8	0.2	0.6	0.2	1.3	0.6	1.4	0.4	0.9	0.5
I κ B α	1.9	2.6	1.9	3.6	0.9	0.3	0.7	1.2	1.3	3.5
JNK	BD	BD	BD	BD	BD	BD	BD	BD	BD	BD
P21	0.7	ND	0.73	ND	0.64	ND	1.1	ND	1.9	ND

Values represent band intensities of phosphorylated protein normalized to that of total protein.

ND: Not determined; BD: Below detection

Cytokines/ Chemokines in AdEHCD40L Treated T47D Cultures

Chemokines and cytokines have been shown to act as intermediate mediators of growth regulatory responses. To identify the chemokines and cytokines that may be produced by AdEHCD40L treatment, multiplex cytokine analysis was carried out with T47D cultures supernatants at 6 hours post infection. IL-1 α , IL-1 β , IL-6, IL-10, IFN α , IL-12p40, GM-CSF and MIP-1 α levels were below the detection limit (10 pg/ml) in virally treated as well as untreated cultures. The chemokines, RANTES was up-regulated moderately in AdEHCD40L treated (13 pg/ml) and recombinant CD40L treated (42 pg/ml) cultures, but not in other virus-treated cells. However, IL-8 and TNF α were only up-regulated in cells that were treated with the recombinant CD40L protein (Figure 5.8). While VEGF, an angiogenic mediator, was expressed in untreated and AdEHNull treated cultures, this cytokine was not detected in cells treated with the both AdEHCD40L and recombinant CD40L protein. These preliminary studies suggest that both the recombinant CD40L protein and AdEHCD40L up-regulated RANTES and down-regulated VEGF.

Discussion

The use of an oncolytic virus for CD40L transgene delivery implies a combined anti-tumor outcome derived from CD40 ligation and the viral oncolytic process. The underlying mechanisms of tumor cell killing by an oncolytic adenovirus remains unclear. By comparison, a number of pathways have been shown to be associated with the positive and negative growth regulatory effects of CD40 ligation. Individual pathways

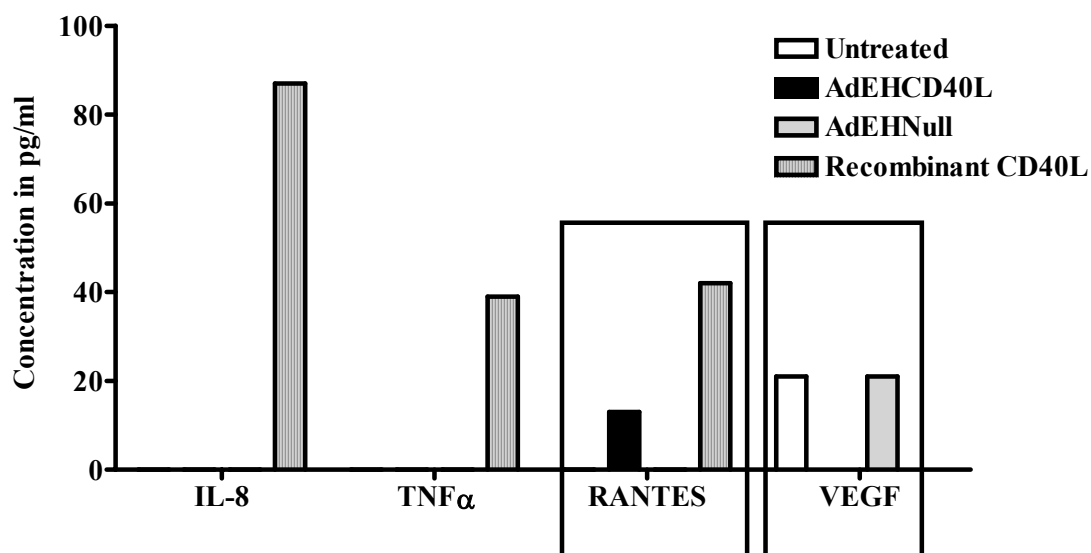


Figure 5.8: Luminex analysis of chemokines and cytokines. T47D cultures were infected with either AdEHCD40L, the control virus AdEHNull (MOI=1) and the recombinant CD40L protein (1 μ g/ml) for 6 hours. Supernatants were collected and subjected to multiplex luminex analysis. Values represented are based on a single experiment run in duplicates. Concentrations below 10 pg/ml were considered as negative and below the detection limit of the assay.

that are activated appear to be cell specific and are also depend on the strength and duration of CD40 ligation. PI3Kinase, NFkB, JNK, p38, and Erk1,2 have been shown to be involved in opposing CD40L mediated apoptotic responses^{38, 40, 149, 163}. We previously reported that breast cancer growth inhibition by recombinant CD40L was accompanied by apoptosis, with a corresponding up regulation of the apoptotic mediator Bax³⁰. These findings suggest that Bcl-2 family members may contribute to the growth inhibitory outcome.

The delivery of CD40L by a non replicative adenovirus has been demonstrated in hematological malignancies, and shown to mediate its anti-tumor efficacy through an increased sensitivity to Fas mediated apoptosis¹⁰⁴. However, there is little indication that similar mechanisms manifest in cells that were infected by AdEHCD40L.

The role of NFkB in regulating cell growth in cancer cells is well established¹⁶⁴⁻¹⁶⁶. A number of studies have shown that CD40L growth inhibitory activity is observed only when NFkB activation is blocked. This suggests that NFkB activation negatively regulates cell growth. We observed that AdEHCD40L treatment decreased the level of phosphorylated IκBα. These findings indirectly support the notion that reduced NFkB activity accompanied the CD40L-mediated growth inhibitory event. The blocking of IκBα phosphorylation provided an additive effect to the control adenoviruses but not to the AdEHCD40L mediated cytotoxicity. These finding suggest that AdEHCD40L already involved the NFkB pathway (Figure 5.9).

Unlike our previous observations with recombinant CD40L³⁰, AdEHCD40L mediated growth inhibition was not accompanied by an increased apoptotic activity. However, the proportion of non-viable cells were observed by propidium iodide staining, which correlated to a recent report suggesting that conditionally replicative adenovirus kill tumor cells via an independent mechanism that resembles “necrosis like” programmed cell death¹⁶⁷. This is not surprising as the adenovirus is equipped with survival mechanisms that counteract host cell apoptotic machinery in order to facilitate the viral replicative process^{101, 168, 169}. However, further evaluations are needed, including the characterization of other apoptosis parameters like DNA fragmentation and

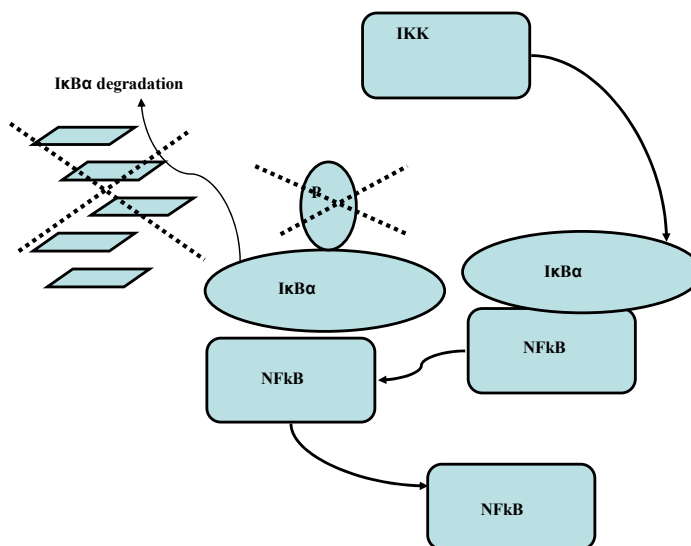


Figure 5.9: Putative mechanism of AdEHCD40L perturbation of NFκB pathway. The putative mechanisms of NFκB by AdEHCD40L, suggests blockage of IκBα phosphorylation by the inhibitor IκBα kinase (IKK) which was not observed by the control AdEHNull or Adv-WT control viruses. This blockage might contribute to NFκB inactivity thus enhancing the cell killing properties of AdEHCD40L.

the characterization of apoptotic mediators in order to exclude the involvement of apoptosis in the cell killing process by AdEHCD40L. Both adenovirus and CD40L may affect the cancer cell growth process via cell cycle accumulation¹⁶⁹⁻¹⁷¹. AdEHNull treatment produced an S phase blockage while AdEHCD40L resulted in both S and G2/M phase arrests that were followed by an increased apoptotic population. The ability of AdEHNull and AdEHCD40L to cause cells to accumulate in the S phase is not surprising considering the adenovirus has the ability to drive the cell through the S phase via its E1A early proteins.

p21^{Waf1/cip1} is known to negatively regulate cell cycle¹⁷², inhibit apoptosis¹⁷³ and induce S phase arrest^{161, 174}. The context in which p21^{Waf1/cip1} induces cell cycle

arrest is dependent on the interactions with cyclin-cdk's. Our preliminary studies show that p21^{Waf1/cip1} was up-regulated in the control virally treated groups and not in the AdEHCD40L group. Given the role of p21^{Waf1/cip1} in regulating cell cycle, further evaluations on the implications of p21^{Waf1/cip1}, its role in cell cycle arrest and apoptosis are needed to better define the mechanism of AdEH mediated anti-tumor activity.

VEGF is a well known cytokine that is produced by breast cancer cells for their pro-angiogenic activity^{175, 176}. AdEHCD40L and the recombinant CD40L protein treatments were accompanied by reduced VEGF production. This is in contrast to other studies that have shown that CD40 triggered by a monoclonal antibody increased VEGF secretion in endothelial cells, multiple myeloma and monocytes^{33, 177, 178}. One possible explanation for the decrease in VEGF observed by us might be that CD40L regulation of VEGF maybe dependent on the source of CD40L and dependent on the cell type.

RANTES, is a chemokine previously described to be up-regulated by CD40L interaction and implicated in breast cancer progression¹⁷⁹⁻¹⁸¹. We observed that RANTES was up-regulated in culture supernatants of AdEHCD40L and recombinant CD40L treated T47D breast cancer cells indicating that CD40 ligation is likely to contribute to their expression. The relevance of these findings needs to be further investigated as their altered levels are far below those that can attain patho-physiological effects or impact cell growth in culture¹⁸²⁻¹⁸⁴.

Our preliminary evaluations indicate that the AdEHCD40L mediated the growth regulatory outcome was accompanied by unique cellular and molecular outcomes. They

are attributable to viral oncolytic and CD40 dependent events (Figure 5.10) involved in cell cycle progression, apoptotic regulation and cytokine production. Further studies will elucidate the relative importance of these events in order to optimize anti-tumor outcome.

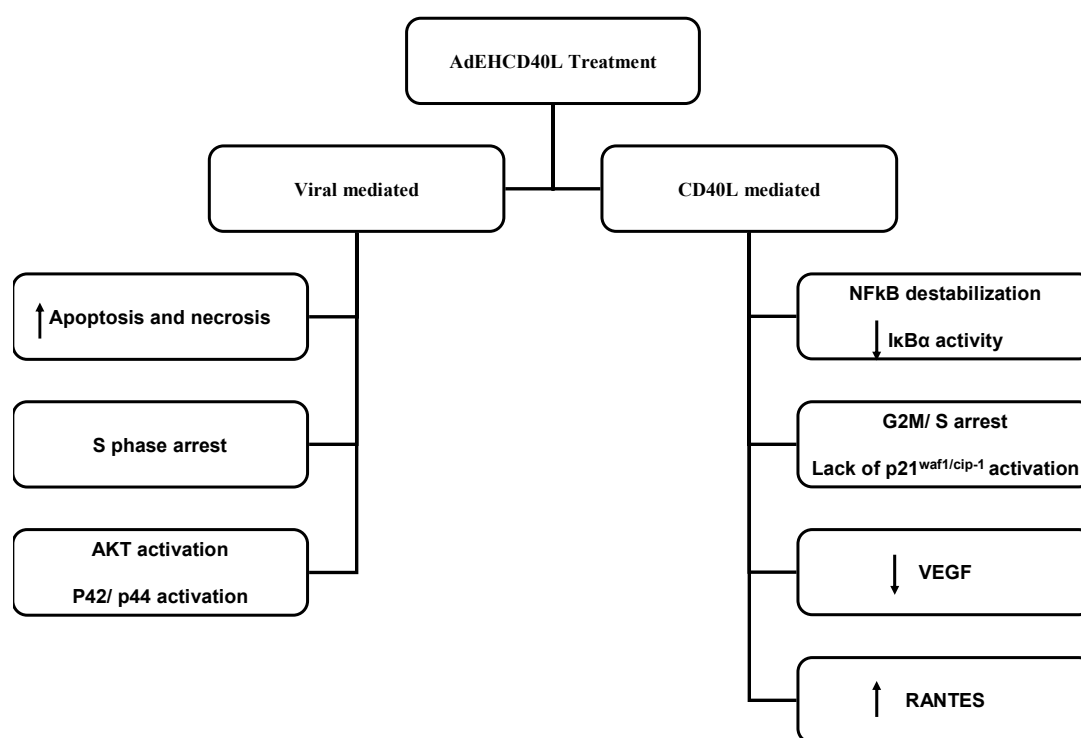


Figure 5.10: Schematic of pathways affected by AdEHCD40L.

CHAPTER SIX

Conclusion and Future Studies

The ability of CD40L to concomitantly impact cell growth and activate the immune system makes it an excellent candidate for the targeted therapy of cancer. Additionally, the widespread expression of its target molecule CD40 on various hematological and solid tumors suggests that CD40L therapy can be used for treatment of a wide array of cancers.

Hypoxia has been correlated with poor prognosis in breast cancer patients and associated with the estrogen unresponsiveness and the resistance to traditional therapies. In our study we have utilized the tumor hypoxic environment to facilitate selective expression of CD40L by a replicative adenovirus. My data support our previous findings with recombinant CD40L that CD40L can directly inhibit the growth of breast cancer cells. The enhanced anti-tumor response by the CD40L transgene was mediated by viral oncolysis and CD40L toxicity in vitro, which proved to be markedly more efficient than the recombinant CD40L protein. AdEHCD40L can regulate viral replication and CD40L in the context of the hypoxic status of the cells. Perturbation of cellular signaling by the CD40L transgene did not appear to be antagonistic to the adenovirus replicative activity, even though CD40L and the adenovirus may modulate similar signaling pathways¹⁵². Preliminary findings underlying the mechanisms of AdEHCD40L cytotoxicity indicated an increased apoptotic (Annexin V+) and necrotic (propidium iodide incorporation)

activities that were accompanied by reduced I κ B α phosphorylation, lack of p21^{waf1/cip-1} activation, G₂M/S cell cycle arrest, and differential chemokine and cytokine expression. Given the role of p21^{waf1/cip-1} in cell cycle progression, NF κ B regulation, and apoptosis, further studies are needed to define mechanisms governing the role of p21^{waf1/cip-1} and its relation to cell cycle arrest, NF κ B blockage and apoptosis.

AdEHCD40L and AdEHNull can inhibit tumor cell growth by 44 - 58% in breast cancer hu-mouse xenografts. The optimal dosage of AdEHCD40L to enhance tumor growth inhibition needs to be further explored and seems to be dependent on the growth rate of the tumor and the viral dose. A viral dose of MOI = 1 and below of the AdEH virus is optimal based in our in vitro findings. This suggests that therapeutic outcome can be attained by administering lower doses of adenovirus. This would help further our hypothesis that AdEHCD40L enhances tumor cell growth when compared to the parental AdEHNull construct.

Future Studies

Cancer-selective biotherapy or gene therapy approaches have widely been considered to be the next horizon towards developing a cure for breast cancer. Due to the rapid immune clearance of the virus by the host immune system, the systemic anti-tumor activity of AdEHCD40L will be evaluated in a SCID models initially either by determining the viral effect on a contra-lateral implanted tumor or by using an intravenous model. Further, given the ability of CD40L to directly impact cell growth and activate the immune system, a syngeneic breast cancer mouse model will be considered to evaluate the impact of AdEHCD40L on anti-tumor immunity. The

hypothetical mode of action of AdEHCD40L in an immune competent system has been outlined in figure 6.1.

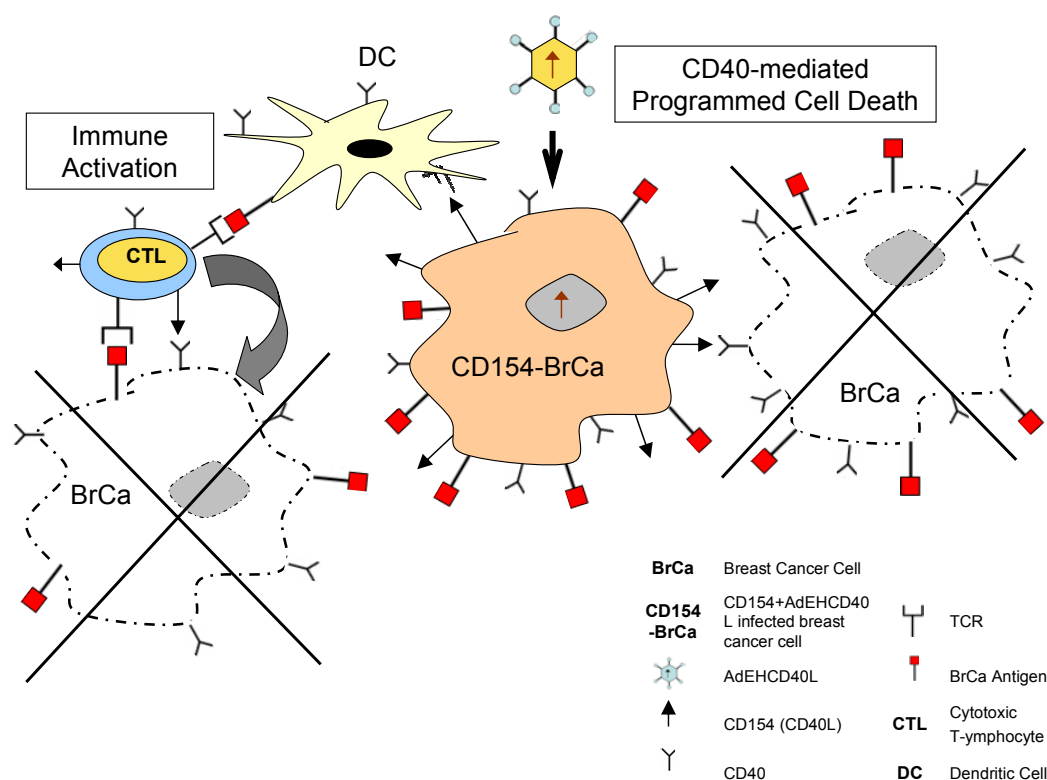


Figure 6.1: Hypothetical anti-tumor activity of AdEHCD40L. Potential anti-tumor activities of an oncolytic virus delivering CD40L include the direct growth inhibition through CD40-CD40L interactions and viral oncolysis. Additionally, bystander immune activation is expected. Dendritic cell tumor antigen uptake and CD40L stimulation could enhance culminating the generation of cytotoxic T cells that would result in inhibition of tumor growth.

Micro-arrays represent an important high throughput tool in analyzing gene expression profiles at the transcriptional level. Over 46,000 genes differentially expressed in treated controls can be compared to the normal counterparts and this approach can

accelerate the identification of important transcripts and key pathways involved in the therapeutic outcome

Primary breast cancer cells harbor mammary self-renewing stem cells that have oncogenic potential^{185, 186}. Given the recent findings by others that hypoxia plays a role in the survival of breast cancer stem cell markers^{71, 187, 188}, the ability of the hypoxia regulated AdEHCD40L to inhibit the growth of the cancer stem cell population will be considered.

APPENDICES

APPENDIX A

Cloning of the AdEH Recombinant Adenoviral Constructs

Modification of the Viral Genome

The genome of adenovirus was modified in order to include the following features:

- Deletion of the endogenous E1A promoter and substitution by the 5XEH3 promoter
- Deletion of the endogenous E4 promoter and substitution by the E2F-1 promoter (obtained by PCR from human genomic DNA using the following set of primers:
- 5'TACTGTAAC TATAACGGTCCTAAGGTAGCGTGGTACCATCCGGACAAAGCC-3', and 5'TAAGTATT TAAATGGCGAGGGCTCGATCCCCGC-3')
- Introduction of an insulator sequence between the packaging signal and the E1A promoter. This sequence (bovine growth hormone transcriptional stop signal) was obtained from the plasmid pCDNA3 (Invitrogen) by digestion with the restriction endonucleases PvuII and NotI.
- Deletion of the genes encoding the gp19K/6.7K proteins in the E3 region, and substitution with the CD40L cDNA.

As starting material, the pSEHE2F plasmid was used ⁷⁰. This plasmid already contains the modifications of the E1 and E4 promoters, and the insulator sequence. The introduction of the CD40L transgene was performed in several steps, as follows:

- Isolation of the 4.7kb fragment obtained by digestion of pSEHE2F with AgeI.
- Introduction of this fragment in the AgeI site of the plasmid pMIB/V5-HisC (invitrogen). This intermediate plasmid was named pMIB-AgeC. The purpose of this step is to isolate the viral fragment from the rest of the adenoviral genome in a smaller plasmid that contains AgeI restriction sites. This is needed to perform the following modifications in this fragment.
- Construction of a fragment that contains a XmnI restriction site in the position 28555 of adenovirus type 5 sequence. It was obtained by PCR using the plasmid pSEHE2F as a template, with the following set of primers (the XmnI site is underlined): 5'AAGGACTAGTTTCGCGCCCTTTCTCAAATTTAAGC3' and 5'CCGATTCTAGAGAAACCTGAATTAGAATAGCCCGTAGAGTTGCTTGAAATTGTTCTAAACCCAC 3'.
- Digestion of pMIB-AgeC with SpeI and XbaI and introduction of the PCR fragment described above. The new plasmid was named pMIB-E3Xmn.
- Digestion of pMIB-E3Xmn with MunI (in position 29355 relative to adenovirus type 5 sequence) and simultaneous partial digestion XmnI. A partial digestion with XmnI was needed in order to cut only in position 28555. This way, the fragment comprised between the nucleotides 28555 and 29355 of the adenoviral sequence (corresponding to the sequence of gp19k/6.7k) is excised from the plasmid.
- In this location, a cassette containing the recognition sequence for the enzyme PstI-SceI (PI-SceI adapter) was introduced by ligation. The adapter was obtained by hybridization of the following oligonucleotides: 5'ACGTAATCTATGTCGGGT

GCGGAGAAAGAGGTAATGAAATGGCA3' and TGCCATTTTCATTACCTC TTTCTCCGCACCCGACATAGATTACGT3'. The resulting plasmid was named pMIB-PI-SceI. This construct allows the introduction of foreign sequences in the E3 region, using the enzyme PI-SceI.

- The pMIB-PI-SceI plasmid was digested with the enzymes AgeI and ScaI simultaneously, and the 4.7 kb fragment was subcloned into the same sites of the pSEHE2F plasmid. This way the mutated E3 region was introduced into a partial viral genome. This intermediate construct was digested with SwaI and SpeI, and the 7.7 kb fragment obtained was subcloned again in the pSEHE2F plasmid, in order to reconstruct a fully functional recombinant adenoviral sequence.
- The recombinant adenoviral sequence was digested with PI-SceI, and the CD40L cDNA was introduced in this site by ligation, using the PI-SceI adapters.
- The resulting plasmid (pSEH40L) contains the same modification of viral promoters E1A and E4 as the pSEHE2F plasmid, plus the CD40L inserted into the E3 region. This location allows the transcriptional control of the transgene by the endogenous adenoviral late promoter, which is active once the viral replication has started¹⁸⁹.

Generation of Viral Particles

The pSEH40L plasmid was digested with PacI in order to liberate the viral genome. After phenol/chloroform extraction and ethanol precipitation, the DNA was resuspended in 10 mM Tris pH 8.1 and transfected in 293 cells using the Calcium Phosphate method. Once cytopathic effect was evident, the cells were collected and lysed by three cycles of freezing and thawing. The supernatant was used to re-infect

A549 cells treated with Cobalt Chloride in order to induce stabilization of HIF-1 α . The cells were covered with soft-agar, and viral plaques were isolated 10 days later. The viral clones were confirmed by PCR amplification of critical regions and sequencing of the products (E1A, E4 and E3 regions). One of the clones was amplified in A549 cells, purified using a double cesium Chloride gradient, and desalted using a sepharose column. The quantification was performed by spectrophotometer (particles) and plaque forming assay (pfu).

APPENDIX B

Purification, Titration and Genomic Validation of AdEHCD40L

Material and Methods

Purification and Titration of Adenovirus

Purification and titration of the recombinant adenoviral vectors (AdEHCD40L and AdEHNull) as well as the wild type (Adv-WT) control virus is schematically represented in Figure A.1. Unlike the wild type (Adv-WT) vector, cesium chloride (CsCl) centrifugation of recombinant AdEH constructs yields two bands on the gradient formed with a final concentration of 1.33 gm/ml and 1.45 gm/ml. The lower band is collected as it contains the infectious virus.

Polymerase chain reactions (PCR) were carried out to validate the genomic configuration of the viral construct. Viral DNA was extracted with the QIAamp deoxyribonucleic acid (DNA) blood mini kit using the manufacturer's protocol (Qiagen, Valencia, CA). Briefly purified virus was treated with proteinase K and lysis buffer. The mixture was heated at 56°C for 10 minutes. The viral lysate was then treated with 100% ethanol, pulse vortexed briefly and then loaded onto a QIAamp spin column. DNA was eluted in 60 µl of elution buffer after appropriate washes in between. The extracted DNA (60 ng) was amplified by PCR (GeneAmp RNA PCR kit, Perkin Elmer, Foster City, CA) using sequence specific primers for adenoviral E1, E3 and E4 modified regions (Figure A.2). PCR amplification conditions were: an initial/ denaturation of 95°C for 1 minute

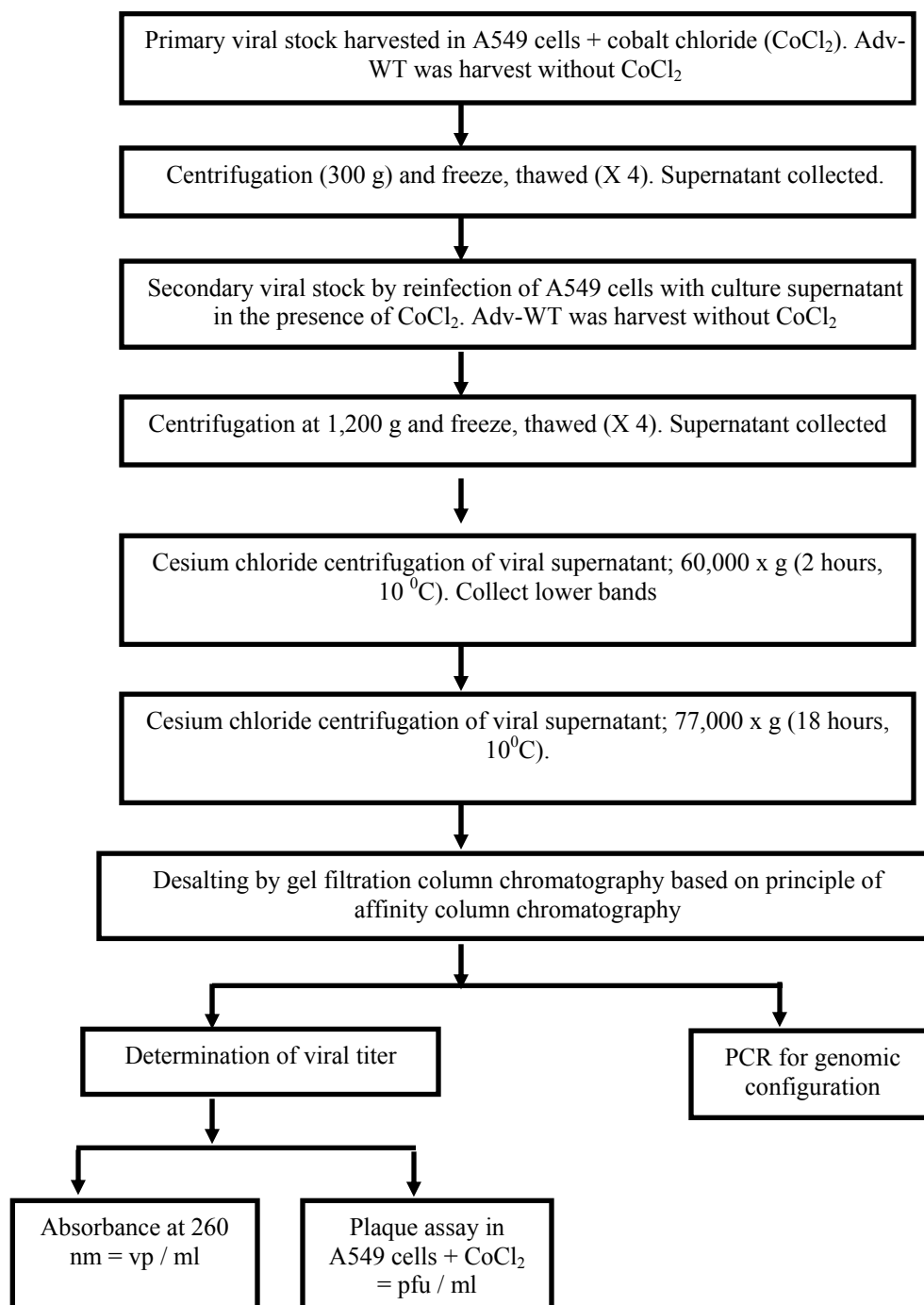


Figure B.1: Schematic for viral purification, quantification and validation of genomic integrity.

E1A

- 1- Forward 5' TAGTGTGGCGGAAGTGTGATGTTG 3'
- 2- Reverse 5' TCTTCGGTAATAACACCTCCGTGG 3'

E3

- 3- Forward 5' AAGGACTAGTTTCGCGCCCTTTCTCAAATTTAAGC 3'
- 4- Reverse 5' TTGGTCATCTCTGTTAGGGTGGG 3'

E4

- 5- Forward 5' AAAGTGGTCACCGTGATTAAAAAG 3'
- 6- Reverse 5' CGATCATTAATTAACATCATCAATAATATACC 3'

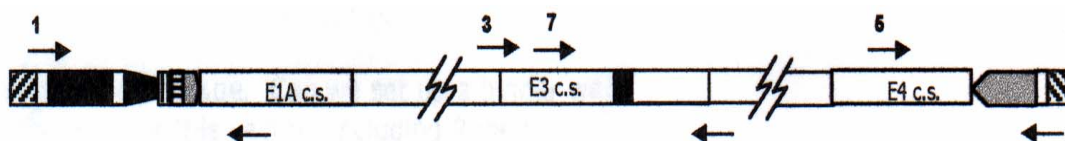


Figure B.2: Primer sequences and schematic of primer position used for PCR amplification of E1, E3 and E4 modified sequences.

followed by 35 cycles of 94°C for 1 minute; annealing of 55°C for 45 seconds; elongation of 72°C for 1 minute. The reaction was terminated with a final elongation step of 72 °C for 5 minutes. Wild type adenovirus (Adv-WT) was used as positive control for sequence specific amplification.

Sequencing of the CD40L cDNA Inserted into AdEH

Dideoxy sequencing was carried out to verify the fidelity of the inserted cDNA sequence. 60 ng of purified DNA from AdEHCD40L was amplified by PCR with forward primer 5'AAGGACTAGTTTC GCGCCCTTTCTCAAATTTAAGC3' and reverse primer 5'TTGGTCATCTCTGTTAGGGTGGG3' flanking the CD40L insert. The PCR products were verified by agarose (1.5%) gel electrophoresis and purified using

the QIAquick gel extraction kit (QIAGEN, Valencia, CA) according to the manufacturer's protocol. The concentration of the purified products was determined by densitometric gel band analysis using the Alphamanager 2000D and Scion Image Software ¹⁹⁰, and the PCR products were sequenced by the BigDye dideoxy cycle sequencing method (BigDye terminator cycle sequencing kit; Applied Biosystems, Foster City, CA). 60 ng of purified PCR products were used as template and the sequencing primers include forward (5'CAGGAGGTGAGCTTAGAAAACCCTTAG3') and reverse (5'TTCTCCTGTGTTGCATCTCTGT 3') corresponding to residues corresponding to residue 28484 of the adenovirus through the PI-sce-I cloning sites and 228 - 249 bp (base pair) of CD40L cDNA; forward (5'CAGATGATTGGGTCAGCACT 3') and reverse (5'GTCACCTTCTGTTCCAATCG3') corresponding to residues 124 – 143 bp and residues 595 – 614 bp of CD40L cDNA; forward (5'GGATACTACACCATGAGCAACA3') and reverse (5'TTCATTACCTCTTTCTCCTGGGCTTAAG3') corresponding to residues 451 – 473 bp of the CD40L cDNA and residue 27077-27111 bp of the adenovirus. The products were separated from the unincorporated terminators and purified by spin column purification (Centri-sep spin columns, Princeton separation, Adelphia, NJ). Each sample was suspended in 25 µl of template suppression reagent (TSR) (Applied Biosystems), denatured by heating at 95°C for 2 minutes and run on an ABI prism 310 genetic analyzer (Applied Biosystems) with an injection speed of 6 seconds. The sequencing data was analyzed bi-directionally and aligned with the known sequence of the human CD40L cDNA ¹⁹¹.

Plaque Assay

To determine the infectious titers of the purified virus, a plaque forming assay was performed. A549 (1.25×10^6) cells were dispensed in a 60 mm petri dish and grown to 70 - 80% confluent at time of viral infection. Purified virus were serially diluted (10^2 - 10^{10}) in media (DMEM + 2 % FBS + 100 μ M CoCl₂). Two milliliters (mls) of serially diluted virus were added to the A549 culture and incubated at 37°C, 5 % CO₂ for 90 minutes. The virus inoculant was decanted and the cell culture rinsed with phosphate buffer saline (PBS). The infected cells were over-layered with 5 mls of DMEM/agarose mixture (1:2) containing 2X DMEM + 1:100 antibiotics + 4% FBS + 200 μ M CoCl₂. The plates were allowed to solidify and placed in a 37°C, 5% CO₂ incubator. Viral plaques were evident within 4 – 5 days of culture and viral titer was determined at day 10 for recombinant viruses. Calculations for determination of viral titer is based on infected cultures that contained between 20 and 100 plaques per plate and calculated with the formulae: plaque forming units (pfu/ml) = [(Mean number of plaques) X dilution factor (D)] / volume of infective medium used. The Adv-WT was used as a positive reference control while mock treated cultures with media alone were used as negative controls.

Quantification of Viral Yield

The purified virus (10 μ l) was denatured with 10% sodium dodecylsulfate (SDS) at 56°C for 10 minutes, which disassembles the virus into its protein components and then briefly centrifuged (300 g, 7 minutes). UV-absorbance of the lysed virus was measured at 260 nm for its DNA content against an AD buffer reference (appendix II).

The viral particle concentration is calculated according to ¹⁹², where a 1.00 absorbance unit (AU) (1 cm pathlength) at 260 nm corresponds to 1.1×10^{12} viral particles (vp) /ml.

Results

Validation of Genomic Configuration of Purified Adenoviral Vectors

To attain conditional replicative activity in cancer cells, the AdEHCD40L adenovector incorporates hypoxic response element (HRE) and estrogen response element (ERE) and E2F-1 promoters that restricts the viral replication and CD40L transgene expression to cancer cells over-expressing HIF-1 α (prevalent in the hypoxic environment), estrogen and E2F-1. To verify that these genetic modifications were retained after the viral expansion and purification, PCR using sequence specific primers for viral E1, E3 and E4 regions (Figure A.3) were carried out to define the expected molecular configuration of the construct carrying CD40L (AdEHCD40L), as well as the control virus lacking the transgene (AdEHNull). Amplification products of the expected size for AdEHCD40L (1000 bp); E3 (2431 bp) and E4 (850 bp) were compared with their wild type counterparts (497 bp, 2421 bp and 708 bp, respectively) (Figure A.3) and found to retain the inserted modifications. Bidirectional DNA sequencing was also carried out to verify that the CD40L transgene cDNA insert was of the wild type genotype (Figure A.4). These findings indicate that adenovirus vectors maintained the expected molecular configuration throughout the expansion and purification processes.

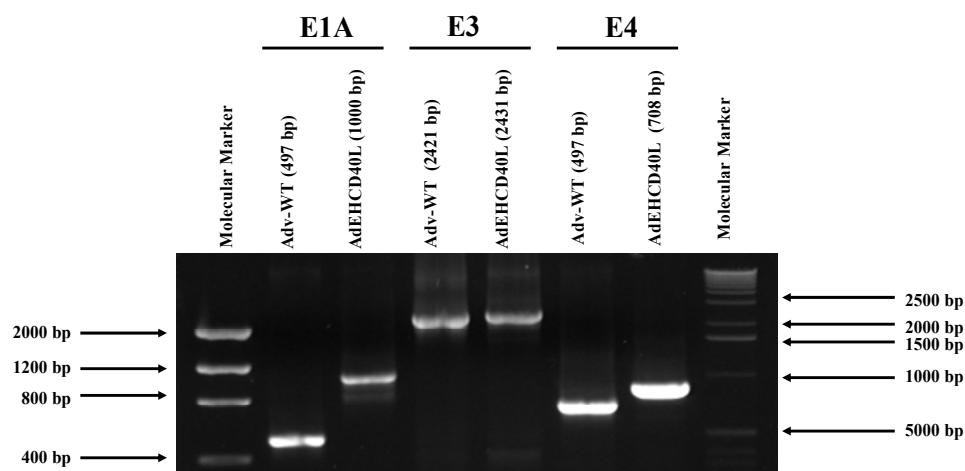


Figure B.3: Sequence specific amplification of the viral construct. Amplification products of the expected size was observed for recombinant AdEHCD40L E1A (lane 3, 1000 bps), E3 (lane 5, 2431 bps) and E4 (lane 7, 850 bps) regions using sequence specific primers at 35 cycles. Control E1A (lane2, 497 bps), E3 (Lane 4, 2421 bps) and E4 (lane 6, 708 bps) regions were amplified with the Adv-WT adenovirus DNA template to identify location of the of the unmodified E1A, E3 and E4 regions. Lanes 1, 8: Low molecular weight and high molecular weight DNA markers.

Adenoviral Titration

The expansion of recombinant adenovirus vectors commonly yields infectious particles as well as non infectious particles, whose relative distribution that can be determined by quantification of viral particles (vp) as well as enumeration of plaque forming units (pfu). The quality of the viral preparation is inversely related to the vp/pfu ratio. Viral particles (infectious and non infectious) for the Adv-WT and the recombinant constructs (AdEHCD40L and AdEHNull), ranged from 10^{12} - 10^{13} vp/ml according to spectrophotometric analysis.

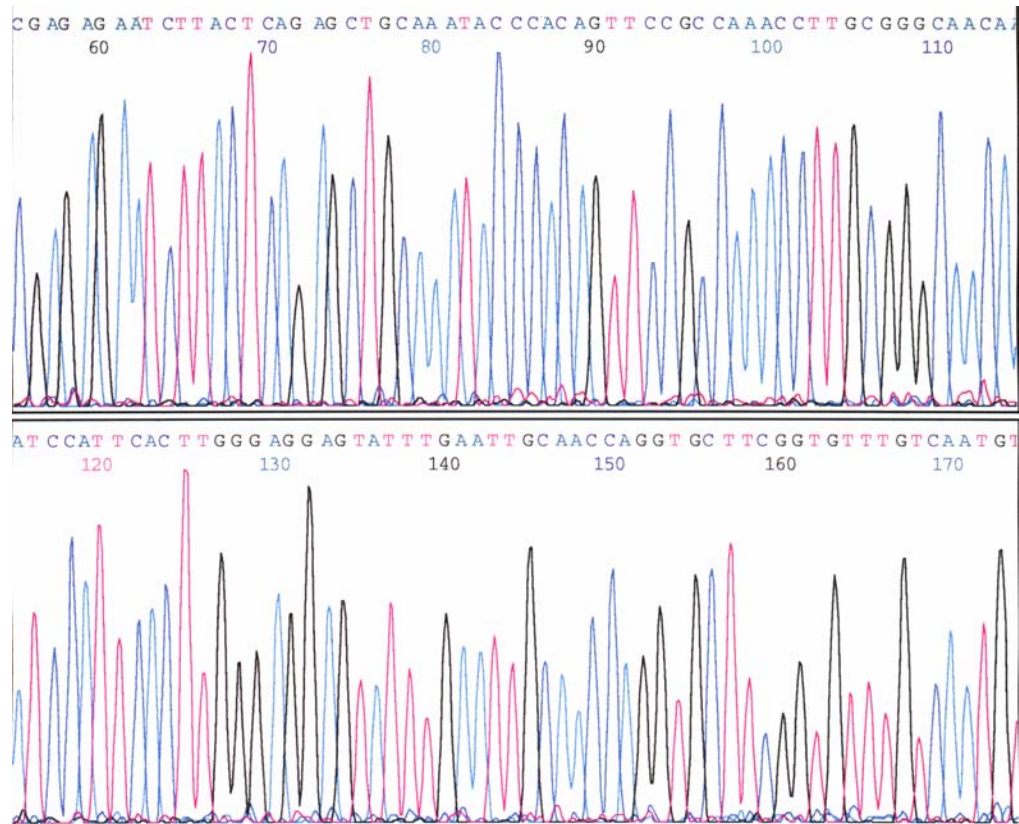


Figure B.4: Bidirectional DNA sequencing data of the CD40L transgene by the dye terminator labeling method. Each of the four dideoxy terminators (ddNTP's) is tagged with a different fluorescent dye. The growing chain is terminated and labelled with the dye that corresponds to A: Green, C: Blue, G: Black, T: Red.

Discussion

By using a standard plaque forming assay the minimal titer needed to infect, replicate, and lyse the cells was determined using the human embryonic kidney cell line (293 cells), an E1A transformed cell line^{193, 194}. Viral titers for AdEHCD40L and the control virus, AdEHNull range from 60 - 600 vp /pfu, as compared with a ratio of 43 for the wild type adenovirus preparation (Table A.1). This range of infectivity may be attributable to the variation in the recovering of infectious viral particles from different culture batches. However, for all experiment carried out with the AdEHCD40L and

Table B.1: Quantification of viral yield by spectrophotometry and plaque forming assay.

Cell lines	Virus	CoCl ₂	Viral titers		vp/pfu ratio
			pfu/ml	vp/ml	
A549	Adv-WT	None	1.3×10^{11}	3.7×10^{12}	26.4
A549	Adv-WT	100 μ M	1.5×10^{11}	3.7×10^{12}	28.8
293	Adv-WT	100 μ M	1.4×10^{11}	3.7×10^{12}	25.1
A549	AdEHCD40L	100 μ M	1.0×10^9	6.3×10^{11}	618
A549	AdEHCD40L	100 μ M	2.0×10^{10}	1.5×10^{12}	73
A549	AdEHCD40L	100 μ M	2.5×10^9	5.6×10^{11}	219
A549	AdEHNull	100 μ M	2.1×10^9	8.4×10^{11}	409.8
A549	AdEHNull	100 μ M	8.9×10^9	8.6×10^{11}	97
A549	AdEHNull	100 μ M	4.4×10^9	9.4×10^{11}	216

AdEHNull comparable vp/pfu ratios were used. This negates discrepancies that might occur due to variations in the non-infectious particles used to determine the biological outcome. Comparable titers were obtained in A549 lung epithelial cell lines. Cobalt chloride, which stabilizes/induces hypoxic inducible factor (HIF-1 α), did not affect the viral yield (Table A.1).

We were able to expand and purify the AdEH constructs by cesium chloride centrifugation without losing the inserted transgenes and modified promoters. Due to the presence of the tumor specific promoters that restrict viral E1A expression, the virus can only replicate and lyse cells under hypoxic conditions or in cell lines that are

transformed to express E1A. Previous reports recommend early passage HEK 293 cell line as an appropriate candidate to determine adenoviral titers due to their trans acting E1A transformed components (^{193, 195}). However, this cell lines tends to loose its trans-acting E1A component over passing of cells. We were able to attain comparable titers with A549 cells in the presence of CoCl_2 hence obviating utilization of low passage HEK 293 cells that are commonly required for viral titer validations ^{193, 194}.

In conclusion we were able to expand and purify the AdEH constructs without loosing the incorporated promoter and transgene modifications.

APPENDIX C

CD40L Sequence

1 tctgccagaa gataccattt caactttaac acagcatgat cgaaacatac aaccaaactt
61 ctecccgatc tgcggccact ggactgccca tcagcatgaa aatttttatg tatttactta
121 ctgttttct taccaccag atgattgggt cagcactttt tgctgtgtat cttcatagaa
181 gggtggacaa gatagaagat gaaaggaatc ttcatagaaga tttgtattc atgaaaacga
241 tacagagatg caacacagga gaaagatcct tatecttact gaactgtgag gagattaaaa
301 gccagtttga aggctttgtg aaggatataa tgtaaacaag agaggagacg aagaaagaaa
361 acagcttga aatgcaaaaa ggtgatcaga atcctcaaat tgcggcacat gtcataagtg
421 aggccagcag taaaacaaca tctgtgttac agtgggctga aaaaggatac tacaccatga
481 gcaacaactt ggtaaccctg gaaaatggga aacagctgac cgtaaaaaga caaggactct
541 attatatcta tgccaagtc accttctgtt ccaatcggga agcttcgagt caagctccat
601 ttatagccag cctctgccta aagtcccccg gtagattcga gagaatctta ctcagagctg
661 caaataccca cagttccgcc aaaccttgcg ggcaacaatc cattcacttg ggaggagtat
721 ttgaattgca accaggtgct tcggtgttg tcaatgtgac tgatccaagc caagtgagcc
781 atggcactgg cttcacgtcc ttggcttac taaactctg aacagtgtca cttgcaggc
841 tgtgtggag ctgacgtgg gagtcttcat

REFERENCES

1. Guarneri, V.; Conte, P. F., The curability of breast cancer and the treatment of advanced disease. *Eur J Nucl Med Mol Imaging* **2004**, 31 Suppl 1, S149-61.
2. Kim, J. A., Targeted therapies for the treatment of cancer. *Am J Surg* **2003**, 186, (3), 264-8.
3. Links, M.; Lewis, C., Chemoprotectants: a review of their clinical pharmacology and therapeutic efficacy. *Drugs* **1999**, 57, (3), 293-308.
4. Tripathy, D., Targeted therapies in breast cancer. *Breast J* **2005**, 11 Suppl 1, S30-5.
5. Emens, L. A., Trastuzumab: targeted therapy for the management of HER-2/neu-overexpressing metastatic breast cancer. *Am J Ther* **2005**, 12, (3), 243-53.
6. Armitage, R. J.; Sato, T. A.; Macduff, B. M.; Clifford, K. N.; Alpert, A. R.; Smith, C. A.; Fanslow, W. C., Identification of a source of biologically active CD40 ligand. *Eur J Immunol* **1992**, 22, (8), 2071-6.
7. Hehlhans, T.; Pfeffer, K., The intriguing biology of the tumour necrosis factor/tumour necrosis factor receptor superfamily: players, rules and the games. *Immunology* **2005**, 115, (1), 1-20.
8. Idriss, H. T.; Naismith, J. H., TNF alpha and the TNF receptor superfamily: structure-function relationship(s). *Microsc Res Tech* **2000**, 50, (3), 184-95.
9. Hehlhans, T.; Mannel, D. N., The TNF-TNF receptor system. *Biol Chem* **2002**, 383, (10), 1581-5.
10. van Kooten, C.; Banchereau, J., CD40-CD40 ligand. *J Leukoc Biol* **2000**, 67, (1), 2-17.

11. Tong, A. W.; Stone, M. J., Prospects for CD40-directed experimental therapy of human cancer. *Cancer Gene Ther* **2003**, 10, (1), 1-13.
12. Uckun, F. M.; Gajl-Peczalska, K.; Myers, D. E.; Jaszczyk, W.; Haissig, S.; Ledbetter, J. A., Temporal association of CD40 antigen expression with discrete stages of human B-cell ontogeny and the efficacy of anti-CD40 immunotoxins against clonogenic B-lineage acute lymphoblastic leukemia as well as B-lineage non-Hodgkin's lymphoma cells. *Blood* **1990**, 76, (12), 2449-56.
13. Biancone, L.; Cantaluppi, V.; Camussi, G., CD40-CD154 interaction in experimental and human disease (review). *Int J Mol Med* **1999**, 3, (4), 343-53.
14. Gauchat, J. F.; Henchoz, S.; Fattah, D.; Mazzei, G.; Aubry, J. P.; Jomotte, T.; Dash, L.; Page, K.; Solari, R.; Aldebert, D.; et al., CD40 ligand is functionally expressed on human eosinophils. *Eur J Immunol* **1995**, 25, (3), 863-5.
15. Grewal, I. S.; Flavell, R. A., CD40 and CD154 in cell-mediated immunity. *Annu Rev Immunol* **1998**, 16, 111-35.
16. Henn, V.; Steinbach, S.; Buchner, K.; Presek, P.; Kroczyk, R. A., The inflammatory action of CD40 ligand (CD154) expressed on activated human platelets is temporally limited by coexpressed CD40. *Blood* **2001**, 98, (4), 1047-54.
17. Bishop, G. A.; Hostager, B. S., The CD40-CD154 interaction in B cell-T cell liaisons. *Cytokine Growth Factor Rev* **2003**, 14, (3-4), 297-309.
18. Arpin, C.; Dechanet, J.; Van Kooten, C.; Merville, P.; Grouard, G.; Briere, F.; Banchereau, J.; Liu, Y. J., Generation of memory B cells and plasma cells in vitro. *Science* **1995**, 268, (5211), 720-2.
19. Garrone, P.; Neidhardt, E. M.; Garcia, E.; Galibert, L.; van Kooten, C.; Banchereau, J., Fas ligation induces apoptosis of CD40-activated human B lymphocytes. *J Exp Med* **1995**, 182, (5), 1265-73.
20. Korthauer, U.; Graf, D.; Mages, H. W.; Briere, F.; Padayachee, M.; Malcolm, S.; Ugazio, A. G.; Notarangelo, L. D.; Levinsky, R. J.; Kroczyk, R. A., Defective expression of T-cell CD40 ligand causes X-linked immunodeficiency with hyper-IgM. *Nature* **1993**, 361, (6412), 539-41.

21. Callard, R. E.; Armitage, R. J.; Fanslow, W. C.; Spriggs, M. K., CD40 ligand and its role in X-linked hyper-IgM syndrome. *Immunol Today* **1993**, 14, (11), 559-64.
22. Durandy, A.; Schiff, C.; Bonnefoy, J. Y.; Forveille, M.; Rousset, F.; Mazzei, G.; Milili, M.; Fischer, A., Induction by anti-CD40 antibody or soluble CD40 ligand and cytokines of IgG, IgA and IgE production by B cells from patients with X-linked hyper IgM syndrome. *Eur J Immunol* **1993**, 23, (9), 2294-9.
23. Lougaris, V.; Badolato, R.; Ferrari, S.; Plebani, A., Hyper immunoglobulin M syndrome due to CD40 deficiency: clinical, molecular, and immunological features. *Immunol Rev* **2005**, 203, 48-66.
24. Young, L. S.; Eliopoulos, A. G.; Gallagher, N. J.; Dawson, C. W., CD40 and epithelial cells: across the great divide. *Immunol Today* **1998**, 19, (11), 502-6.
25. Paulie, S.; Ehlin-Henriksson, B.; Mellstedt, H.; Koho, H.; Ben-Aissa, H.; Perlmann, P., A p50 surface antigen restricted to human urinary bladder carcinomas and B lymphocytes. *Cancer Immunol Immunother* **1985**, 20, (1), 23-8.
26. Posner, M. R.; Cavacini, L. A.; Upton, M. P.; Tillman, K. C.; Gornstein, E. R.; Norris, C. M., Jr., Surface membrane-expressed CD40 is present on tumor cells from squamous cell cancer of the head and neck in vitro and in vivo and regulates cell growth in tumor cell lines. *Clin Cancer Res* **1999**, 5, (8), 2261-70.
27. Cooke, P. W.; James, N. D.; Ganesan, R.; Wallace, M.; Burton, A.; Young, L. S., CD40 expression in bladder cancer. *J Pathol* **1999**, 188, (1), 38-43.
28. Sabel, M. S.; Yamada, M.; Kawaguchi, Y.; Chen, F. A.; Takita, H.; Bankert, R. B., CD40 expression on human lung cancer correlates with metastatic spread. *Cancer Immunol Immunother* **2000**, 49, (2), 101-8.
29. van den Oord, J. J.; Maes, A.; Stas, M.; Nuyts, J.; Battocchio, S.; Kasran, A.; Garmyn, M.; De Wever, I.; De Wolf-Peeters, C., CD40 is a prognostic marker in primary cutaneous malignant melanoma. *Am J Pathol* **1996**, 149, (6), 1953-61.
30. Tong, A. W.; Papayoti, M. H.; Netto, G.; Armstrong, D. T.; Ordonez, G.; Lawson, J. M.; Stone, M. J., Growth-inhibitory effects of CD40 ligand (CD154) and its endogenous expression in human breast cancer. *Clin Cancer Res* **2001**, 7, (3), 691-703.

31. de Toter, D.; Meazza, R.; Zupo, S.; Cutrona, G.; Matis, S.; Colombo, M.; Balleari, E.; Pierri, I.; Fabbi, M.; Capaia, M.; Azzarone, B.; Gobbi, M.; Ferrarini, M.; Ferrini, S., Interleukin-21 receptor (IL-21R) is up-regulated by CD40 triggering and mediates proapoptotic signals in chronic lymphocytic leukemia B cells. *Blood* **2006**, 107, (9), 3708-15.
32. Tong, A. W.; Seamour, B.; Chen, J.; Su, D.; Ordonez, G.; Frase, L.; Netto, G.; Stone, M. J., CD40 ligand-induced apoptosis is Fas-independent in human multiple myeloma cells. *Leuk Lymphoma* **2000**, 36, (5-6), 543-58.
33. Tai, Y. T.; Li, X.; Tong, X.; Santos, D.; Otsuki, T.; Catley, L.; Tournilhac, O.; Podar, K.; Hideshima, T.; Schlossman, R.; Richardson, P.; Munshi, N. C.; Luqman, M.; Anderson, K. C., Human anti-CD40 antagonist antibody triggers significant antitumor activity against human multiple myeloma. *Cancer Res* **2005**, 65, (13), 5898-906.
34. Afford, S. C.; Ahmed-Choudhury, J.; Randhawa, S.; Russell, C.; Youster, J.; Crosby, H. A.; Eliopoulos, A.; Hubscher, S. G.; Young, L. S.; Adams, D. H., CD40 activation-induced, Fas-dependent apoptosis and NF-kappaB/AP-1 signaling in human intrahepatic biliary epithelial cells. *Faseb J* **2001**, 15, (13), 2345-54.
35. Lee, J. K.; Seki, N.; Sayers, T. J.; Subleski, J.; Gruys, E. M.; Murphy, W. J.; Wiltrot, R. H., Constitutive expression of functional CD40 on mouse renal cancer cells: induction of Fas and Fas-mediated killing by CD40L. *Cell Immunol* **2005**, 235, (2), 145-52.
36. Voorzanger-Rousselot, N.; Blay, J. Y., Coexpression of CD40 and CD40L on B lymphoma and carcinoma cells: an autocrine anti-apoptotic role. *Leuk Lymphoma* **2004**, 45, (6), 1239-45.
37. Goldstein, M. D.; Watts, T. H., Identification of distinct domains in CD40 involved in B7-1 induction or growth inhibition. *J Immunol* **1996**, 157, (7), 2837-43.
38. Tsukamoto, N.; Kobayashi, N.; Azuma, S.; Yamamoto, T.; Inoue, J., Two differently regulated nuclear factor kappaB activation pathways triggered by the cytoplasmic tail of CD40. *Proc Natl Acad Sci U S A* **1999**, 96, (4), 1234-9.

39. He, X.; Brenchley, P. E.; Jayson, G. C.; Hampson, L.; Davies, J.; Hampson, I. N., Hypoxia increases heparanase-dependent tumor cell invasion, which can be inhibited by antiheparanase antibodies. *Cancer Res* **2004**, 64, (11), 3928-33.
40. Eliopoulos, A. G.; Wang, C. C.; Dumitru, C. D.; Tsiachlis, P. N., Tpl2 transduces CD40 and TNF signals that activate ERK and regulates IgE induction by CD40. *Embo J* **2003**, 22, (15), 3855-64.
41. Young, L. S.; Searle, P. F.; Onion, D.; Mautner, V., Viral gene therapy strategies: from basic science to clinical application. *J Pathol* **2006**, 208, (2), 299-318.
42. Garnett, C. T.; Erdman, D.; Xu, W.; Gooding, L. R., Prevalence and quantitation of species C adenovirus DNA in human mucosal lymphocytes. *J Virol* **2002**, 76, (21), 10608-16.
43. Neumann, R.; Genersch, E.; Eggers, H. J., Detection of adenovirus nucleic acid sequences in human tonsils in the absence of infectious virus. *Virus Res* **1987**, 7, (1), 93-7.
44. Zubko, L. A.; Zatsepin, N. I., [Detection of latent adenoviruses in tonsil and adenoid tissues after ultraviolet irradiation]. *Vopr Virusol* **1967**, 12, (5), 587-90.
45. Davies, C. C.; Bem, D.; Young, L. S.; Eliopoulos, A. G., NF-kappaB overrides the apoptotic program of TNF receptor 1 but not CD40 in carcinoma cells. *Cell Signal* **2005**, 17, (6), 729-38.
46. Eliopoulos, A. G.; Young, L. S., The role of the CD40 pathway in the pathogenesis and treatment of cancer. *Curr Opin Pharmacol* **2004**, 4, (4), 360-7.
47. Gallagher, N. J.; Eliopoulos, A. G.; Agathangelo, A.; Oates, J.; Crocker, J.; Young, L. S., CD40 activation in epithelial ovarian carcinoma cells modulates growth, apoptosis, and cytokine secretion. *Mol Pathol* **2002**, 55, (2), 110-20.
48. Grammer, A. C.; Lipsky, P. E., CD154-CD40 interactions mediate differentiation to plasma cells in healthy individuals and persons with systemic lupus erythematosus. *Arthritis Rheum* **2002**, 46, (6), 1417-29.

49. Quezada, S. A.; Jarvinen, L. Z.; Lind, E. F.; Noelle, R. J., CD40/CD154 interactions at the interface of tolerance and immunity. *Annu Rev Immunol* **2004**, 22, 307-28.
50. Kanerva, A.; Hemminki, A., Adenoviruses for treatment of cancer. *Ann Med* **2005**, 37, (1), 33-43.
51. Xia, X. Z.; Treanor, J.; Senaldi, G.; Khare, S. D.; Boone, T.; Kelley, M.; Theill, L. E.; Colombero, A.; Solovyev, I.; Lee, F.; McCabe, S.; Elliott, R.; Miner, K.; Hawkins, N.; Guo, J.; Stolina, M.; Yu, G.; Wang, J.; Delaney, J.; Meng, S. Y.; Boyle, W. J.; Hsu, H., TACI is a TRAF-interacting receptor for TALL-1, a tumor necrosis factor family member involved in B cell regulation. *J Exp Med* **2000**, 192, (1), 137-43.
52. Tong, A. W., Oncolytic viral therapy for human cancer: challenges revisited. *Drug Development Research* **2006**, 66, 260-277.
53. Relph, K. L.; Harrington, K. J.; Pandha, H., Adenoviral strategies for the gene therapy of cancer. *Semin Oncol* **2005**, 32, (6), 573-82.
54. Glasgow, J. N.; Bauerschmitz, G. J.; Curiel, D. T.; Hemminki, A., Transductional and transcriptional targeting of adenovirus for clinical applications. *Curr Gene Ther* **2004**, 4, (1), 1-14.
55. Ganly, I.; Kim, D.; Eckhardt, G.; Rodriguez, G. I.; Soutar, D. S.; Otto, R.; Robertson, A. G.; Park, O.; Gulley, M. L.; Heise, C.; Von Hoff, D. D.; Kaye, S. B., A phase I study of Onyx-015, an E1B attenuated adenovirus, administered intratumorally to patients with recurrent head and neck cancer. *Clin Cancer Res* **2000**, 6, (3), 798-806.
56. Lamont, J. P.; Nemunaitis, J.; Kuhn, J. A.; Landers, S. A.; McCarty, T. M., A prospective phase II trial of ONYX-015 adenovirus and chemotherapy in recurrent squamous cell carcinoma of the head and neck (the Baylor experience). *Ann Surg Oncol* **2000**, 7, (8), 588-92.
57. Dotti, G.; Savoldo, B.; Takahashi, S.; Goltsova, T.; Brown, M.; Rill, D.; Rooney, C.; Brenner, M., Adenovector-induced expression of human-CD40-ligand (hCD40L) by multiple myeloma cells. A model for immunotherapy. *Exp Hematol* **2001**, 29, (8), 952-61.

58. Kater, A. P.; Dicker, F.; Mangiola, M.; Welsh, K.; Houghten, R.; Ostresh, J.; Nefzi, A.; Reed, J. C.; Pinilla, C.; Kipps, T. J., Inhibitors of XIAP sensitize CD40-activated chronic lymphocytic leukemia cells to CD95-mediated apoptosis. *Blood* **2005**, 106, (5), 1742-8.
59. Dzotic, H.; Loskog, A.; Totterman, T. H.; Essand, M., Adenovirus-mediated CD40 ligand therapy induces tumor cell apoptosis and systemic immunity in the TRAMP-C2 mouse prostate cancer model. *Prostate* **2006**.
60. Sims-Mourtada, J. C.; Bruce, S.; McKeller, M. R.; Rangel, R.; Guzman-Rojas, L.; Cain, K.; Lopez, C.; Zimonjic, D. B.; Popescu, N. C.; Gordon, J.; Wilkinson, M. F.; Martinez-Valdez, H., The human AKNA gene expresses multiple transcripts and protein isoforms as a result of alternative promoter usage, splicing, and polyadenylation. *DNA Cell Biol* **2005**, 24, (5), 325-38.
61. Lucas, A.; Kremer, E. J.; Hemmi, S.; Luis, J.; Vignon, F.; Lazennec, G., Comparative transductions of breast cancer cells by three DNA viruses. *Biochem Biophys Res Commun* **2003**, 309, (4), 1011-6.
62. Lu, H.; Qin, H.; Zhang, Y., [Down regulation of HER2/neu expression by adenovirus E1A and its anti-tumor activity]. *Zhonghua Zhong Liu Za Zhi* **2000**, 22, (5), 370-3.
63. Stutz, A. M.; Hoeck, J.; Natt, F.; Cuenoud, B.; Woisetschlager, M., Inhibition of interleukin-4- and CD40-induced IgE germline gene promoter activity by 2'-aminoethoxy-modified triplex-forming oligonucleotides. *J Biol Chem* **2001**, 276, (15), 11759-65.
64. Yoo, G. H.; Hung, M. C.; Lopez-Berestein, G.; LaFollette, S.; Ensley, J. F.; Carey, M.; Batson, E.; Reynolds, T. C.; Murray, J. L., Phase I trial of intratumoral liposome E1A gene therapy in patients with recurrent breast and head and neck cancer. *Clin Cancer Res* **2001**, 7, (5), 1237-45.
65. Hortobagyi, G. N.; Hung, M. C.; Lopez-Berestein, G., A Phase I multicenter study of E1A gene therapy for patients with metastatic breast cancer and epithelial ovarian cancer that overexpresses HER-2/neu or epithelial ovarian cancer. *Hum Gene Ther* **1998**, 9, (12), 1775-98.
66. Kaplan, J. M., Adenovirus-based cancer gene therapy. *Curr Gene Ther* **2005**, 5, (6), 595-605.

67. Wilson, D. R., Viral-mediated gene transfer for cancer treatment. *Curr Pharm Biotechnol* **2002**, 3, (2), 151-64.
68. Williams, M. A.; Tan, J. T.; Adams, A. B.; Durham, M. M.; Shirasugi, N.; Whitmire, J. K.; Harrington, L. E.; Ahmed, R.; Pearson, T. C.; Larsen, C. P., Characterization of virus-mediated inhibition of mixed chimerism and allospecific tolerance. *J Immunol* **2001**, 167, (9), 4987-95.
69. Breidenbach, M.; Rein, D. T.; Schondorf, T.; Khan, K. N.; Herrmann, I.; Schmidt, T.; Reynolds, P. N.; Vlodavsky, I.; Haviv, Y. S.; Curiel, D. T., A new targeting approach for breast cancer gene therapy using the Heparanase promoter. *Cancer Lett* **2005**.
70. Hernandez-Alcoceba, R.; Pihalja, M.; Qian, D.; Clarke, M. F., New oncolytic adenoviruses with hypoxia- and estrogen receptor-regulated replication. *Hum Gene Ther* **2002**, 13, (14), 1737-50.
71. Axelson, H.; Fredlund, E.; Ovenberger, M.; Landberg, G.; Pahlman, S., Hypoxia-induced dedifferentiation of tumor cells--a mechanism behind heterogeneity and aggressiveness of solid tumors. *Semin Cell Dev Biol* **2005**, 16, (4-5), 554-63.
72. Brahimi-Horn, C.; Berra, E.; Pouyssegur, J., Hypoxia: the tumor's gateway to progression along the angiogenic pathway. *Trends Cell Biol* **2001**, 11, (11), S32-6.
73. Prosnitz, R. G.; Yao, B.; Farrell, C. L.; Clough, R.; Brizel, D. M., Pretreatment anemia is correlated with the reduced effectiveness of radiation and concurrent chemotherapy in advanced head and neck cancer. *Int J Radiat Oncol Biol Phys* **2005**, 61, (4), 1087-95.
74. Kurebayashi, J., Resistance to endocrine therapy in breast cancer. *Cancer Chemother Pharmacol* **2005**, 56 Suppl 1, 39-46.
75. Kurebayashi, J.; Otsuki, T.; Moriya, T.; Sonoo, H., Hypoxia reduces hormone responsiveness of human breast cancer cells. *Jpn J Cancer Res* **2001**, 92, (10), 1093-101.
76. Liu, G. Y.; Shen, K. W.; Shao, Z. M.; Shen, Z. Z., [Hypoxia induces down-regulation of estrogen receptor alpha in human breast cancer.]. *Zhonghua Zhong Liu Za Zhi* **2004**, 26, (11), 664-8.

77. Gruber, M. F.; Bjorndahl, J. M.; Nakamura, S.; Fu, S. M., Anti-CD45 inhibition of human B cell proliferation depends on the nature of activation signals and the state of B cell activation. A study with anti-IgM and anti-CDw40 antibodies. *J Immunol* **1989**, 142, (12), 4144-52.
78. Quintero, M.; Mackenzie, N.; Brennan, P. A., Hypoxia-inducible factor 1 (HIF-1) in cancer. *Eur J Surg Oncol* **2004**, 30, (5), 465-8.
79. Bos, R.; van der Groep, P.; Greijer, A. E.; Shvarts, A.; Meijer, S.; Pinedo, H. M.; Semenza, G. L.; van Diest, P. J.; van der Wall, E., Levels of hypoxia-inducible factor-1alpha independently predict prognosis in patients with lymph node negative breast carcinoma. *Cancer* **2003**, 97, (6), 1573-81.
80. Bos, R.; van Diest, P. J.; de Jong, J. S.; van der Groep, P.; van der Valk, P.; van der Wall, E., Hypoxia-inducible factor-1alpha is associated with angiogenesis, and expression of bFGF, PDGF-BB, and EGFR in invasive breast cancer. *Histopathology* **2005**, 46, (1), 31-6.
81. Bos, R.; van Diest, P. J.; van der Groep, P.; Shvarts, A.; Greijer, A. E.; van der Wall, E., Expression of hypoxia-inducible factor-1alpha and cell cycle proteins in invasive breast cancer are estrogen receptor related. *Breast Cancer Res* **2004**, 6, (4), R450-9.
82. Axelrod, D. M.; Menendez-Botet, C. J.; Kinne, D. W.; Osborne, M. P., Levels of estrogen and progesterone receptor proteins in patients with breast cancer during various phases of the menses. *Cancer Invest* **1988**, 6, (1), 7-14.
83. Osborne, C. K.; Schiff, R.; Fuqua, S. A.; Shou, J., Estrogen receptor: current understanding of its activation and modulation. *Clin Cancer Res* **2001**, 7, (12 Suppl), 4338s-4342s; discussion 4411s-4412s.
84. Vaupel, P.; Mayer, A.; Briest, S.; Hockel, M., Hypoxia in breast cancer: role of blood flow, oxygen diffusion distances, and anemia in the development of oxygen depletion. *Adv Exp Med Biol* **2005**, 566, 333-42.
85. Belozarov, V. E.; Van Meir, E. G., Hypoxia inducible factor-1: a novel target for cancer therapy. *Anticancer Drugs* **2005**, 16, (9), 901-9.

86. Hirano, A.; Longo, D. L.; Taub, D. D.; Ferris, D. K.; Young, L. S.; Eliopoulos, A. G.; Agathangelou, A.; Cullen, N.; Macartney, J.; Fanslow, W. C.; Murphy, W. J., Inhibition of human breast carcinoma growth by a soluble recombinant human CD40 ligand. *Blood* **1999**, 93, (9), 2999-3007.
87. Wingett, D. G.; Vestal, R. E.; Forcier, K.; Hadjokas, N.; Nielson, C. P., CD40 is functionally expressed on human breast carcinomas: variable inducibility by cytokines and enhancement of Fas-mediated apoptosis. *Breast Cancer Res Treat* **1998**, 50, (1), 27-36.
88. Howard, L. M.; Miller, S. D., Immunotherapy targeting the CD40/CD154 costimulatory pathway for treatment of autoimmune disease. *Autoimmunity* **2004**, 37, (5), 411-8.
89. Kato, Y.; Tsuda, T.; Hosaka, Y.; Takahashi, T.; Shirakawa, K.; Furusako, S.; Mizuguchi, K.; Mochizuki, H., Effect of trapidil on effector functions of monocytes related to atherosclerotic plaque. *Eur J Pharmacol* **2001**, 428, (3), 371-9.
90. Wierda, W. G.; Cantwell, M. J.; Woods, S. J.; Rassenti, L. Z.; Prussak, C. E.; Kipps, T. J., CD40-ligand (CD154) gene therapy for chronic lymphocytic leukemia. *Blood* **2000**, 96, (9), 2917-24.
91. Liu, Y.; Xia, D.; Li, F.; Zheng, C.; Xiang, J., Intratumoral administration of immature dendritic cells following the adenovirus vector encoding CD40 ligand elicits significant regression of established myeloma. *Cancer Gene Ther* **2005**, 12, (2), 122-32.
92. Lin, E.; Nemunaitis, J., Oncolytic viral therapies. *Cancer Gene Ther* **2004**, 11, (10), 643-64.
93. Polak, M. E.; Johnson, P.; Di Palma, S.; Higgins, B.; Hurren, J.; Borthwick, N. J.; Jager, M. J.; McCormick, D.; Cree, I. A., Presence and maturity of dendritic cells in melanoma lymph node metastases. *J Pathol* **2005**, 207, (1), 83-90.
94. Kirn, D.; Hermiston, T.; McCormick, F., ONYX-015: clinical data are encouraging. *Nat Med* **1998**, 4, (12), 1341-2.

95. Tokatli, F.; Altaner, S.; Uzal, C.; Ture, M.; Kocak, Z.; Uygun, K.; Bilgi, S., Association of HER-2/neu overexpression with the number of involved axillary lymph nodes in hormone receptor positive breast cancer patients. *Exp Oncol* **2005**, 27, (2), 145-9.
96. Qi, C.; Zhu, Y. T.; Chang, J.; Yeldandi, A. V.; Rao, M. S.; Zhu, Y. J., Potentiation of estrogen receptor transcriptional activity by breast cancer amplified sequence 2. *Biochem Biophys Res Commun* **2005**, 328, (2), 393-8.
97. Vaupel, P.; Mayer, A.; Hockel, M., Tumor hypoxia and malignant progression. *Methods Enzymol* **2004**, 381, 335-54.
98. Chen, W. T.; Huang, C. J.; Wu, M. T.; Yang, S. F.; Su, Y. C.; Chai, C. Y., Hypoxia-inducible factor-1 α is associated with risk of aggressive behavior and tumor angiogenesis in gastrointestinal stromal tumor. *Jpn J Clin Oncol* **2005**, 35, (4), 207-13.
99. Baxendale, A. J.; Dawson, C. W.; Stewart, S. E.; Mudaliar, V.; Reynolds, G.; Gordon, J.; Murray, P. G.; Young, L. S.; Eliopoulos, A. G., Constitutive activation of the CD40 pathway promotes cell transformation and neoplastic growth. *Oncogene* **2005**, 24, (53), 7913-23.
100. Gorgoulis, V. G.; Zacharatos, P.; Mariatos, G.; Kotsinas, A.; Bouda, M.; Kletsas, D.; Asimacopoulos, P. J.; Agnantis, N.; Kittas, C.; Papavassiliou, A. G., Transcription factor E2F-1 acts as a growth-promoting factor and is associated with adverse prognosis in non-small cell lung carcinomas. *J Pathol* **2002**, 198, (2), 142-56.
101. Zhang, S. Y.; Liu, S. C.; Al-Saleem, L. F.; Holloran, D.; Babb, J.; Guo, X.; Klein-Szanto, A. J., E2F-1: a proliferative marker of breast neoplasia. *Cancer Epidemiol Biomarkers Prev* **2000**, 9, (4), 395-401.
102. Piret, J. P.; Mottet, D.; Raes, M.; Michiels, C., CoCl₂, a chemical inducer of hypoxia-inducible factor-1, and hypoxia reduce apoptotic cell death in hepatoma cell line HepG2. *Ann N Y Acad Sci* **2002**, 973, 443-7.
103. Dery, C. V.; Herrmann, C. H.; Mathews, M. B., Response of individual adenovirus promoters to the products of the E1A gene. *Oncogene* **1987**, 2, (1), 15-23.

104. Chu, P.; Deforce, D.; Pedersen, I. M.; Kim, Y.; Kitada, S.; Reed, J. C.; Kipps, T. J., Latent sensitivity to Fas-mediated apoptosis after CD40 ligation may explain activity of CD154 gene therapy in chronic lymphocytic leukemia. *Proc Natl Acad Sci U S A* **2002**, 99, (6), 3854-9.
105. Jakubczak, J. L.; Ryan, P.; Gorziglia, M.; Clarke, L.; Hawkins, L. K.; Hay, C.; Huang, Y.; Kaloss, M.; Marinov, A.; Phipps, S.; Pinkstaff, A.; Shirley, P.; Skripchenko, Y.; Stewart, D.; Forry-Schaudies, S.; Hallenbeck, P. L., An oncolytic adenovirus selective for retinoblastoma tumor suppressor protein pathway-defective tumors: dependence on E1A, the E2F-1 promoter, and viral replication for selectivity and efficacy. *Cancer Res* **2003**, 63, (7), 1490-9.
106. Zelzer, E.; Levy, Y.; Kahana, C.; Shilo, B. Z.; Rubinstein, M.; Cohen, B., Insulin induces transcription of target genes through the hypoxia-inducible factor HIF-1alpha/ARNT. *Embo J* **1998**, 17, (17), 5085-94.
107. Stiehl, D. P.; Jelkmann, W.; Wenger, R. H.; Hellwig-Burgel, T., Normoxic induction of the hypoxia-inducible factor 1alpha by insulin and interleukin-1beta involves the phosphatidylinositol 3-kinase pathway. *FEBS Lett* **2002**, 512, (1-3), 157-62.
108. Doronzo, G.; Russo, I.; Mattiello, L.; Riganti, C.; Anfossi, G.; Trovati, M., Insulin activates hypoxia-inducible factor-1alpha in human and rat vascular smooth muscle cells via phosphatidylinositol-3 kinase and mitogen-activated protein kinase pathways: impairment in insulin resistance owing to defects in insulin signalling. *Diabetologia* **2006**.
109. Salceda, S.; Caro, J., Hypoxia-inducible factor 1alpha (HIF-1alpha) protein is rapidly degraded by the ubiquitin-proteasome system under normoxic conditions. Its stabilization by hypoxia depends on redox-induced changes. *J Biol Chem* **1997**, 272, (36), 22642-7.
110. Bilton, R.; Mazure, N.; Trottier, E.; Hattab, M.; Dery, M. A.; Richard, D. E.; Pouyssegur, J.; Brahimi-Horn, M. C., Arrest-defective-1 protein, an acetyltransferase, does not alter stability of hypoxia-inducible factor (HIF)-1alpha and is not induced by hypoxia or HIF. *J Biol Chem* **2005**, 280, (35), 31132-40.
111. Bi, M.; Naczki, C.; Koritzinsky, M.; Fels, D.; Blais, J.; Hu, N.; Harding, H.; Novoa, I.; Varia, M.; Raleigh, J.; Scheuner, D.; Kaufman, R. J.; Bell, J.; Ron, D.; Wouters, B. G.; Koumenis, C., ER stress-regulated translation increases tolerance to extreme hypoxia and promotes tumor growth. *Embo J* **2005**, 24, (19), 3470-81.

112. Aminova, L. R.; Chavez, J. C.; Lee, J.; Ryu, H.; Kung, A.; Lamanna, J. C.; Ratan, R. R., Prosurvival and prodeath effects of hypoxia-inducible factor-1alpha stabilization in a murine hippocampal cell line. *J Biol Chem* **2005**, 280, (5), 3996-4003.
113. Kim, H. J.; Yang, S. J.; Kim, Y. S.; Kim, T. U., Cobalt chloride-induced apoptosis and extracellular signal-regulated protein kinase activation in human cervical cancer HeLa cells. *J Biochem Mol Biol* **2003**, 36, (5), 468-74.
114. Piret, J. P.; Lecocq, C.; Toffoli, S.; Ninane, N.; Raes, M.; Michiels, C., Hypoxia and CoCl₂ protect HepG2 cells against serum deprivation- and t-BHP-induced apoptosis: a possible anti-apoptotic role for HIF-1. *Exp Cell Res* **2004**, 295, (2), 340-9.
115. Vengellur, A.; LaPres, J. J., The role of hypoxia inducible factor 1alpha in cobalt chloride induced cell death in mouse embryonic fibroblasts. *Toxicol Sci* **2004**, 82, (2), 638-46.
116. Bauzon, M.; Castro, D.; Karr, M.; Hawkins, L. K.; Hermiston, T. W., Multigene expression from a replicating adenovirus using native viral promoters. *Mol Ther* **2003**, 7, (4), 526-34.
117. Putzer, B. M.; Hitt, M.; Muller, W. J.; Emtage, P.; Gauldie, J.; Graham, F. L., Interleukin 12 and B7-1 costimulatory molecule expressed by an adenovirus vector act synergistically to facilitate tumor regression. *Proc Natl Acad Sci U S A* **1997**, 94, (20), 10889-94.
118. Hawkins, L. K.; Hermiston, T. W., Gene delivery from the E3 region of replicating human adenovirus: evaluation of the ADP region. *Gene Ther* **2001**, 8, (15), 1132-41.
119. Gu, Z.; Belzer, S. W.; Gibson, C. S.; Bankowski, M. J.; Hayden, R. T., Multiplexed, real-time PCR for quantitative detection of human adenovirus. *J Clin Microbiol* **2003**, 41, (10), 4636-41.
120. Zheng, M.; Ramsay, A. J.; Robichaux, M. B.; Norris, K. A.; Kliment, C.; Crowe, C.; Rapaka, R. R.; Steele, C.; McAllister, F.; Shellito, J. E.; Marrero, L.; Schwarzenberger, P.; Zhong, Q.; Kolls, J. K., CD4⁺ T cell-independent DNA vaccination against opportunistic infections. *J Clin Invest* **2005**, 115, (12), 3536-44.

121. Holub, M.; Zakeri, S. M.; Lichtenberger, C.; Pammer, J.; Paolini, P.; Leifeld, L.; Rockenschaub, S.; Wolschek, M. F.; Steger, G.; Willheim, M.; Gangl, A.; Reinisch, W., Heterogeneous expression and regulation of CD40 in human hepatocellular carcinoma. *Eur J Gastroenterol Hepatol* **2003**, 15, (2), 119-26.
122. Gao, Y. L.; Shi, H. Z.; Liu, M.; Gu, X. S., [Inhibition of human glioma cell growth by a soluble recombinant human CD40 ligand]. *Ai Zheng* **2002**, 21, (10), 1112-5.
123. Cui, W.; Li, L. Y., [Functional significance of CD40 and CD40 ligand linking on human lung cells]. *Zhonghua Yi Xue Za Zhi* **2003**, 83, (20), 1807-11.
124. Preuss, M. A.; Lam, J. T.; Wang, M.; Leath, C. A., 3rd; Kataram, M.; Mahasreshti, P. J.; Alvarez, R. D.; Curiel, D. T., Transcriptional blocks limit adenoviral replication in primary ovarian tumor. *Clin Cancer Res* **2004**, 10, (9), 3189-94.
125. Clesham, G. J.; Adam, P. J.; Proudfoot, D.; Flynn, P. D.; Efstathiou, S.; Weissberg, P. L., High adenoviral loads stimulate NF kappaB-dependent gene expression in human vascular smooth muscle cells. *Gene Ther* **1998**, 5, (2), 174-80.
126. O'Shea, C.; Klupsch, K.; Choi, S.; Bagus, B.; Soria, C.; Shen, J.; McCormick, F.; Stokoe, D., Adenoviral proteins mimic nutrient/growth signals to activate the mTOR pathway for viral replication. *Embo J* **2005**, 24, (6), 1211-21.
127. Cho, W. K.; Seong, Y. R.; Lee, Y. H.; Kim, M. J.; Hwang, K. S.; Yoo, J.; Choi, S.; Jung, C. R.; Im, D. S., Oncolytic effects of adenovirus mutant capable of replicating in hypoxic and normoxic regions of solid tumor. *Mol Ther* **2004**, 10, (5), 938-49.
128. Schuler, W.; Bosma, M. J., Nature of the scid defect: a defective VDJ recombinase system. *Curr Top Microbiol Immunol* **1989**, 152, 55-62.
129. Schuler, W.; Weiler, I. J.; Schuler, A.; Phillips, R. A.; Rosenberg, N.; Mak, T. W.; Kearney, J. F.; Perry, R. P.; Bosma, M. J., Rearrangement of antigen receptor genes is defective in mice with severe combined immune deficiency. *Cell* **1986**, 46, (7), 963-72.

130. Kubota, T.; Yamaguchi, H.; Watanabe, M.; Yamamoto, T.; Takahara, T.; Takeuchi, T.; Furukawa, T.; Kase, S.; Kodaira, S.; Ishibiki, K.; et al., Growth of human tumor xenografts in nude mice and mice with severe combined immunodeficiency (SCID). *Surg Today* **1993**, 23, (4), 375-7.
131. Paine-Murrieta, G. D.; Taylor, C. W.; Curtis, R. A.; Lopez, M. H.; Dorr, R. T.; Johnson, C. S.; Funk, C. Y.; Thompson, F.; Hersh, E. M., Human tumor models in the severe combined immune deficient (scid) mouse. *Cancer Chemother Pharmacol* **1997**, 40, (3), 209-14.
132. Mullen, P.; Ritchie, A.; Langdon, S. P.; Miller, W. R., Effect of Matrigel on the tumorigenicity of human breast and ovarian carcinoma cell lines. *Int J Cancer* **1996**, 67, (6), 816-20.
133. Tong, A. W.; Nemunaitis, J.; Su, D.; Zhang, Y.; Cunningham, C.; Senzer, N.; Netto, G.; Rich, D.; Mhashilkar, A.; Parker, K.; Coffee, K.; Ramesh, R.; Ekmekcioglu, S.; Grimm, E. A.; van Wart Hood, J.; Merritt, J.; Chada, S., Intratumoral injection of INGN 241, a nonreplicating adenovector expressing the melanoma-differentiation associated gene-7 (mda-7/IL24): biologic outcome in advanced cancer patients. *Mol Ther* **2005**, 11, (1), 160-72.
134. Wood, M.; Perrotte, P.; Onishi, E.; Harper, M. E.; Dinney, C.; Pagliaro, L.; Wilson, D. R., Biodistribution of an adenoviral vector carrying the luciferase reporter gene following intravesical or intravenous administration to a mouse. *Cancer Gene Ther* **1999**, 6, (4), 367-72.
135. Tritos, N. A.; Segal-Lieberman, G.; Vezeridis, P. S.; Maratos-Flier, E., Estradiol-induced anorexia is independent of leptin and melanin-concentrating hormone. *Obes Res* **2004**, 12, (4), 716-24.
136. Heise, C. C.; Williams, A. M.; Xue, S.; Propst, M.; Kim, D. H., Intravenous administration of ONYX-015, a selectively replicating adenovirus, induces antitumoral efficacy. *Cancer Res* **1999**, 59, (11), 2623-8.
137. Sinek, J.; Frieboes, H.; Zheng, X.; Cristini, V., Two-dimensional chemotherapy simulations demonstrate fundamental transport and tumor response limitations involving nanoparticles. *Biomed Microdevices* **2004**, 6, (4), 297-309.

138. Loskog, A.; Dzojic, H.; Vikman, S.; Ninalga, C.; Essand, M.; Korsgren, O.; Totterman, T. H., Adenovirus CD40 ligand gene therapy counteracts immune escape mechanisms in the tumor Microenvironment. *J Immunol* **2004**, 172, (11), 7200-5.
139. Paielli, D. L.; Wing, M. S.; Rogulski, K. R.; Gilbert, J. D.; Kolozsvary, A.; Kim, J. H.; Hughes, J.; Schnell, M.; Thompson, T.; Freytag, S. O., Evaluation of the biodistribution, persistence, toxicity, and potential of germ-line transmission of a replication-competent human adenovirus following intraprostatic administration in the mouse. *Mol Ther* **2000**, 1, (3), 263-74.
140. Taki, M.; Kagawa, S.; Nishizaki, M.; Mizuguchi, H.; Hayakawa, T.; Kyo, S.; Nagai, K.; Urata, Y.; Tanaka, N.; Fujiwara, T., Enhanced oncolysis by a tropism-modified telomerase-specific replication-selective adenoviral agent OBP-405 ('Telomelysin-RGD'). *Oncogene* **2005**, 24, (19), 3130-40.
141. Green, N. K.; Herbert, C. W.; Hale, S. J.; Hale, A. B.; Mautner, V.; Harkins, R.; Hermiston, T.; Ulbrich, K.; Fisher, K. D.; Seymour, L. W., Extended plasma circulation time and decreased toxicity of polymer-coated adenovirus. *Gene Ther* **2004**, 11, (16), 1256-63.
142. Bauerschmitz, G. J.; Kanerva, A.; Wang, M.; Herrmann, I.; Shaw, D. R.; Strong, T. V.; Desmond, R.; Rein, D. T.; Dall, P.; Curiel, D. T.; Hemminki, A., Evaluation of a selectively oncolytic adenovirus for local and systemic treatment of cervical cancer. *Int J Cancer* **2004**, 111, (2), 303-9.
143. Grammer, A. C.; Swantek, J. L.; McFarland, R. D.; Miura, Y.; Geppert, T.; Lipsky, P. E., TNF receptor-associated factor-3 signaling mediates activation of p38 and Jun N-terminal kinase, cytokine secretion, and Ig production following ligation of CD40 on human B cells. *J Immunol* **1998**, 161, (3), 1183-93.
144. Ahonen, C.; Manning, E.; Erickson, L. D.; O'Connor, B.; Lind, E. F.; Pullen, S. S.; Kehry, M. R.; Noelle, R. J., The CD40-TRAF6 axis controls affinity maturation and the generation of long-lived plasma cells. *Nat Immunol* **2002**, 3, (5), 451-6.
145. Ricote, M.; Garcia-Tunon, I.; Fraile, B.; Fernandez, C.; Aller, P.; Paniagua, R.; Royuela, M., p38 MAPK protects against TNF-alpha-provoked apoptosis in LNCaP prostatic cancer cells. *Apoptosis* **2006**.

146. Coltella, N.; Rasola, A.; Nano, E.; Bardella, C.; Fassetta, M.; Filigheddu, N.; Graziani, A.; Comoglio, P. M.; Di Renzo, M. F., p38 MAPK turns hepatocyte growth factor to a death signal that commits ovarian cancer cells to chemotherapy-induced apoptosis. *Int J Cancer* **2006**, 118, (12), 2981-90.
147. Koizumi, K.; Tanno, S.; Nakano, Y.; Habiro, A.; Izawa, T.; Mizukami, Y.; Okumura, T.; Kohgo, Y., Activation of p38 mitogen-activated protein kinase is necessary for gemcitabine-induced cytotoxicity in human pancreatic cancer cells. *Anticancer Res* **2005**, 25, (5), 3347-53.
148. Ahmed-Choudhury, J.; Russell, C. L.; Randhawa, S.; Young, L. S.; Adams, D. H.; Afford, S. C., Differential induction of nuclear factor-kappaB and activator protein-1 activity after CD40 ligation is associated with primary human hepatocyte apoptosis or intrahepatic endothelial cell proliferation. *Mol Biol Cell* **2003**, 14, (4), 1334-45.
149. Davies, C. C.; Mason, J.; Wakelam, M. J.; Young, L. S.; Eliopoulos, A. G., Inhibition of phosphatidylinositol 3-kinase- and ERK MAPK-regulated protein synthesis reveals the pro-apoptotic properties of CD40 ligation in carcinoma cells. *J Biol Chem* **2004**, 279, (2), 1010-9.
150. Melotti, P.; Nicolis, E.; Tamanini, A.; Rolfini, R.; Pavirani, A.; Cabrini, G., Activation of NF-kB mediates ICAM-1 induction in respiratory cells exposed to an adenovirus-derived vector. *Gene Ther* **2001**, 8, (18), 1436-42.
151. O'Connell, P. J.; Morelli, A. E.; Logar, A. J.; Thomson, A. W., Phenotypic and functional characterization of mouse hepatic CD8 alpha⁺ lymphoid-related dendritic cells. *J Immunol* **2000**, 165, (2), 795-803.
152. Palmer, D. H.; Chen, M. J.; Searle, P. F.; Kerr, D. J.; Young, L. S., Inhibition of NF-kappaB enhances the cytotoxicity of virus-directed enzyme prodrug therapy and oncolytic adenovirus cancer gene therapy. *Gene Ther* **2005**, 12, (15), 1187-97.
153. Tibbles, L. A.; Spurrell, J. C.; Bowen, G. P.; Liu, Q.; Lam, M.; Zaiss, A. K.; Robbins, S. M.; Hollenberg, M. D.; Wickham, T. J.; Muruve, D. A., Activation of p38 and ERK signaling during adenovirus vector cell entry lead to expression of the C-X-C chemokine IP-10. *J Virol* **2002**, 76, (4), 1559-68.
154. Ormerod, M. G., *Flow cytometry a practical approach, second edition*. Oxford University Press, Inc., New York, NY: 1992.

155. Liu, K. J.; Lu, L. F.; Cheng, H. T.; Hung, Y. M.; Shiou, S. R.; Whang-Peng, J.; Juang, S. H., Concurrent delivery of tumor antigens and activation signals to dendritic cells by irradiated CD40 ligand-transfected tumor cells resulted in efficient activation of specific CD8⁺ T cells. *Cancer Gene Ther* **2004**, 11, (2), 135-47.
156. Wuerzberger-Davis, S. M.; Chang, P. Y.; Berchtold, C.; Miyamoto, S., Enhanced G2-M arrest by nuclear factor- κ B-dependent p21waf1/cip1 induction. *Mol Cancer Res* **2005**, 3, (6), 345-53.
157. Savickiene, J.; Treigyte, G.; Magnusson, K. E.; Navakauskiene, R., p21 (Waf1/Cip1) and FasL gene activation via Sp1 and NF κ B is required for leukemia cell survival but not for cell death induced by diverse stimuli. *Int J Biochem Cell Biol* **2005**, 37, (4), 784-96.
158. Kim, Y. A.; Lee, W. H.; Choi, T. H.; Rhee, S. H.; Park, K. Y.; Choi, Y. H., Involvement of p21WAF1/CIP1, pRB, Bax and NF- κ B in induction of growth arrest and apoptosis by resveratrol in human lung carcinoma A549 cells. *Int J Oncol* **2003**, 23, (4), 1143-9.
159. Pestell, R. G.; Albanese, C.; Reutens, A. T.; Segall, J. E.; Lee, R. J.; Arnold, A., The cyclins and cyclin-dependent kinase inhibitors in hormonal regulation of proliferation and differentiation. *Endocr Rev* **1999**, 20, (4), 501-34.
160. Flores-Rozas, H.; Kelman, Z.; Dean, F. B.; Pan, Z. Q.; Harper, J. W.; Elledge, S. J.; O'Donnell, M.; Hurwitz, J., Cdk-interacting protein 1 directly binds with proliferating cell nuclear antigen and inhibits DNA replication catalyzed by the DNA polymerase delta holoenzyme. *Proc Natl Acad Sci U S A* **1994**, 91, (18), 8655-9.
161. Radhakrishnan, S. K.; Feliciano, C. S.; Najmabadi, F.; Haegbarth, A.; Kandel, E. S.; Tyner, A. L.; Gartel, A. L., Constitutive expression of E2F-1 leads to p21-dependent cell cycle arrest in S phase of the cell cycle. *Oncogene* **2004**, 23, (23), 4173-6.
162. Swaroop, N.; Chen, F.; Wang, L.; Dokka, S.; Toledo, D.; Rojanasakul, Y., Inhibition of nuclear transcription factor- κ B by specific IkappaB kinase peptide inhibitor. *Pharm Res* **2001**, 18, (11), 1631-3.
163. Hanissian, S. H.; Geha, R. S., Jak3 is associated with CD40 and is critical for CD40 induction of gene expression in B cells. *Immunity* **1997**, 6, (4), 379-87.

164. Luo, J. L.; Kamata, H.; Karin, M., IKK/NF-kappaB signaling: balancing life and death--a new approach to cancer therapy. *J Clin Invest* **2005**, 115, (10), 2625-32.
165. Schwartz, S. A.; Hernandez, A.; Mark Evers, B., The role of NF-kappaB/IkappaB proteins in cancer: implications for novel treatment strategies. *Surg Oncol* **1999**, 8, (3), 143-53.
166. Ravi, R.; Bedi, A., NF-kappaB in cancer--a friend turned foe. *Drug Resist Updat* **2004**, 7, (1), 53-67.
167. Abou El Hassan, M. A.; van der Meulen-Muileman, I.; Abbas, S.; Kruij, F. A., Conditionally replicating adenoviruses kill tumor cells via a basic apoptotic machinery-independent mechanism that resembles necrosis-like programmed cell death. *J Virol* **2004**, 78, (22), 12243-51.
168. Manka, D.; Spicer, Z.; Millhorn, D. E., Bcl-2/adenovirus E1B 19 kDa interacting protein-3 knockdown enables growth of breast cancer metastases in the lung, liver, and bone. *Cancer Res* **2005**, 65, (24), 11689-93.
169. Ben-Israel, H.; Kleinberger, T., Adenovirus and cell cycle control. *Front Biosci* **2002**, 7, d1369-95.
170. Wang, T. L.; Huang, J. A.; Yu, G. H.; Mao, Y. X.; Wang, G. J.; Zhang, X. G., [Biological effects of soluble CD40 ligand on lung cancer cell line A549 and its mechanism.]. *Ai Zheng* **2004**, 23, (11), 1278-82.
171. Yamada, M.; Shiroko, T.; Kawaguchi, Y.; Sugiyama, Y.; Egilmez, N. K.; Chen, F. A.; Bankert, R. B., CD40-CD40 ligand (CD154) engagement is required but not sufficient for modulating MHC class I, ICAM-1 and Fas expression and proliferation of human non-small cell lung tumors. *Int J Cancer* **2001**, 92, (4), 589-99.
172. Gartel, A. L.; Serfas, M. S.; Tyner, A. L., p21--negative regulator of the cell cycle. *Proc Soc Exp Biol Med* **1996**, 213, (2), 138-49.
173. el-Deiry, W. S.; Tokino, T.; Velculescu, V. E.; Levy, D. B.; Parsons, R.; Trent, J. M.; Lin, D.; Mercer, W. E.; Kinzler, K. W.; Vogelstein, B., WAF1, a potential mediator of p53 tumor suppression. *Cell* **1993**, 75, (4), 817-25.

174. Gartel, A. L.; Tyner, A. L., The role of the cyclin-dependent kinase inhibitor p21 in apoptosis. *Mol Cancer Ther* **2002**, 1, (8), 639-49.
175. Bobrovnikova-Marjon, E. V.; Marjon, P. L.; Barbash, O.; Vander Jagt, D. L.; Abcouwer, S. F., Expression of angiogenic factors vascular endothelial growth factor and interleukin-8/CXCL8 is highly responsive to ambient glutamine availability: role of nuclear factor-kappaB and activating protein-1. *Cancer Res* **2004**, 64, (14), 4858-69.
176. Hampl, M.; Tanaka, T.; Albert, P. S.; Lee, J.; Ferrari, N.; Fine, H. A., Therapeutic effects of viral vector-mediated antiangiogenic gene transfer in malignant ascites. *Hum Gene Ther* **2001**, 12, (14), 1713-29.
177. Melter, M.; Reinders, M. E.; Sho, M.; Pal, S.; Geehan, C.; Denton, M. D.; Mukhopadhyay, D.; Briscoe, D. M., Ligation of CD40 induces the expression of vascular endothelial growth factor by endothelial cells and monocytes and promotes angiogenesis in vivo. *Blood* **2000**, 96, (12), 3801-8.
178. Cho, C. S.; Cho, M. L.; Min, S. Y.; Kim, W. U.; Min, D. J.; Lee, S. S.; Park, S. H.; Choe, J.; Kim, H. Y., CD40 engagement on synovial fibroblast up-regulates production of vascular endothelial growth factor. *J Immunol* **2000**, 164, (10), 5055-61.
179. Basok, A.; Shnaider, A.; Man, L.; Chaimovitz, C.; Douvdevani, A., CD40 is expressed on human peritoneal mesothelial cells and upregulates the production of interleukin-15 and RANTES. *J Am Soc Nephrol* **2001**, 12, (4), 695-702.
180. Woltman, A. M.; de Haij, S.; Boonstra, J. G.; Gobin, S. J.; Daha, M. R.; van Kooten, C., Interleukin-17 and CD40-ligand synergistically enhance cytokine and chemokine production by renal epithelial cells. *J Am Soc Nephrol* **2000**, 11, (11), 2044-55.
181. Azenshtein, E.; Luboshits, G.; Shina, S.; Neumark, E.; Shahbazian, D.; Weil, M.; Wigler, N.; Keydar, I.; Ben-Baruch, A., The CC chemokine RANTES in breast carcinoma progression: regulation of expression and potential mechanisms of promalignant activity. *Cancer Res* **2002**, 62, (4), 1093-102.

182. Adams, J.; Carder, P. J.; Downey, S.; Forbes, M. A.; MacLennan, K.; Allgar, V.; Kaufman, S.; Hallam, S.; Bicknell, R.; Walker, J. J.; Cairnduff, F.; Selby, P. J.; Perren, T. J.; Lansdown, M.; Banks, R. E., Vascular endothelial growth factor (VEGF) in breast cancer: comparison of plasma, serum, and tissue VEGF and microvessel density and effects of tamoxifen. *Cancer Res* **2000**, 60, (11), 2898-905.
183. Noris, M.; Daina, E.; Gamba, S.; Bonazzola, S.; Remuzzi, G., Interleukin-6 and RANTES in Takayasu arteritis: a guide for therapeutic decisions? *Circulation* **1999**, 100, (1), 55-60.
184. Niwa, Y.; Akamatsu, H.; Niwa, H.; Sumi, H.; Ozaki, Y.; Abe, A., Correlation of tissue and plasma RANTES levels with disease course in patients with breast or cervical cancer. *Clin Cancer Res* **2001**, 7, (2), 285-9.
185. Dontu, G.; Al-Hajj, M.; Abdallah, W. M.; Clarke, M. F.; Wicha, M. S., Stem cells in normal breast development and breast cancer. *Cell Prolif* **2003**, 36 Suppl 1, 59-72.
186. Al-Hajj, M.; Wicha, M. S.; Benito-Hernandez, A.; Morrison, S. J.; Clarke, M. F., Prospective identification of tumorigenic breast cancer cells. *Proc Natl Acad Sci USA* **2003**, 100, (7), 3983-8.
187. Helczynska, K.; Kronblad, A.; Jogi, A.; Nilsson, E.; Beckman, S.; Landberg, G.; Pahlman, S., Hypoxia promotes a dedifferentiated phenotype in ductal breast carcinoma in situ. *Cancer Res* **2003**, 63, (7), 1441-4.
188. Krishnamurthy, P.; Ross, D. D.; Nakanishi, T.; Bailey-Dell, K.; Zhou, S.; Mercer, K. E.; Sarkadi, B.; Sorrentino, B. P.; Schuetz, J. D., The stem cell marker Bcrp/ABCG2 enhances hypoxic cell survival through interactions with heme. *J Biol Chem* **2004**, 279, (23), 24218-25.
189. Hawkins, L. K.; Johnson, L.; Bauzon, M.; Nye, J. A.; Castro, D.; Kitzes, G. A.; Young, M. D.; Holt, J. K.; Trown, P.; Hermiston, T. W., Gene delivery from the E3 region of replicating human adenovirus: evaluation of the 6.7 K/gp19 K region. *Gene Ther* **2001**, 8, (15), 1123-31.
190. Zhang, Y. A.; Nemunaitis, J.; Scanlon, K. J.; Tong, A. W., Anti-tumorigenic effect of a K-ras ribozyme against human lung cancer cell line heterotransplants in nude mice. *Gene Ther* **2000**, 7, (23), 2041-50.

191. Hollenbaugh, D.; Grosmaire, L. S.; Kullas, C. D.; Chalupny, N. J.; Braesch-Andersen, S.; Noelle, R. J.; Stamenkovic, I.; Ledbetter, J. A.; Aruffo, A., The human T cell antigen gp39, a member of the TNF gene family, is a ligand for the CD40 receptor: expression of a soluble form of gp39 with B cell co-stimulatory activity. *Embo J* **1992**, 11, (12), 4313-21.
192. Maizel, J. V., Jr.; White, D. O.; Scharff, M. D., The polypeptides of adenovirus. II. Soluble proteins, cores, top components and the structure of the virion. *Virology* **1968**, 36, (1), 126-36.
193. Medhora, M.; Daniels, J.; Munday, K.; Fisslthaler, B.; Busse, R.; Jacobs, E. R.; Harder, D. R., Epoxygenase-driven angiogenesis in human lung microvascular endothelial cells. *Am J Physiol Heart Circ Physiol* **2003**, 284, (1), H215-24.
194. van Rooij, E.; Doevendans, P. A.; de Theije, C. C.; Babiker, F. A.; Molkentin, J. D.; de Windt, L. J., Requirement of nuclear factor of activated T-cells in calcineurin-mediated cardiomyocyte hypertrophy. *J Biol Chem* **2002**, 277, (50), 48617-26.
195. Park, M. T.; Lee, M. S.; Kim, S. H.; Jo, E. C.; Lee, G. M., Influence of culture passages on growth kinetics and adenovirus vector production for gene therapy in monolayer and suspension cultures of HEK 293 cells. *Appl Microbiol Biotechnol* **2004**, 65, (5), 553-8.